EXPERIMENTAL AND NUMERICAL STUDIES TO DETERMINE THE SUBGRADE SOIL RESILIENT MODULUS USING REPEATED LOAD CBR TEST

A thesis submitted to the Indian Institute of Technology Guwahati
for the partial fulfilment of the award of the degree

of

Doctor of Philosophy

In Civil Engineering with a Specialization in
'Transportation Systems Engineering'

by

SUPRATIM KAUSHIK
(Roll no.- 176104012)

Under the guidance of
Dr. Anjan Kumar Siddagangaiah

DEPARTMENT OF CIVIL ENGINEERING
INDIAN INSTITUTE OF TECHNOLOGY GUWAHATI
GUWAHATI - 781039, INDIA

AUGUST 2023

Dedication

Dedicated to my parents for their constant support and encouragement during my PhD & my dear friend Dr. Avilash Sahoo, who is no more with us today

Certificate

This is to certify that the thesis titled "***Numerical and experimental studies to determine the subgrade soil resilient modulus using the RLCBR test***" submitted by ***Supratim Kaushik (Roll No.:176104012)*** to the Indian Institute of Technology Guwahati for the award of the degree of Doctor of Philosophy is a record of bonafide research work carried out by him under my supervision and guidance. In my opinion, the thesis work has reached the requisite standard fulfilling the requirement for the degree of Doctor of Philosophy.

The findings presented in this thesis have not been submitted in part or full to any other university or institute for the award of any degree or diploma.

Dr. Anjan Kumar S.
Associate professor
Department of Civil Engineering
Indian Institute of Technology Guwahati
Assam - 781039, India

Place: IIT Guwahati

Date: 10/08/2023

Declaration

I declare that this written submission represents my ideas in my own words. Where others' thoughts and words have been included, I have adequately cited and referenced the original sources. I also declare that I have adhered to all academic honesty and integrity principles and have not misinterpreted, fabricated, or falsified any idea/ data/ fact/ source in my submission. This thesis, in any way, does not purport to endorse any proprietary products or technologies.

Supratim Kaushik

Place: IIT Guwahati

Date: 10/08/2023

Supratim Kaushik

Roll: 176104012

Acknowledgement

I extend my heartfelt appreciation and profound thanks to my supervisor, Dr. Anjan Kumar S., for his unwavering support and invaluable guidance during my PhD journey. His extensive expertise and constant motivation have been instrumental in shaping my research and completing this thesis. I am genuinely grateful for the significant amount of time he dedicated to me throughout my academic pursuit.

I would also like to extend my heartfelt gratitude to my Doctoral committee members Dr. C. Mallikarjuna, Dr. Hrishikesh Sharma and Dr. Pankaj Biswas for their inputs and opinions which have helped me shape this thesis.

Personally, I would like to offer my sincere gratitude to Mr. Kuldeep Kalita, Mr. Mrinal Sarmah, and Mr. Balen Kalita of the Transportation Systems Engineering Division for their support during my laboratory experiments. The support provided by the Department of Civil Engineering, NIT Meghalaya during the course of my M.Tech and PhD is hereby acknowledged. My heartfelt thanks go out to the National Rural Infrastructure Development authority (NRIDA), Govt. of India for providing support for field visits and collection of soil samples and field testing.

I would like to thank my friends and co-researchers: Miss Ibaiahun Nongbet Sohlang, Dr. Bhaskar Pratim Das, Mrs. Saswati Das, Dr. Santanu Pathak, Dr. Nishant Bhargava, Mr. Harish Nanda for their constant support and encouragement during the course of my PhD work. Without their constant backing and encouragement, it would have been impossible for me to manage the rigours of being a part time research scholar. Special thanks to my friend and former colleague in NIT Meghalaya, Dr. Suman Kumar, for the help and support provided in carrying out the numerical simulations used in this research. I would like to thank Mr. Akshai Chandran, Mr. Shaikhul Islam Prodhani, former M.tech students in the Department of Civil Engineering, IIT Guwahati for helping me in carrying out the experiments required for the research.

Last (but certainly not least), I would also like to thank my family for their continuous encouragement, love, and support. A special mention for my friend Miss Pallabi Sarma, for supporting me in every step during the course of my PhD.

Supratim Kaushik

LIST OF ABBREVIATIONS

Acronym	*Meaning*
AASHTO	American Association for State Highway and Transport Officials
SSV	Soil Support Value
CBR	California Bearing Ratio
MEPDG	Mechanistic Empirical Pavement Design Guide
NCHRP	National Cooperative Highway Research Program
IRC	Indian Roads Congress
RLTT	Repeated Load Triaxial Test
RLCBR	Repeated Load CBR
FEM	Finite Element Method
HRB	Highway Research Board
WASHO	Western Association of State Highway Officials
MSA	Million Standard Axles
RC	Resonant Column
FFRC	Free Free Resonant Column
UCS	Unconfined Compressive Strength
LVDT	Linear Variable Differential Transducer
FWD	Falling Weight Deflectometer
SPA/PSPA	Seismic Pavement Analyzer/Portable Seismic Pavement Analyzer
LWD	Light Weight Deflectometer
DCP	Dynamic Cone Penetrometer
ASTM	American Society for Testing and Materials
DST	Direct Shear Test
CI	Intermediate Compressible Clay
CL	Low Compressible Clay
MI	Intermediate Compressible Clay
OMC	Optimum Moisture Content
MDD	Maximum Dry Density
MAE	Mean Absolute Error
MSE	Mean Square Error
RMSE	Root Mean Square Error

Abstract

Subgrade characterization in terms of resilient modulus is an important aspect of mechanistic pavement design methods. The resilient modulus is analogous to the Elastic modulus; however, repeated loads are applied instead of monotonic load and is expressed as the ratio of deviatoric stress to the resilient strain. The most commonly used laboratory method to determine resilient modulus is the Repeated Load Triaxial Test (RLTT). However, the test is complex, requires expensive test setup, skilled personnel and is time-consuming. Therefore, an alternate simple and cost-effective method for subgrade resilient modulus characterization using the simple CBR apparatus has been explored in this study. This study aims to characterize the subgrade resilient modulus using the Repeated Load CBR (RLCBR) test and compare it with the field modulus. It combines numerical modelling of the CBR test, with laboratory studies using the Repeated load CBR (RLCBR) test to propose methodologies and predictive models to characterize the subgrade resilient modulus using the RLCBR test. A total of twelve soils were tested in the laboratory in the present study. RLCBR tests were conducted on all twelve soils in deformation-controlled mode and five soils (out of twelve) in load-controlled mode. The laboratory resilient modulus was compared with the field resilient modulus determined using the Light Weight Deflectometer and the Dynamic Cone Penetrometer (DCP) tests.

A 3D Finite Element Model of the CBR test was formulated in the commercial package LS-DYNA® to understand the mechanics of the test. The soil was modelled as an elastoplastic material using the Mohr-Coulomb Failure criterion. Appropriate boundary conditions for the mould, surcharge load and penetrating plunger were considered to simulate the laboratory conditions. A mesh sensitivity analysis was conducted by considering mesh sizes of 1.25 mm, 2.5 mm, 5 mm, 7.5 mm and 10 mm. Results showed that the load penetration graphs and the CBR values were not affected significantly when the mesh size was increased from 1.25 mm to 2.5 mm and therefore were used for further analysis. Validation with data from the literature and laboratory test results showed that the model could predict the CBR value with errors within 5%. Further, it was observed from load penetration curves obtained from the numerical model that for the kind of soils considered in the study, the yielding of the soils took place after 3 mm penetration of the plunger. Therefore, simulations were performed by considering the material as elastic up to 3 mm penetration using probable values of Elastic modulus and Poisson's ratio, resulting in 180 simulations. The objective was to obtain mathematical relationships between the octahedral shear stress and the bulk

stress with the plunger stress, which can be measured experimentally. Results showed that a linear relationship between the bulk stress and octahedral shear stress with the plunger stress can be assumed under elastic conditions.

For laboratory studies, soils were collected from ten in-service low-volume roads in the states of Assam and Meghalaya, and two soils were collected from within the IIT Guwahati campus roads. Standard size 50 cm x 50 cm pits were excavated to the subgrade level. Before collecting soil specimens, field tests like field density using the core cutter and sand replacement methods and moisture content determination were carried out. This was followed by conducting a solitary Dynamic Cone Penetration test and a Light Weight Deflectometer (LWD) test to determine the field modulus. Post this, soils in sufficient quantity were transported to the IIT Guwahati laboratory for testing. Initial Laboratory testing consisted of basic characterization of soil. Tests included conducting Atterberg's limits test, particle size distribution test, and determining the soil's compaction characteristics and strength characteristics using soaked and unsoaked CBR tests. Results showed that the soils collected were fine-grained, with CI, CL and MI classifications. Further, the soils can be classified as low and medium plastic soils based on plasticity index values. Additional laboratory tests included a Direct shear test to obtain shear strength parameters for eight soils, while elastic modulus was obtained by conducting Unconfined Compressive Strength (UCS) tests.

RLCBR tests were carried out in two modes: (i) Deformation controlled mode (ii) Load controlled mode. The deformation-controlled RLCBR tests load the specimen to a target deformation and unload it. In contrast, the load-controlled mode subjected the specimen to predefined target load and unloading cycles. The deformation-controlled RLCBR tests were used to standardize the test and propose a predictive model which estimates the subgrade resilient modulus at stress levels typical of a subgrade soil element. In contrast, the load-controlled test results were used for stress-based non-linear elastic characterization of subgrade soils.

RLCBR tests in the deformation-controlled mode were conducted on the twelve soils collected at three moisture contents at a target deformation of 1.5 mm. Three replicates were tested at each test condition, and the average of the results was used. The plunger stress obtained experimentally was used to obtain the octahedral shear stress and the bulk stress of the CBR specimens under plunger loading using the mathematical relationships developed using the numerical model. The computed octahedral shear stress and the bulk stress were used in the MEPDG constitutive model with model coefficients obtained empirically to compute the resilient modulus of the soils at each test condition (24 test conditions). The plunger stress, resilient deformation

and the resilient modulus for the eight soils (24 test conditions) were used to carry out a non-linear least square regression to fit the RLCBR model parameters and propose a predictive model. The model was validated by computing the RLCBR modulus for the remaining 4 soils and comparing it with the resilient modulus at recommended stress levels. Results showed that the proposed RLCBR model agreed with the modulus calculated at the recommended stress levels using the MEPDG model. Further, statistical analysis of the proposed model showed that the model could capture the effects of moisture on the resilient modulus.

Load-controlled RLCBR tests were carried out on five of the twelve soils used in the study. The loads were applied as proportions of the peak load obtained from the Unsoaked CBR tests. The peak load here is the load at which the behaviour of the soil changes from elastic to plastic regime. Eight load sequences were applied on the soils at OMC-3, OMC, whereas five were applied on the specimens at OMC+3. The bulk and octahedral stresses for each load sequence were calculated using the relationships developed from the FEM. The resilient modulus for each stress sequence was computed using the model proposed earlier using the deformation-controlled tests. The bulk stress, octahedral shear stress and resilient modulus were then used in a non-linear least square regression analysis to obtain the model coefficients of the MEPDG constitutive model for the five soils at each test condition. The results showed that the proposed methodology predicted the MEPDG model coefficients with an $R^2 > 0.8$ for all the cases. Further, the model coefficients were validated with those obtained from empirical correlations and showed promising agreement. The proposed methodology can be cost-effective in characterizing resilient moduli for MEPDG Level 1 applications.

Finally, the computed laboratory resilient modulus was compared with the field-evaluated elastic modulus. The laboratory-resilient modulus was much higher than the field modulus obtained using the DCP and the LWD due to variations in field and laboratory moisture-density conditions. However, it was also observed that as the moisture and density conditions were nearer to the laboratory conditions, the RLCBR and field modulus approached each other. The comparison assessment of the field and RLCBR test results suggest that a reference modulus from the laboratory RLCBR test can be used to evaluate the construction quality in the field in terms of modulus in addition to traditional density checking. Hence the resilient modulus prediction model developed using RLCBR, a quick and simple test, could provide more inputs to design and quality control characteristics in the field for constructing subgrade soils.

Keywords: RLCBR, LWD, DCP, Finite Element Modelling.

Table of Contents

List of Tables

List of Figures

CHAPTER 1

Introduction

1.1 General

A typical pavement structure consists of soil subgrade, the granular layers (sub-base and base) and the bituminous layers. The soil subgrade is the foundation layer of the pavement to which all the load wheel stresses are transmitted. Therefore, a pavement structure must have a strong subgrade with adequate bearing capacity and stiffness (Yoder & Witczak, 1975). The subgrade can be made up of either natural soil or compacted. Pavement performance can be defined as the ability of pavement to serve traffic over time (AASHTO,1993) satisfactorily. The optimal performance of a pavement structure is assured when three key aspects namely, pavement design, quality of construction, and proper pavement maintenance are integrated. Designing and constructing a pavement with sufficient strength and stiffness is critical for long-term durability. During the design phase, proper material characterization in the laboratory ensures a structurally sound structure. Whereas quality control measures during construction impart durability over its service life.

Over the years, pavement design methods have undergone significant evolution, transitioning from purely empirical approaches to mechanistic empirical methods (Pereira and Pais, 2017). In the empirical design methods, subgrade characterization was done based on empirical parameters such as the CBR and the soil support value (SSV) used in the initial AASHTO guide for designing pavement structures in 1961(AASHTO, 1961). However, CBR and SSV were based on empirical tests, which did not represent a fundamental material property. As an improvement over this limitation, in 1986, the AASHTO pavement design method introduced the concept of resilient modulus (M_r) to characterise subgrade soils (AASHTO,1986). The resilient modulus is the elastic modulus determined based on repeated deviatoric stress and the resilient strain. The resilient modulus characterizes the subgrade's nonlinear elastic behaviour and represents the dynamic pavement loading. The primary advantage of using the resilient modulus in pavement design is that it can be used as an input in layered elastic computer programs, which can be used to calculate pavement responses (Stresses and strains) to wheel loads, which can then be empirically correlated to

pavement performance. There are two ways to characterize the resilient modulus for mechanistic pavement design: (i) a single representative value that is representative of the state of stress of the subgrade (used in MEPDG Level 2 and most mechanistic design methods worldwide) (ii) characterization of stress-dependent behaviour of the soil (MEPDG Level 1). Resilient modulus is well accepted for subgrade characterization in mechanistic pavement analysis and design (Shell pavement design manual,1978 ; MS-2:Asphalt Mix Design Methods, 2015; IRC 37,2018; Austroads, 2012 ;AASHTO Mechanistic-empirical pavement design guide (MEPDG), 2008). Therefore, a precise estimate of the subgrade resilient modulus is important for the design of durable and cost-effective pavements.

The Repeated Load Triaxial Test (RLTT) is the most commonly used laboratory method for estimating soil resilient modulus (Puppala, 2008). However, owing to the complexity and high cost of the RLTT, attempts have been made to use simple, cost-effective equipment like the static triaxial test apparatus, the oedometer and the CBR to mimic the repeated loading of the RLTT (Kim *et al*., 2001 ; Nagula *et al.*, 2018; Araya, 2011). The most popular among the alternate methods is the Repeated load CBR (RLCBR) test, which has drawn significant research interest in the last decade (Molenaar, 2007; Araya, 2011;Hao and Pabst, 2021; Haghighi *et al*., 2018; Narzary and Ahamad, 2020). The repeated load CBR (RLCBR) test was first utilized in the 1980s by Loach (1987), who conducted tests on reconstituted soils with known effective stress and stress history. Later, Molenaar (2007) used the RLCBR test to characterize fine-grained soils, including swelling clays, laterites, and volcanic materials like cinder. The test was shown to provide reasonable estimates of the resilient deformation of the soils. The set up used for a RLCBR test is similar to that of a standard CBR test, but repeated loads are applied instead of the conventional loading. The soil particles undergo permanent and recoverable deformations under multiple load repetitions at the same deformation rate. After a few repetitions, the permanent deformation ceases, and only stable recoverable or resilient deformation is observed. Due to a CBR specimen's complex stress state, the soil's resilient modulus cannot be directly computed as in the case of RLTT. Instead, the resilient deformation and the plunger load are used in an elastic model based on a quasi-static infinite half-space under a circular load based on elastic theory to compute the resilient modulus. Araya (2011) extended the use of the RLCBR test to granular materials and proposed a regression model based on finite element analysis for estimating the stiffness modulus of granular materials. Since then,

several studies have been carried out to utilize the RLCBR test for the characterization of the resilient behaviour of granular materials, soils, waste rocks and chemically treated materials (Sas *et al*., 2013; Bhattacharjee and Bandyopadhyay, 2015; Haghighi *et al*., 2018; Hao and Pabst, 2021).

1.2 Research gap

Earlier research on the RLCBR test and the proposed models did not consider the state of stress at which the modulus has been reported. For use in a mechanistic-empirical design, the resilient modulus must be calculated at the recommended stress level representative of an in-service pavement. Therefore, a better understanding of the state of stress of a CBR specimen is required to completely understand the mechanics of the test before the RLCBR modulus can be used as input in mechanistic design programs. Moreover, limited research is available on the stress-based nonlinear elastic characterization of subgrade soils using the RLCBR test, which can be used as inputs in MEPDG level 1 analysis.

1.3 Research objective

This study aims to characterize the subgrade soil resilient modulus for use in mechanistic pavement design using the RLCBR test. The following tasks were carried out to achieve the objective:

- **Task 1**: Selection and collection of soils from in-service pavements and basic soil properties characterization in the laboratory.
- **Task 2**: Conducting RLCBR test on the selected subgrade soils at various moisture contents in deformation-controlled and load-controlled modes.
- **Task 3**: Finite element modelling of the CBR test and parametric analysis.
- **Task 4**: Development of resilient modulus predictive model from the load-controlled RLCBR test results and the FEM at specified stress state.
- **Task 5**: Propose a methodology for the stress-based characterization of subgrade soils using the RLCBR test
- **Task 6**: Compare RLCBR modulus with field modulus.

1.4 Organization of report

The contents of this thesis are organized into eight chapters. Chapter 1 introduces the research area, provides background information on the requirement of resilient modulus characterization for mechanistic pavement design, and highlights the research problem and objectives of the research work. Chapter 2 presents a detailed review of the literature related to this research work. Firstly, the historical evolution of pavement design methods was reviewed, emphasizing subgrade characterization methods. This was followed by reviewing various state-of-the-art laboratory and in situ practices to determine resilient modulus. Finally, a detailed review of the literature of the RLCBR test and the identification of research gaps is presented. Chapter 3 describes the various materials, laboratory and field-testing protocols used in this research. In chapter 4, the details of the developed numerical model of CBR are presented along with validation. Chapter 5 presents the results of the laboratory RLCBR tests conducted using the deformation mode. Test protocols and prediction models have also been proposed for resilient modulus estimation using the RLCBR test. Further a simple range comparison was made with the field modulus. Chapter 6 presents the results of the load-controlled RLCBR test and proposes a novel methodology to characterize the stress-dependent behaviour of soils. The summary of findings, salient conclusions, and the way forward of this research work is presented in chapter 7.

CHAPTER 2

Literature Review

2.1 General

A sustainable pavement structure depends on three main aspects, namely, pavement design, quality of construction and maintenance. To efficiently design a pavement, proper material characterization is very important. The properties of materials in each layer: the subgrade, the granular layers, and the bituminous layer, must be ascertained before we arrive at the most appropriate design thickness. The subgrade soil characterization over the years has evolved from empirical methods such as the SSV, R-value and CBR to the use of resilient modulus in the mechanistic design procedures. This section provides a detailed review of the evolution of the methods of subgrade characterization with a focus on current state-of-the-art practices.

2.2 Design of flexible pavements: A historical perspective

In the context of pavement design, the primary objective of a design method is to determine the thickness of individual pavement layers to be constructed over the subgrade. It ascertains a suitable composition and thickness of individual pavement layers that can perform satisfactorily over the design period for the projected traffic load and given environmental conditions. Over the past few decades, pavement design has transitioned from an empirical approach to a mechanistic-empirical one. A detailed discussion of the evolution of pavement design methods is presented in this section. A timescale of the important milestones in the design of flexible pavements is presented in Figure 2.1.

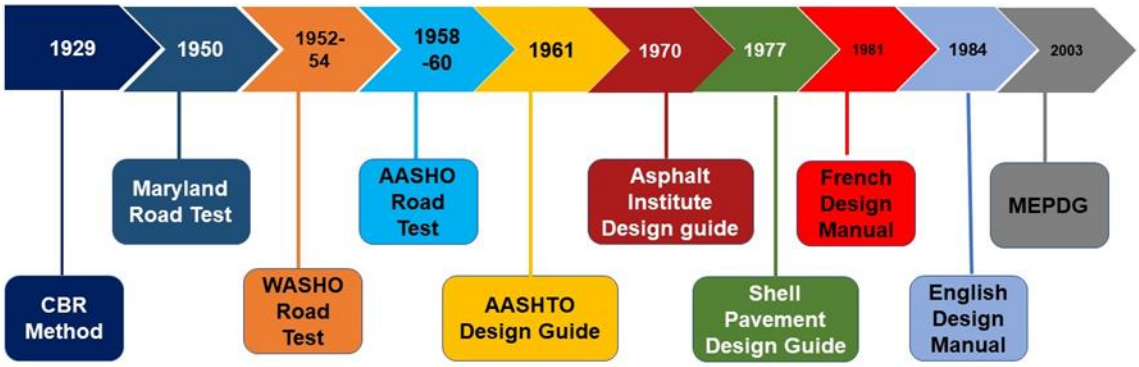

Figure 2.1: Timeline of evolution of pavement design methods

2.2.1 Empirical pavement design

Initial flexible pavement design methods were based on empirical procedures, which involved the determination of the thickness of individual layers with or without a soil strength test (Huang, 1993). The empirical method that doesn't involve a strength test has been used since the development of the Public Roads (PR) soil classification (Hogentogler and Terzaghi, 1929). The system classified the subgrade as uniform from A-1 to A-8 and nonuniform from B-1 to B-3. The Highway Research Board (HRB) later modified this system in 1945 by grouping soils from A-1 to A-7 and adding a group index to differentiate soils within each group (HRB,1945). Steele(1945) discussed using the HRB classification and group index to estimate subbase and total pavement thickness without a strength test. In 1929,the California Highway Department pioneered the empirical method with a strength test, which related pavement thickness to the California Bearing Ratio (CBR). The CBR measures a subgrade soil's penetration resistance relative to a standard crushed rock. After extensive study by the U.S. Corps of Engineers during World War II, the CBR design method gained popularity and became widely used (U.S Army Corps of Engineers, 1945). Apart from the CBR, the Soil Stability Value and the Hveem R-value were the predominantly used soil strength parameters (Puppala, 2008).

Full-scale road tests were a significant advancement in pavement design using empirical methods as they addressed critical factors such as traffic, climatic conditions, and pavement distresses. These tests became the main support for the development of a new approach to pavement design, which is still used in many pavement analyses and design methods today. The Maryland road test was the first to be conducted in the United States to determine the relative effects of different axle loadings (HRB, 1952).

The Western Association of State Highway Officials (WASHO) road test followed, investigating the effect of axle loadings on pavement cracking for different asphalt layer thicknesses The WASHO road test also introduced the Benkelman Beam device, which measured pavement deflection under slow-moving wheel loads, providing an early indication of pavement performance. The AASHO road test, undertaken from 1958 to 1960, was a landmark test under real traffic conditions and contributed to improving pavement design (HRB, 1962). The AASHO road test resulted in the development of the pavement serviceability concept, equations relating serviceability, load, and thickness design of both flexible and rigid pavements, which were used in pavement design guides such as the AASHTO design guides AASHTO (1961;1972;1986) and Asphalt Institute MS-1 (1970).

In India, the initial recommendations for the design of flexible pavements were made in 1970 with the introduction of the 1st edition of the IRC:37. The design method was based on two factors: (i) the strength of the subgrade (foundation) measured by the California Bearing Ratio, and (ii) the traffic, quantified by the number of commercial vehicles weighing 3 tonnes or more. These guidelines underwent revision in 1984, considering the design traffic measured by the cumulative number of equivalent standard axle loads of 80 kN. Design charts for traffic volumes up to 30 million standard axle repetitions were provided. The 1970 and 1984 guidelines were based on an empirical approach derived from experience (IRC 37,1970;IRC 37,1984).

An empirical method is limited to applying only to specific environments, materials, and loading conditions. Any deviation from these conditions renders the design invalid, and a new method has to be developed through trial and error to fit the new conditions. This is because the association between the factors contributing to pavement failures, such as loads, materials, layer configurations, and environmental factors, is established based on experience, empirical experimentation, or a blend of both. It is not recommended to use an empirical relationship to describe phenomena occurring outside the range of data used to establish the relationship (Pereira and Pais, 2017). Further, the design method is based on empirical test parameters like CBR, SSV, etc., which are not fundamental material properties (Puppala, 2008).

2.2.2 Mechanistic empirical pavement design methods

Mechanistic-empirical design methods marked a significant advancement over empirical approaches in pavement design. These methods incorporate the principles of mechanics to predict the induced states of stresses and strains within the pavement structure. By considering the effects of traffic loading and environmental conditions, computer software programs have been developed to implement mechanics-based predictions, typically using a layered elastic model (Huang, 1993). The stresses and strains calculated from elastic theory are then empirically correlated to the pavement failure by computing the number of loading cycles to failure. A reliability component is usually introduced that considers the various sources of variability that can affect the design process. This integration of mechanics and empirical observations allows for more accurate and reliable assessments of pavement performance, enabling engineers to make informed decisions during the design process. Figure 2.2 shows a typical mechanistic empirical pavement design framework.

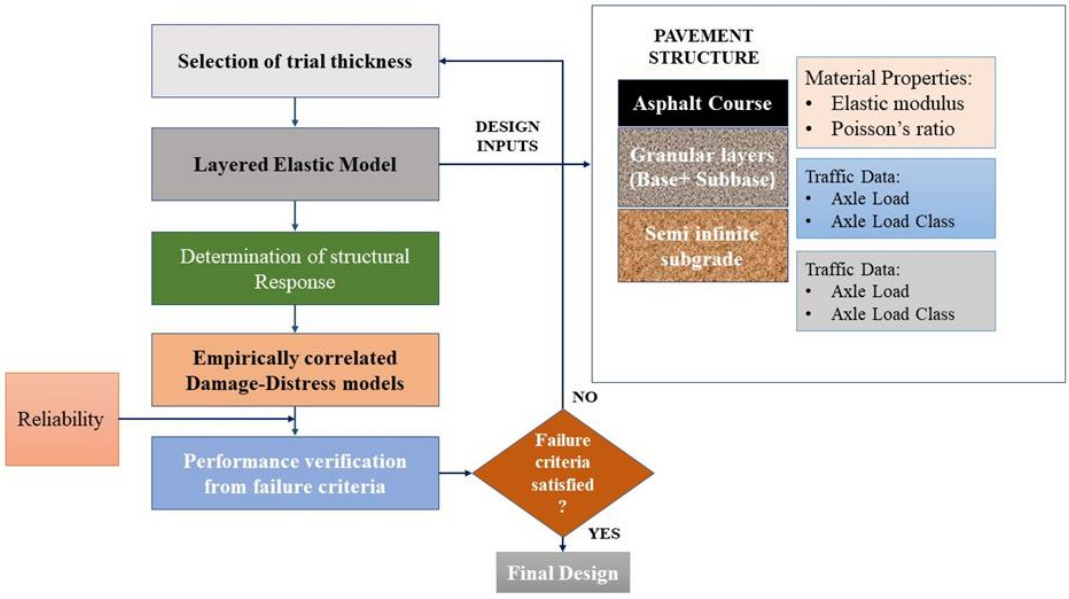

Figure 2.2: Framework of a Mechanistic-Empirical design

Over the years, several mechanistic pavement design methods have been developed across the world, which work on the framework presented in Figure 2.2 (Shell pavement design manual,1978;Shook,1982; LCPC,1981; Powell *et al.*,1984). The French pavement design method (LCPC, 1981) stands out as the most comprehensive design approach currently employed in Europe (Pereira and Pais, 2017). In the Indian context, mechanistic pavement design was introduced with the 2002 edition of the Indian Roads Congress Publication 37 based on the findings of R-6 and

R-56 research initiatives by the Ministry of Road Transport and Highways (IRC 37, 2002) .The design of flexible pavements incorporated mechanistic-empirical performance models for subgrade rutting and bottom-up cracking in the bottom bituminous layer derived from these research projects. The analysis of pavements was carried out using the FPAVE software, specifically developed for the R-56 research scheme to analyze linear elastic layered pavement systems. Thickness charts developed provided design guidelines for traffic levels up to 150 million standard axles (msa) repetitions. Further revisions were made in 2012 and 2018, where provisions were made for higher traffic, alternate materials and a new advanced version of the FPAVE known as IIT PAVE was introduced (IRC 37,2012; IRC 37, 2018)

The Mechanistic-Empirical Pavement Design Guide (MEPDG) was developed as part of the NCHRP 1-37A project and is considered the most comprehensive of all the mechanistic design methods in practice around the world (AASHTO Mechanistic-empirical pavement design guide (MEPDG), 2008). This method integrated calibrated models specific to the United States to predict various distresses caused by traffic loads and environmental conditions. Unlike the previous approach, MEPDG considered vehicle class, load distributions, and seasonal effects on pavement performance, an improvement over the earlier mechanistic design methods. The MEPDG method employed a seasonal-based approach to assessing pavement performance, allowing for the consideration of the effect of climate conditions on material behaviour over time. The structural responses, such as stresses, strains, and deflections, were calculated using a mechanistic approach considering material properties, environmental conditions, and loading characteristics. These calculated responses were then used as inputs in empirical models to predict distress in the pavement. By iteratively comparing predicted performance against design criteria, the composition and material selection of the pavement structure were adjusted to achieve a satisfactory design outcome. Based on the importance of the projects and the input data considered, MEPDG projects are classified into levels 1 to 3.

- Level 1: Material properties are determined using routine laboratory tests and used for projects of very high significance.
- Level 2: Material properties are determined using empirical correlations with other parameters and are used for less significant projects.

- Level 3: Material properties are determined from an existing database based on experience and are applicable for low-volume pavements or for preliminary design.

2.3 Characterization of pavement materials for mechanistic design

The review of different design methods reveals the significance of material characterization as a vital element in any mechanistic design approach. Precise determination of the resilient modulus (M_r) of compacted subgrade soil is crucial for ensuring the safe and sustainable design of flexible pavement systems (Kardani *et al*., 2022; Nazarian *et al*., 2003; Puppal, 2008). The subgrade layer is the foundation layer of the pavement to which all the loads are finally transferred. Therefore, it is a fundamental requirement of a pavement structure to have a sufficiently strong subgrade with adequate bearing capacity and stiffness (Yoder and Witzack,1975). Specifically, subgrade characterization in the empirical methods was on the basis of empirical tests such as the CBR, SSV and the R-value. However, with the introduction of resilient modulus (M_r) in the 1986 edition of the AASHTO, a shift in the characterization methods was observed (AASHTO,1986). The subgrade layer is now characterized in terms of its elastic properties which are signified by the elastic modulus or resilient modulus.

2.4 Resilient modulus of subgrade

Soil is a highly complex material, whose stiffness behaviour depends on numerous factors. The most important factors effecting the stiffness or elastic modulus of soil are: soil type, moisture content, soil density, type of modulus estimated and stress history of the soil. A particular value of elastic moduli for a soil can be associated only to a particular test condition. As the test condition changes, wide variation can be observed in the estimated moduli, thus defining an elastic modulus for a soil which accurately represents the field conditions and design requirement can prove to be a challenging task. The elastic modulus of soil is therefore, one of the most complex parameters, whose estimation requires a thorough understanding of the conditions and the purpose for which it is estimated. Generally speaking, the elastic modulus is the ratio of the applied deviatoric stress to the resulting strain of the material. However, for the same soil, numerous modulus values may be obtained depending on the strain level, stress history of the soil, drainage conditions, moisture and compaction of the soil (Briaud, 2001). The elastic modulus of soil can be of the following types:

- Initial tangent modulus: The initial slope of the stress-strain curve is termed the initial tangent modulus (E_{max}).
- Secant modulus: The secant modulus (E_1) is defined as the slope of the line that joins the origin to a point on the stress-strain curve that represents half the ultimate deviatoric stress at which the sample fails.

The different soil moduli are pictorially illustrated in Figure 2.3**: Different types of soil moduli**

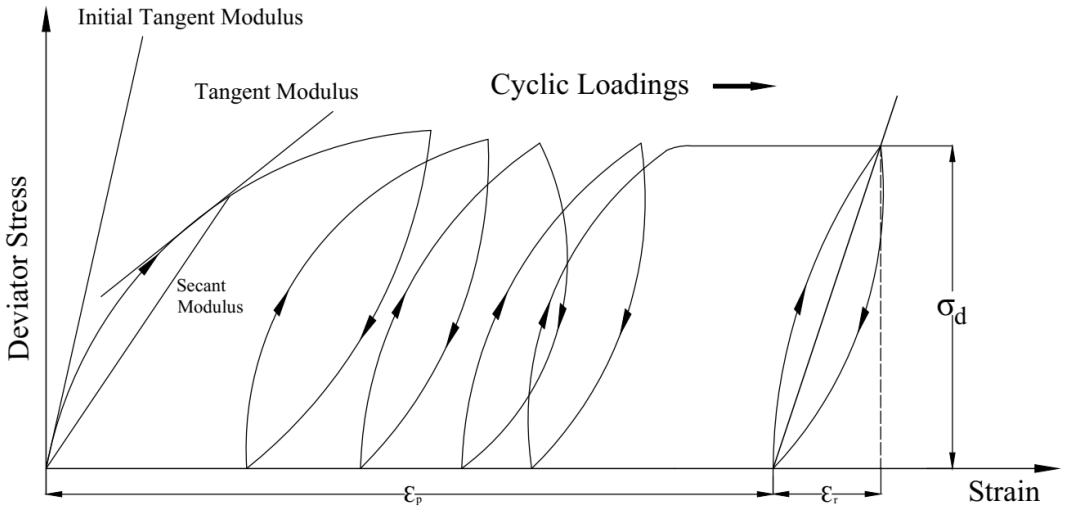

Figure 2.3: Different types of soil moduli

In pavement engineering, to consider the cyclic nature of the traffic loads, the resilient modulus is commonly preferred. The resilient modulus is equivalent to an elastic modulus used in elastic theories, with the exception that it is determined by applying a repeated deviatoric load instead of a monotonic load and is defined as the ratio of the repeated deviatoric stress to the recoverable or resilient strain. The resilient modulus (M_r) represents the secant modulus of the stress-strain curve of the soil after a particular number of load repetitions. Mathematically, M_r is computed as shown in Equation 2.1.

$$M_r = \frac{\sigma_d}{\varepsilon_r} \qquad (2.1)$$

where

M_r = Resilient modulus

σ_d = Deviatoric stress applied

ε_r = Recoverable or resilient strain

Most subgrade soils are not linearly elastic but experience permanent deformation under repeated loads (Uzan, 1985). However, when the loads are much smaller than the ultimate loads at failure and repeated for a large number of cycles, the permanent deformation ceases, and the resulting deformation is considered entirely recoverable or elastic. This resulting deformation is then used to calculate the resilient modulus or simply the stiffness. NCHRP 1-28A (2003) and (AASHTO T307,2003) resilient modulus testing protocols are based on this principle.

However, problems associated with field sampling, specimen preparation, and expertise required for performing the test have prompted many transportation agencies to adopt in situ stiffness determination methods, especially for widening and rehabilitation projects. A wide variety of field and laboratory equipment are used to determine the modulus of subgrade soils for use in pavement design, each having different operational principles. Therefore, the obtained moduli for the same soil are distinctly different for the various types of equipment used, as each apparatus measures different elastic moduli at different strain levels. The laboratory methods measure the resilient modulus, while the field NDT devices measure the Elastic modulus.

It becomes essential to understand the strain level and stress state at which the modulus is measured to interpret the moduli obtained. The variability in the measured modulus may thus have a significant impact on the design thicknesses obtained in a pavement design. Therefore, it becomes fundamental for a pavement engineer to critically understand the operational and functional differences between the field and laboratory-measured moduli to achieve more realistic resilient modulus values.

2.5 Factors affecting subgrade soil resilient modulus

Numerous studies conducted over the years have revealed that the resilient modulus of subgrade soils is not constant. Instead, it is primarily influenced by three factors: (1) state of stress (confining stress, deviatoric stress) and (2) soil physical state, including moisture and density.

A slight increase in the resilient modulus was observed with an increase in confining stress for fine-grained soils (Ooi *et al*.,2004; Elliott and Thornton,1988). On the other hand, Sargand et al., (2000) reported the negligible effect of confining stress on fine-grained soils. In the case of coarse-grained soils, the resilient modulus was

observed to increase with an increase in confining stress (Figueroa and Thompson, 1980; Farrar and Turner, 1991; Lekarp *et al*., 2000).

Sensitivity to deviatoric stress manifests in two distinct behaviours: hardening and softening (Tamrakar and Nazarian, 2016). Hardening increases strength and stiffness under repeated deviatoric loads, while softening causes a reduction in material strength and stiffness under repeated deviatoric loads. The characterization of these behaviours in subgrade can be accomplished through tests such as the resilient modulus test conducted under repeated load triaxial conditions. Coarse-grained soils are usually referred to as strain-hardening materials, whereas fine-grained soils are referred to as strain-softening materials. The primary reason for strain hardening behaviour is the rearrangement of particles under repeated deviatoric loading, which enhances the density of the material and, in turn, increases the material stiffness. Additionally, studies have shown that there remains a critical degree of saturation (80-85%) above which granular or coarse-grained materials undergo rapid degradation. For a typically consolidated cohesive soil, a strain softening behaviour is mostly observed under repeated loading with an increase in deviatoric stress (Khasawneh and Al-jamal, 2019). However, whether a normally consolidated cohesive soil will undergo hardening or softening depends on several factors:(i) cyclic stress ratio (ii) the over-consolidation ratio (OCR) (iii) the frequency of cyclic loading (iv) type of compaction effort (Seed and McNeill, 1958;Zhou and Gong, 2001;Narzary and Ahamad, 2021). A significant decrease in the resilient modulus can be observed for both coarse-grained and fine-grained soils with an increase in moisture content (Hicks and Monismith,1971; Barksdale and Itani, 1989;Dawson *et al.*, 1996 ; Heydinger *et al*., 1996 ;Khoury and Zaman, 2004). Under repeated loading, saturated granular materials and fine-grained soils experience the development of excess pore-water pressure. As pore-water pressure increases, the effective stress within the material decreases, resulting in a decrease in both strength and stiffness. Thom and Brown (1987) presented the argument that the presence of moisture in an aggregate assembly has a lubricating effect on the particles. According to their hypothesis, this lubrication would lead to increased deformation in the aggregate assembly, resulting in a reduction of the resilient modulus, even in the absence of pore-water pressure generation. To validate their hypothesis, Thom and Brown conducted a series of repeated load triaxial tests on crushed rock, where they varied the moisture content as one of the parameters. These tests, conducted with

drained conditions and loading frequencies ranging from 0.1 to 3 Hz, did not show any significant development of pore pressures for degrees of saturation up to 85%. Despite the absence of pore pressure, the test results demonstrated a reduction in the resilient modulus with increasing moisture content, which was attributed to the lubricating effect of water.

The increase in density leads to an increase in resilient modulus for coarse-grained soils (Robinson, 1974;Rada and Witczak, 1981; Kolisoja, 1997). With an increase in density due to additional compaction of the particulate system, the number of particle contacts per particle significantly increases. As a consequence, the average contact stress corresponding to a given external load decreases. This reduction in deformation within the particle contacts leads to an increase in the resilient modulus, as highlighted by Kolisoja (1997). In the case of fine-grained soils, a higher compaction effort may lead to a reduction in soil resilient modulus (Lee *et al*., 1997). A similar observation was made by Narzary and Ahamad (2021), who postulated that a reduction in resilient modulus was observed for samples compacted with heavy compaction, whereas an increase in modulus was observed under repeated loading for samples compacted using light compaction. Resilient modulus is also affected by the method of compaction. Usually, static compaction yields a higher modulus than the kneading method of compaction (Lee *et al*., 1997).

2.6 Laboratory evaluation methods of subgrade resilient modulus

Seed and McNeill (1958) previously demonstrated the distinctions between the initial tangent elastic modulus and resilient modulus. Their work highlighted the importance of creating laboratory methods that mimic real-world traffic loading conditions. Several methods have been developed and used over the years to characterize the resilient modulus. These methods have been discussed in brief in this section:

- **Repeated Load Triaxial Test (RLTT):** The RLT test equipment is used to perform the resilient modulus test, which involves subjecting compacted soil specimens to a series of cyclic loads to simulate traffic wheel loading. The AASHTO T307 (2003) provides detailed guidelines for specimen size, preparation, and data acquisition, which are currently followed to determine the resilient modulus. The stress levels used for testing the specimens are based on their location within the pavement structure, and each test comprises a

conditioning and testing phase. A total of 15 stress sequences are applied during the testing phase at three confining pressures (13.8 kPa,27.6 kPa and 41.4 kPa) and five deviatoric stresses (13.8 kPa, 27.6 kPa, 41.4 kPa, 55.2 kPa and 68.9 kPa). An analysis of the stress sequences shows that a triaxial soil specimen in an RLTT is subjected to a bulk stress (θ) in the range of 55-193 MPa and an octahedral shear stress of 6-33 MPa, which is the expected stress state of a soil element in a typical pavement structure. As the load applications are repeated, the deformation becomes entirely resilient. Finally, the resilient modulus is determined by calculating the ratio of the applied deviatoric stress to the resilient strain. The resilient modulus obtained from the RLTT is a medium to high-strain resilient modulus (Puppala, 2008).

- **Resonant Column Test:** Originally created in the 1930s for studying the dynamic properties of materials similar to rocks, the Resonant Column (RC) test has been consistently updated to facilitate the dynamic characterization of geomaterials. During the test, the specimens are placed on a pedestal with a securely attached top cap and torsional drive plate. The top end of the specimen is subjected to torsional excitation with a constant amplitude and varying frequency using the drive plate. By recording the variation of peak torsional displacement with frequency, a frequency response curve is obtained. From this, the small strain shear modulus is calculated and subsequently converted into the resilient modulus using constitutional relations.
- **Simple Shear Test:** The determination of resilient modulus in this method involves subjecting a soil specimen to shear stresses in both directions. This method is capable of mimicking the stress reversal phenomenon that occurs due to traffic wheel load movements, making it more representative of field conditions. However, a study by Barksdale *et al.* (1997) revealed that the stress paths of the soil specimen and in situ soil in the field differ. Additionally, there are limitations to this method, such as the stress-induced anisotropy of the soil specimen and the difficulty in applying uniform stress.
- **Free Free Resonant Column test (FFRC):** Initially intended for testing concrete (ASTM C215), the testing method was later adapted by Nazarian *et al.*(2003) to evaluate the characteristics of base and subgrade materials. The testing apparatus involves an instrumented hammer, which acts as an impulse

source to generate waves over a range of frequencies. Additionally, an accelerometer is used to capture the generated waves, while a data acquisition system is employed for data collection. The low strain elastic modulus is obtained by using the longitudinal resonant frequency, which is acquired from the frequency response function.

- **Hollow Cylinder test:** The hollow cylinder test is a highly accurate method for simulating actual field conditions by replicating the stress reversal phenomenon that occurs due to the movement of wheel loads, as demonstrated by Barksdale *et al.* (1997). This test involves placing a hollow cylindrical soil specimen inside a rubber membrane, which is then subjected to vertical, torsional, and radial stresses.

For the past thirty years, the RLTT test equipment has been primarily used to determine resilient modulus. While several other testing apparatuses have been described, there have been limited studies on their widespread implementation. Consequently, this review will mainly focus on the studies conducted using the RLTT to characterize subgrade modulus. Seed *et al*. (1962) conducted one of the earliest studies on the determination of resilient modulus, where they evaluated a variety of soils under different compaction conditions. Barksdale (1971, 1972) and Terrel *et al*. (1974) studied the loading pulse shape and duration of the RLT laboratory test. Hicks and Monismith (1971) documented the factors affecting resilient modulus determination for unbound bases, while Kalcheff and Hicks (1973) recommended potential stress sequence and ratios for granular base materials. In the first attempts to model resilient modulus, Thompson and Robnett (1976) proposed an arithmetic model for describing the resilient properties of fine-grained soils. Shook *et al*. (1982) used a bulk stress model to predict the resilient behavior of fine-grained soils, and Uzan (1985) introduced a two-parameter model incorporating both bulk and deviatoric stresses to simulate the resilient behavior of subsoils. Therefore, the initial studies on resilient modulus mainly focused on developing test procedures and equipment modifications for testing granular and fine-grained soils. Furthermore, preliminary studies on mathematical modelling of the resilient modulus as a function of stress state, and introducing empirical correlations based on simple empirical tests like CBR and UCS and basic soil properties to predict resilient modulus were also explored.

Following the recommendation of the AASHTO 1986 interim design guide, many DOTs initiated funded projects to use resilient modulus for subgrade characterization. In the 1990s and early 2000s, much research focused on developing different resilient modulus testing protocols, such as T-292, T-294 & P-46, and AASHTO T307, which consisted of a conditioning phase followed by a testing phase with varying stress sequences for both granular materials and subgrade soils. Differences between protocols included the position of LVDTs, with some suggesting internal LVDTs and others external measurements. Currently, the accepted protocol for conducting RLTT tests is the AASHTO T307 (2003).

By the early 2000s, the impact of moisture and density effects on the moduli of geomaterials had gained importance. As a result, attempts were made to quantify the effects of moisture on soil resilient modulus by incorporating moisture as a parameter in the constitutive models (Dunlap,1963 ; Seed *et al*., 1967; Uzan,1985; Pezo,1994). To account for moisture effects, the AASHTO Mechanistic-empirical Pavement Design Guide (MEPDG,2008) proposed an adjustment model to estimate changes in M_r with moisture content once the resilient modulus at a specific moisture content and stress state is known. However, it has been pointed out that instead of studying the resilient modulus variation with moisture content, it is more logical to relate resilient modulus to matric suction as a stress state variable (Zapata *et al.*, 2007). Strong correlation exists between the resilient modulus and matric suction of a soil (Khoury and Zaman, 2004; Yang *et al*., 2005; Fredlund *et al*.,1977 ; Vanapalli *et al*.,1999). Most research from 2010 onwards therefore focussed on development of constitutive models for incorporation of suction as a stress state variable using the principles of unsaturated soil mechanics (Parreira and Gonçalves, 2000; Yang *et al*., 2005; Liang *et al.*, 2008 ; Cary and Zapata, 2011). Section 2.7 presents the details of various resilient modulus prediction models in use in pavement engineering.

2.7 Resilient modulus prediction models

Conducting resilient modulus test using the RLTT can be a complicated and time-consuming process that may not be practical for less critical projects due to the associated costs, time and requirement of skilled manpower. Furthermore, it can be challenging to predict and replicate the in-situ conditions, particularly in terms of stress and moisture content, which adds to the complexity of using resilient modulus testing. Consequently, correlations with simple empirical tests and soil properties are sought

for estimating the resilient modulus, particularly in projects of less importance in MEPDG Level 2 or 3 design and analysis. A lot of research has been put into developing prediction models for the soil resilient modulus. The predictive resilient modulus models can be broadly divided into three categories: (i) Empirical correlations with simple tests (ii) Constitutive models (iii) Empirical correlations with soil basic properties. The empirical predictive models are developed by means of statistical regression and can prove to be a suitable tool for quick estimation of resilient modulus in the absence of RLTT, specially for projects of lesser importance. Further, the constitutive models are used to model the stress dependent non-linear behaviour of subgrade soils. The constitutive models are comprised of several constant parameters, which can be determined using a model fitting regression analysis using the RLTT data, or using empirical correlations relating soil basic properties to the model parameters. A brief overview of various resilient modulus models is presented in this section.

2.7.1 Empirical correlations of resilient modulus (M_r)

Correlations exist between empirical tests like the California Bearing Ratio (CBR) and basic tests like the unconfined compressive strength (UCS). However, CBR being the more familiar test among the pavement engineers, CBR based correlations are still widely used in many semi mechanistic design approaches, which require a single representative value of the M_r. The empirical correlations of the resilient modulus with the CBR are summarized in Table 2.1.

Table 2.1: Correlations of resilient modulus with California Bearing ratio (CBR)

Year	Author	Model
1962	Heukelom & Klomp	$M_r(MPa) = 10 * CBR\ for\ CBR \leq 5$ $M_r(MPa) = 17.6 * CBR^{0.64}$
1975	Green and Hall	$M_r(MPa) = 38 * CBR^{0.711}$
1987	Lister & Powell	$M_r(MPa) = 18 * CBR^{0.64}$
1997	Ayres	$M_r(MPa) = 21 * CBR^{0.65}$

Note: CBR: Soaked California Bearing Ratio in percentage; Mr= Resilient modulus of soil (MPa).

Several researchers, including Porter (1938,1950), Hight and Stevens (1982) and Fleming and Rogers (1995) have highlighted that the California Bearing Ratio (CBR) is more indicative of bearing capacity and strength rather than recoverable behavior of materials. Thompson and Robnett (1979) were unable to establish a suitable

correlation between CBR and resilient modulus (M_r). Hight and Stevens (1982) noted that CBR does not consistently correlate with either strength or stiffness, while Sukumaran *et al*. (2004) observed a significant variation in M_r values obtained using CBR, which is influenced by numerous factors. However, despite its various shortcomings, CBR is widely accepted, due to the ease of conducting the test and its cost effectiveness.

The UCS was shown to have a stronger correlation with M_r than the CBR by Hossain (2008). Over the years several empirical correlations have been developed for predicting the resilient modulus with the results of the unconfined compressive strength test, like the initial tangent modulus and the stress at 10% strain levels (Lee *et al*.,1997; Drumm *et al*.,1990 ; Hossain and Kim, 2015). More extensive models include soil basic properties along with the UCS parameters to predict the resilient modulus. In developing the correlations, the resilient modulus is usually calculated at a recommended stress state which is representative of the stress level usually experienced by subgrade in the field. The various UCS based models available in the literature are summarized in Table 2.2.

Table 2.2: Correlations of resilient modulus with the unconfined compressive strength

Reference	Model	Remarks
Thomson and Robnett (1979)	$M_r(ksi) = 3.49 + 1.9 * Initial\ tangent\ modulus$, R^2=0.53 $M_r(ksi) = 0.86 + 0.307 * Unconfined\ compressive\ strength$, R^2= 0.47	• Fine-grained soils from Illinois were used • Their analysis considered soil classification, including soil index properties, CBR, and stress-strain behaviour from the UC test.
Drumm *et al*. (1990)	$M_r(ksi) = 45.8 + 0.00052\left(\frac{1}{a}\right) + 0.188(q_u) + 0.45\ (PI) - 0.216(\Upsilon_d) - 0.25(S) - 0.15(P_{200})$, R^2= 0.83 Where, a = Initial tangent modulus of a stress–strain curve from UC tests (psi), q_u = Unconfined compressive strength (psi), PI = plasticity index (%), γ_d = dry unit weight (lb/ft^3), S = degree of saturation (%), and P_{200} = percent passing the Number (No.) 200 sieve.	• 11 soils from Tennessee with classifications ranging from CL, SM-CL, ML and SM were used for the study. • Resilient modulus tests were performed on each soil at two levels of saturation, using a deviator stress of 6 psi and a confining stress of zero. Subsequently, the same samples were used for conducting UC tests.
Lee *et al*. (1997)	$M_r = 695.4 * (S_{u1\%}) - 5.93 * (S_{u1\%})^2$, R^2= 0.97 *Where,* M_r = Resilient modulus at deviator stress deviator stress of 6 psi and a confining pressure of 3 psi. $S_{u1\%}$ = Stress at 1% strain from the Unconfined Compressive strength test	• Resilient modulus and UC tests were performed on three different Indiana clayey soils classified as A-4–A-6 (CL), A-6 (CL), and A-7-6 (CH) • Comparison was based on a representative state of stresses with a deviator stress of 6 psi and a confining pressure of 3 psi

Reference	Model	Remarks
Hossain *et al*. (2011)	$\frac{M_r}{P_a} = 2494.2 + 0.6(PI) - 8.66(P_{200}) + 16.4(GI) + 165.53\ (MCR) - 1961\ (DR) + 185.29(\frac{q_u}{P_a})$, $R^2 = 0.44$ Where, M_r = resilient modulus at deviator stress of 41.34 kPa (6 psi) and confining stress of 13.78 kPa (2 psi), P_a= Atmospheric pressure (kPa), *GI* = group index, *MCR* = Moisture content ratio (moisture content/optimum moisture content), and *DR* = Density ratio (dry density/maximum dry density).	• 130 soil samples (including A-4, A-6, and A-7-6) collected from Oklahoma were used to develop the correlation
Hossain and Kim (2015)	$M_r = 657 * (S_{u1\%}) - 6.75 * (S_{u1\%})^2$ M_r = Resilient modulus at deviator stress deviator stress of 6 psi and a confining pressure of 3 psi. $S_{u1\%}$ = Stress at 1% strain from the Unconfined Compressive strength test.	• UC tests were performed on twenty-nine bulk soil samples statically and dynamically compacted in the laboratory and collected from existing construction projects in nine Virginia DOT construction districts.

2.7.2 Constitutive models incorporating stress state

To model the stress dependent non-linear elastic behaviour of subgrade soils, several models have been proposed in the literature. This section provides a brief review of the various models developed over the years to characterize the stress dependent behaviour of the subgrade soils. The constitutive models may be categorized as two parameter or three parameter models depending on the number of unknown constants that need to be determined (Puppala, 2008).

- **Two parameter resilient modulus constitutive models**

The general form of the two-parameter resilient modulus constitutive model is shown in Equation 2.2.

$$M_r = k_1 P_a [f(c)]^{k_2} \qquad (2.2)$$

Where, *f(c)* is a stress attribute representing the state of stress in the material and is represented by either one of the following: deviatoric stress, confining stress, the bulk stress or the octahedral stress. Summary of various two parameter models available in the literature is summarized in Table 2.3.

Dunlap (1963) proposed a two-parameter model with confining stress(σ_3) as the stress attribute. The model is based on only the confining stress and does not consider the effect of deviatoric stress on the soil behaviour. Seed *et al*. (1967) in an improvement over the Dunlap's model, replaced the deviatoric stress with the bulk stress(θ). Although the effect of the deviatoric stress inherently considers the effect of bulk stress, the effect of deviatoric stress cannot be delineated from this model. Moossazadeh and Witczak (1981) used the deviatoric stress as the stress attribute in the two-parameter model. However, the effect of confining stress is neglected in this model. Wolfe and Butalia (2004) put forward a model based on the octahedral normal and shear stresses as the stress attribute. The formulations presented in Table 2.3 are normalized with the atmospheric pressure (P_a) and therefore the model parameters are dimensionless.

Table 2.3: Resilient modulus constitutive models with two model parameters

Year	Author	Model	Stress attribute
1963	Dunlap	$M_r = k_1 P_a (\frac{\sigma_3}{P_a})^{k_2}$	Confining stress
1967	Seed *et al*.	$M_r = k_1 P_a (\frac{\theta}{P_a})^{k_2}$	Bulk stress
1981	Moossazadeh and Witczak	$M_r = k_1 P_a (\frac{\sigma_d}{P_a})^{k_2}$	Deviatoric stress
2004	Wolfe and Butalia	$\frac{M_r}{P_a} = k_1 (\frac{P_a * \sigma_{oct}}{{\tau_{oct}}^2})^{k_2}$	Octahedral normal and shear stress

** Note: σ_3 = Confining stress; θ= Bulk stress = $(\sigma_1 + \sigma_2 + \sigma_3)$; P_a= Atmospheric pressure; σ_d= Deviatoric stress; σ_{oct}= Octahedral normal stress= $(\sigma_1 + \sigma_2 + \sigma_3)/3$; τ_{oct} =Octahedral shear stress=$\frac{1}{3}((\sigma_1 - \sigma_2)^2 + (\sigma_2 - \sigma_3)^2 + (\sigma_3 - \sigma_1)^2)$; k_1, k_2 are model constants.*

- **Three parameter resilient modulus constitutive models**

The general form of a three-parameter resilient modulus constitutive model is shown in Equation 2.3) (Ooi *et al*., 2006)

$$M_r = k_1 P_a [f(c)]^{k_2} [g(s)]^{k_3} \quad (2.3)$$

Where, $f(c)$ is a function of confinement and $g(s)$ is a function of shear.

The effect of confinement is usually represented by the minor principal stress (σ_3), the bulk stress(θ) and the octahedral normal stress (σ_{oct}), whereas the effect of shear stress state is accounted using the octahedral shear stress or the deviatoric stress. The most commonly used three parameter models are summarized in Table 2.4. The earliest three parameter model was introduced by Uzan (1985). The confinement in this model was considered using the bulk stress, whereas the shear stress was characterized by the deviatoric stress. Later, Witczak and Uzan (1988) replaced the deviatoric stress with the octahedral shear stress which was considered more representative of the stress state of the material. Since then, many variations of the three-parameter model have been proposed by several authors, which are summarized in Table 2.4.

Table 2.4: Three Parameter resilient modulus models

Year	Author	Model
1985	Uzan	$M_r = k_1 P_a (\frac{\theta}{P_a})^{k_2} (\frac{\sigma_d}{P_a})^{k_3}$
1988	Witczak and Uzan	$M_r = k_1 P_a (\frac{\theta}{P_a})^{k_2} (\frac{\tau_{oct}}{P_a})^{k_3}$
1994	Pezo	$M_r = k_1 P_a (\frac{\sigma_3}{P_a})^{k_2} (\frac{\sigma_d}{P_a})^{k_3}$
2002	Ni *et al.*	$M_r = k_1 P_a (1 + \frac{\sigma_3}{P_a})^{k_2} (1 + \frac{\sigma_d}{P_a})^{k_3}$
2004	Ooi *et al.*	$M_r = k_1 P_a (1 + \frac{\theta}{P_a})^{k_2} (1 + \frac{\sigma_d}{P_a})^{k_3}$ $M_r = k_1 P_a (1 + \frac{\theta}{P_a})^{k_2} (1 + \frac{\tau_{oct}}{P_a})^{k_3}$
2008	MEPDG	$M_r = k_1 P_a (\frac{\theta}{P_a})^{k_2} (1 + \frac{\tau_{oct}}{P_a})^{k_3}$

** Note: σ_3=Confining stress; θ=Bulk stress=$(\sigma_1 + \sigma_2 + \sigma_3)$; P_a=Atmospheric pressure; σ_d= Deviatoric stress; τ_{oct} = Octahedral shear stress =$\frac{1}{3}((\sigma_1 - \sigma_2)^2 + (\sigma_2 - \sigma_3)^2 + (\sigma_3 - \sigma_1)^2)$; k_1, k_2,,k_3 are model constants.*

The parameters k_1, k_2, and k_3 in the three-parameter model are constants, which depends on the soil type and the soil physical state. The coefficient k_1 is directly proportional to the Young's modulus and is always non-zero and positive. The constant k_2 is always positive, signifying hardening or stiffening of the material with increasing bulk or volumetric stress. The constant k_3 is always negative, indicating softening of the material with an increase in shear stress within the soil element. It must be noted that if the constants k_2 and k_3 are set to zero, the model reduces to a simple linear elastic model.However, whether the soil will exhibit hardening or softening under the simultaneous change in bulk and shear stress is a complex phenomenon and will depend on the nature of stresses and the magnitude of bulk and shear stresses within the specimen (George, 2004).

2.7.3 Constitutive models incorporating stress state and moisture

A compacted geomaterial within a pavement structure undergoes seasonal variations in moisture content due to several environmental factors like rainfall seepage and capillarity and remains in an unsaturated condition for most part of its service life (Han and Vanapalli, 2015). This variation of moisture has a significant impact on the strength and stiffness of the geomaterials which in turn effects the pavement performance over its design life (Huang, 1993; Yoder and Witczak, 1975). Many

researchers have focussed on implicitly considering the effect of moisture on the soil resilient behaviour by modifying the constitutive models. MEPDG (2008) proposed to correct the resilient modulus obtained from the three-parameter constitutive equation using the following relation (Equation 2.4).

$$\log\frac{M_r}{M_{ropt}} = a + \frac{b-a}{1+EXP\left(\ln\frac{-b}{a} + k_m\left(S - S_{opt}\right)\right)} \qquad (2.4)$$

Where, M_r/M_{ropt}= Resilient modulus ratio; M_{ropt}= Resilient Modulus at a reference condition; a = minimum of log (M_r/M_{ropt}); k_m= regression parameter; S = Degree of saturation at a reference condition. Parameter values a = −0.5934, b = 0.4, and k_m = 6.1324 for fine-grained soils, and parameter values a = −0.3123, b = 0.3, and k_m = 6.8157 for coarse-grained soils.

However, studies have confirmed that when considering resilient modulus variation with moisture content, it is more logical to relate resilient modulus to matric suction as a stress state variable. Strong correlations have been found between the resilient modulus and matric suction of a soil (Fredlund *et al*., 1977; Yang *et al*., 2005;.Vanapalli *et al*., 1999). Assuming the soil and pore water as incompressible, the stress state variables for unsaturated soils are net normal stress (σ-u_a) and matric suction ($\psi = u_a - u_w$) where u_a and u_w are pore air and pore water pressure respectively. Now, as the degree of saturation of the soil increases and the soil goes from unsaturated to fully saturated conditions, the matric suction also approaches zero. Therefore, matric suction is the most relevant state variable in unsaturated soil mechanics and is of utmost importance to a pavement engineer. Various models have been proposed in the literature over the last few decades to describe the M_r-ψ relationship. A comprehensive review of the various models can be found in Han and Vanapalli (2016). They categorized the correlations incorporating matric suction into the following three types: Category A: Empirical correlations with resilient modulus (M_r); Category B: Matric suction incorporated into confining and shearing stresses; Category C: Matric suction incorporated as independent stress state variable. A brief review of some widely accepted models is presented in this section.

Parreira and Goncalves (2000) conducted a study on lateritic subgrade soil and investigated the effect of moisture content and soil suction on the resilient modulus. They proposed a simple relationship between the M_r, deviator stress, and matric suction

level (ψ_m) and suggested a set of model parameters using RLT testing data. The simplified Yang *et al*. (2005) model is another M_r model for unsaturated soils that is a function of deviator stress and matric suction. Liang *et al*. (2008) proposed a model based on the effective stress approach which accounts for both the confinement and octahedral shear stress and incorporates the effect of matric suction into the effective stress. Sawangsuriya *et al*. (2009) proposed a five-parameter power function model for the resilient modulus using a total stress approach and a semi-logarithmic function that relates variation of the M_r to matric suction changes. Cary and Zapata (2011) suggested an enhanced matric suction-dependent resilient modulus model, which is also based on the Universal Model with an additional term incorporating the effect of matric suction into the resilient modulus. Ng *et al*. (2013) suggested a similar model to the Cary and Zapata (2011) model but normalized the suction parameter in the last term of the equation with the net bulk stress instead of the constant atmospheric pressure. Furthermore, their model does not account for the pore-water pressure effects under saturated conditions and therefore is not as comprehensive as the Cary and Zapata (2011) model. Table 2.5 describes the commonly used constitutive models based on suction effects.

Table 2.5: Resilient modulus models incorporating moisture effects (matric suction)

Reference	**Model**
Parreira and Goncalves (2000)*	$M_r = k_1 P_a {\sigma_d}^{k_2} \psi_m^{k_3}$
Yang *et al*. (2005)**	$M_r = k_1 P_a (\sigma_d + \chi\psi_m)^{k_2}$
Liang *et al*. (2008)**	$M_r = k_1 P_a (\frac{\theta + \chi\psi_m}{P_a})^{k_2} (\frac{\tau_{oct}}{P_a} + 1)^{k_3}$
Sawangsuriya *et al*. (2009)***	$M_r = k_1 P_a (\frac{\theta - 3k_4}{P_a})^{k_2} (\frac{\tau_{oct}}{P_a} + k_5)^{k_3}$ $M_{r_{opt}} = \frac{M_{rs}}{M_{rs,opt}} = c + d\ log\psi_m$
Cary and Zapata (2011)***	$M_r = k_1 p_a \left(\frac{\theta_{net} - 3\Delta u_{w-sat}}{p_a}\right)^{k_2} \left(\frac{\tau_{oct}}{p_a} + 1\right)^{k_3} \left(\frac{\psi_m - \Delta\psi_m}{p_a} + 1\right)^{k_4}$
Ng *et al*. (2013)**	$M_r = k_1 p_a \left(\frac{\theta_{net}}{p_a}\right)^{k_2} \left(\frac{\tau_{oct}}{p_a} + 1\right)^{k_3} \left(\frac{\psi_m}{\theta_{net}} + 1\right)^{k_4}$

Note: **Category A; **Category B ;***Category C; θ=Bulk stress=$(\sigma_1 + \sigma_2 + \sigma_3)$; ; P_a=Atmospheric pressure; σ_d=Deviatoric stress; τ_{oct}=Octahedral shear*

stress=$\frac{1}{3}((\sigma_1-\sigma_2)^2+(\sigma_2-\sigma_3)^2+(\sigma_3-\sigma_1)^2)$; ψ_m = *Initial soil suction* ;$\Delta\psi_m$= *Relative change of soil suction with respect to* ψ_m *due to build-up of porewater pressure under unsaturated conditions;* χ= *Bishop's effective stress parameter;* θ_{net} = *Net bulk stress* = θ_b-$3u_a$; $\Delta u_{w\text{-}sat}$ = *Build-up of pore-water pressure under saturated conditions.*

2.7.4 Empirical correlations of resilient modulus (M_r) with basic soil properties

Soil properties significantly influence the resilient behaviour of soils. Therefore, it is logical to correlate the resilient modulus with basic soil properties. Over the past decades, several studies have been carried out to correlate the resilient modulus with soil properties (Rahim, 2005; Rahim and George, 2004; George, 2004). Primarily, the resilient modulus is correlated to soil properties in two ways: (i) Resilient modulus correlated directly to the resilient modulus at a reference stress state (ii) Soil properties correlated to the constitutive model parameters.

- **Soil properties correlated directly to the resilient modulus**

  Rahim (2005) correlated the resilient modulus to basic soil properties based on twelve pavement sections of Mississippi at stress levels of 37 kPa (deviator stress) and 14 kPa (confining pressure). Two separate equations were proposed for fine grained and coarse-grained soils (Equations 2.5 and 2.6) as shown. The results were validated by comparison with an independent set of soil data.

$$M_r = 17.29\ [\left(\frac{LL}{w_c+1}*\Upsilon_{dr}\right)^{2.18}+(\frac{\#200}{100})^{-0.609} \quad (2.5)$$

$$M_r = 324.14\left(\frac{\Upsilon_d}{w_c+1}\right)^{0.8998}(\frac{\#200}{\log C_u})^{-0.4652} \quad (2.6)$$

  Rahim and George (2004) conducted a study to examine the significance of soil index properties in predicting the resilient modulus of soils in Mississippi. They proposed two equations, one for fine-grain soils (Equation 2.8) and another for coarse-grain soils (Equation 2.9). The equation for fine-grain soils was developed based on 12 soils from Mississippi and further validated with eight additional soils from the same region.

Fine-grained soil:

$$M_r(MPa) = 16.75\ ((\frac{LL}{w_c \Upsilon_{dr}})^{2.06} + (\frac{P_{200}}{100})^{-0.59} \quad (2.8)$$

Coarse grain soil:

$$M_r(MPa) = 307.4(^{\Upsilon_{dr}}/_{w_c})^{0.86}(^{P_{200}}/_{100})^{-0.59} \quad (2.9)$$

- **Soil properties correlated to model coefficients**

  While estimating M_r from soil physical properties allows for capturing seasonal variations in M_r based on changes in material properties, it does not account for the effects of stress sensitivity. To address this, researchers such as Von Quintus and Killingsworth (1998), Dai and Zollars (2002), Santha (1994) and Mohammad *et al*. (1999) have proposed prediction models for M_r. These equations involve regressing coefficients of selected constitutive equations against soil physical properties to account for the influence of stress sensitivity and physical properties on design M_r. George (2004) presented a detailed comparison of four different studies carried out to correlate the constitutive model coefficients to the soil basic properties. Four studies were considered for the evaluation were: Long Term Pavement Performance (Amber and Von Quintos, 2002), Georgia department of transportation research study (Santha, 1994), Minnesota Road research project (Dai and Zollars, 2002), Louisiana study (Mohammad *et al*.,1999). The results concluded that being developed from an extensive database of soils, the LTPP equations are the most comprehensive of the four models compared. It has the potential to predict M_r of a range of soils with a wide geographical coverage. The LTPP equations correlates the basic properties of soils with the MEPDG model constant parameters as under (Equations 2.10-2.18):

Coarse grained soil:

$$k_1 = 3.2868 - 0.0412\ P_{3/8} + 0.0267\ P_4 + 0.0137\ (\%Clay) + 0.0083\ LL - 0.0379\ w_{opt} - 0.0004\ \gamma_s \quad (2.10)$$

$$k_2 = 0.5670 + 0.0045\ P_{3/8} - 2.98x10\text{-}5\ P_4 - 0.0043\ (\%Silt) - 0.0102\ (\%Clay) - 0.0041LL + 0.0014\ w_{opt} - 3.41x10\text{-}5\ \gamma_s - 0.4582\ (\gamma_s / \gamma_{opt}) + 0.1779\ (w_c/w_{opt}) \quad (2.11)$$

$$k_3 = -3.5677 + 0.1142\ P_{3/8} - 0.0839\ P_4 - 0.1249\ P_{200} + 0.1030\ (\%Silt) + 0.1191(\%Clay) - 0.0069LL - 0.0103\ w_{opt} - 0.0017\ \gamma_s + 4.3177(\gamma_s / \gamma_{opt}) - 1.1095\ (w_c/w_{opt}). \quad (2.12)$$

Fine grain silty soils:

$$k_1 = 1.0480 + 0.0177\ (\%Clay) + 0.0279\ PI - 0.0370 w_c \quad (2.13)$$

$$k_2 = 0.5097 - 0.0286\ PI \quad (2.14)$$

$$k_3 = -0.2218 + 0.0047\ (\%Silt) + 0.0849\ PI - 0.1399\ w_c \quad (2.15)$$

Fine grain clayey soil:

$$k_1 = 1.3577 + 0.0106\ (\%Clay) - 0.0437\ w_c \quad (2.16)$$

$$k_2 = 0.5193 - 0.0073\ P_4 + 0.0095\ P_{40} - 0.0027\ P_{200} - 0.003\ LL - 0.0049\ w_{opt} \quad (2.17)$$

$$k_3 = 1.4258 - 0.0288\ P_4 + 0.0303\ P_{40} - 0.0521\ P_{200} + 0.0251\ (\%Silt) + 0.0535\ LL - 0.0672\ w_{opt} - 0.0026\ \gamma_{opt} + 0.0025\ \gamma_s - 0.6055\ (w_c / w_{opt}) \quad (2.18)$$

Where

M_r = Resilient Modulus, MPa;

$P_{3/8}$ = Percentage passing sieve #3/8;

P_4 = Percentage passing #4 sieve;

P_{40} = Percentage passing #40 sieve;

w_c = Moisture content of the specimen, %;

w_{opt} = Optimum moisture content of the soil, %;

γ_s = Dry density of the sample, kg/m^3;

γ_{opt} = Optimum dry density, kg/m^3

2.8 Field evaluation methods of subgrade resilient modulus

Field evaluation of subgrade modulus has gained tremendous importance with the introduction of modulus-based quality assurance protocols (Nazarian *et al*., 1996; Puppala, 2008). Further, in implementation of projects which require rehabilitation and widening of pavements, the subgrade and base modulus is mostly determined by conducting in situ tests. The in-situ modulus determination methods can be grouped into two categories: (i) Non-Destructive tests (ii) Intrusive test methods. The non-destructive methods usually employ back calculation routines to estimate the stiffness characteristics of pavement layers based on deflection measurements using an impulse load. Whereas, the intrusive methods are destructive in nature and consists of measuring the penetration resistance of the pavement layers. A brief overview of various non-destructive and intrusive test methods is presented in this section.

The various Non-Destructive test methods for in situ determination of modulus are as under:

- ***Dynaflect*:** The Dynaflect is a lightweight two-wheeled trailer that comes equipped with an automated system for data acquisition and control (Puppala,2008). Dynamic loads of 227 kg are generated by means of two counter-rotating eccentric steel weights rotating at a constant frequency of 8 Hz. The corresponding pavement deflections are measured using five geophones placed at intervals of 1 ft. The method of pavement deflection measurement using Dynaflect is standardized by AASHTO T256 and ASTM 695.

- ***Falling Weight Deflectometer (FWD):*** The Falling Weight Deflectometer applies an impulse load by dropping a weight mass from a specified height and then measures the corresponding deflections from a series of geophones placed over the pavement surface (Nazzal *et al*.,2004; Rahim and George, 2003; (Siddharthan *et al*., 1992). Deflection profiles are then analyzed using theoretical models of distinct constitutive behaviors. The Pavement layer moduli are initially assumed and deflections backcalculated using different algorithms. When predicted deflection patterns and magnitudes matches with the measured, the assumed moduli are reported as moduli of the pavement layer.

The FWD measures the secant modulus for the bituminous, granular and top subgrade layers, whereas the initial tangent modulus for a subgrade at a higher depth (Nazarian *et al*., 1996)

- ***Geogauge:*** A Geogauge is a portable instrument that measures the stiffness properties of pavement layers by inducing small displacements to the soil by means of a harmonic oscillator operating over a frequency of 100 to 196 Hz (Lenke *et al*., 2001). Sensors are used to measure both the resulting force and displacement. Stiffness is determined by averaging stiffness at 25 different frequencies.

- ***Seismic Pavement Analyzer (SPA/PSPA):*** The PSPA modulus is either directly measured or back calculated using a small seismic source (Nazarian and Baker ,1995; Nazarian *et al*.,2003; Nazarian, 2005). It consists of two accelerometers and a source packaged into a hand-portable system. The SPA lowers transducers to the pavement and digitally records surface deformations induced by a large or a small hammer. The source produces an impulsive impact generating stress waves which are than captured by the accelerometers. The modulus of the pavement layer is calculated from the phase plot generated. The SPA/PSPA determines the Young's Modulus of Elasticity and Shear modulus. The measured modulus corresponds to the initial tangent modulus since the impact is very small (Small strain moduli) (Nazarian *et al*., 1997).

- ***Light Weight Deflectometer (LWD):*** Similar to FWDs, the LWDs use a dynamic force to create deflection of layers, which are then measured by means of accelerometers or velocity transducers. The modulus can be either directly estimated or back calculated. The portability and ease of use has led to the LWD receiving significant attention from DOTs across the world. The ASTM has standardized the LWD testing procedure in two separate standards: ASTM 2583 and ASTM 2835. The former deals with the LWD apparatus with a load cell, whereas the second standard deals with the LWDs without a load cell and an assumed peak force value. The test consists of subjecting the soil to a pulse load applied via a disk-shaped steel or aluminium plate. The loading mechanism consists of a drop weight, that, once released, falls along a rod until it hits the plate, thus creating a load impulse. The plate and soil now get displaced as a single unit, until at a point at which the plate and soil system detaches. This

displacement is recorded by either a velocity transducer or an accelerometer. The modulus is then calculated based on an equation derived using the Boussinesq's elastic solution for the case of a rigid or flexible plate resting on an elastic half space. The Light Weight Deflectometer measures the composite elastic modulus of the pavement layers within the depth of influence (Puppala, 2008).

The various intrusive methods of in situ determination of resilient modulus are as under:

- ***Dynamic Cone Penetrometer (DCP):*** In the DCP test, a slender shaft is driven into the compacted subgrade using a sliding hammer of weight of 10 Kg. The penetration of the shaft at each hammer drop is measured and a parameter known as the penetration index is calculated, which is then empirically correlated to the subgrade resilient modulus (Hassan, 1996; George and Uddin , 2000; Mohammad *et al*., 2007). The DCP is the most widely used intrusive methods and is standardized by ASTM D6951-03.
- ***Quasistatic Cone Penetrometer:*** Cone penetrometer tests provide two independently measured parameters, the cone tip resistance (q_c) and the cone friction resistance (f_s) along with the pore water pressure (u_t) at one or more locations, measured when the cone penetrometer is fitted with piezometers. All the three parameters can be used to classify soil strata and determine various properties using soil stiffness. Empirical correlations are available in the literature for calculation of soil resilient modulus from the cone penetrometer data (Gudishala, 2004).
- ***Pressuremeter:*** Pressure meter tests may be either stress-controlled or strain-controlled. In stress-controlled mode, the pressure is increased on the membrane, and corresponding displacements are noted. In the strain-controlled mode, the rate of expansion of the membrane is controlled by constant volumetric increments and the corresponding pressures are monitored. The pressure strain profiles of the test are than used to determine stiffness properties of the soil.
- ***Plate Load Test***: The Plate Load test is conducted by incrementally loading a circular plate (Usually 30 cm in diameter) in contact with the layer to be tested and measuring the corresponding deformations. Moduli is than calculated by

means of the load deformation curve obtained from the test. The measured modulus is usually referred to as a composite modulus as the depth of influence extends more than one layer (Abu-Farsakh *et al.*, 2003).

- ***Dilatometer:*** Borden *et al*. (1985) used the dilatometer (DMT) field data to obtain the resilient modulus of the soil. A unique relationship was obtained between the dilatometer modulus with the resilient modulus and the initial tangent modulus. However, no further studies have been reported for the use of dilatometer for resilient modulus evaluation.

Various devices that have been used for in situ subgrade stiffness evaluation have already been summarized in this section. The Geogauge, introduced by Humboldt manufacturing company in the early 2000s, provides stiffness values of subsoils by measuring deformations produced by applying a harmonic load, that is valid for medium levels of shear strains. A comprehensive evaluation of geogauge was conducted by Lenke *et al*. (2001, 2003). The geogauge was found to be very sensitive to moisture and density variations. Good correlations of the measured moduli were obtained with the FWD backcalculated modulus (Nazzal *et al*., 2004). However, limited use of the Geogauge has been reported across the Transportation agencies for QC/QA work and pavement design.

Another NDT device, the Seismic Pavement analyzer (SPA), was analyzed extensively by Nazarian and Baker (1995); Nazarian *et al*.(2003) and Nazarian (2005) for its use in estimating subsoil stiffness. The SPA uses a seismic source to generate vibrations in the material and digitally records the surface deformations. Although initial studies showed a considerable initial promise, the use of the SPA for QC/QA works and estimating moduli for pavement design have been limited. In recent studies, significant efforts have been put into quantifying the effect of moisture and density on the PSPA modulus (Mazari *et al*., 2014; Tamrakar and Nazarian, 2016). However, more research is needed for the widespread implementation of the PSPA in determining the moduli of subsoils.

Several studies have focussed on the use of the FWD for the determination of subsoil properties using backcalculation routines. Choubane and McNamara (2000) assessed the feasibility of using FWD data to predict the moduli of subsoils. Based on

300 field FWD studies, the following Equation 2.19 was developed and recommended for pavement design:

$$E_{FWD} = 0.03764 * (P/d_r) \quad (2.19)$$

Where

E_{FWD} = Subgrade modulus interpreted from FWD; P= Applied load in lbs;
d_r= Distance measure at a radial distance r.

Ping *et al*.(2002) studied and compared in situ FWD determined moduli with laboratory resilient modulus for similar stress conditions. Results showed that the backcalculated E_{FWD} is about 1.65 times higher than the laboratory resilient modulus. This was similar to the AASHTO recommended correction factor of 0.5 to 0.33 to be applied to the E_{FWD} to obtain laboratory M_r value for use in pavement design. Rahim and George (2003) however, stressed the need to revise this factor. The objective of their research was to determine the ratios of resilient modulus values obtained from field and laboratory methods by conducting FWD tests directly on compacted subgrades. The findings also showed lesser variations between measured and predicted moduli, and low strain moduli obtained should be further scrutinized. Malla and Joshi (2006) conducted a comparative analysis and tried to correlate the FWD and laboratory resilient modulus. The researchers concluded that no definite relationship was observed between the FWD and laboratory resilient modulus. However, the field moduli were, in general, higher than the laboratory resilient modulus. They recommended another approach in which M_r was calculated using bulk and octahedral stresses representative of the subgrade soil at the particular depth. Further, the type of backcalculation routine used for estimating the subgrade moduli could also lead to variability in the estimated modulus.

A miniature version of the FWD, the LWD, or the PFWD has garnered considerable interest from the DOTs for its ease of use and simplicity of operation. In one of the earliest studies, Siekmeier *et al*. (2000) correlated the results of LWD and geogauge with FWD backcalculated modulus for base and subgrade materials. It was reported that both the moduli correlated well with the FWD backcalculated modulus. From the early 2000s till 2010, most of the literature was focussed on evaluating the adequacy of the LWD device for in situ evaluation of modulus of geomaterials (Fleming *et al*.,2007; Nazzal *et al*.,2004;Vennapusa and White,2009). This included establishing

correlations with already established methods like the FWD, correlating modulus obtained from different LWDs (of various make) and evaluating the factors affecting LWD modulus. A lot of LWD devices had flooded the market during this period, each manufacturer coming up with different specifications and principles of operation. A comprehensive review of various LWD devices and the influence of LWD parameters on the measured modulus can be found in Venupasa and White (2009). The critical parameters influencing the measured modulus were found to be the size of loading plate, Plate contact stress and plate rigidity. However, ASTM standardized the LWD test in two different standards (ASTM E2385 and ASTM E2583). The former applies to LWDs without a load cell, where the impact load is estimated from the properties of the falling mass and the drop height. At the same time, the latter is applicable for LWDs with an inbuilt load cell to measure the applied load and measures the deflection of the soil layer through a sensor placed within the centre of the plate. Several studies have investigated the stress conditions prevailing under an LWD via numerical modelling and also validated experimentally through instrumentation (Mooney and Miller, 2009; Bilodeau and Doré,2014). Results showed that in situ stress distribution below the LWD is a function of the soil type. It was also found that the influence depth for an LWD varies from 0.9-1.1 times the plate diameter. To employ the LWD as a quality control tool, the target modulus is required. Several studies have been undertaken by various DOTs to estimate the target modulus. Siekmeier *et al*.(2009) derived the LWD target modulus based on the Grading Number and field moisture content by testing the local materials in Minessotta. A range of soils ranging from non-plastic to a plasticity index of 34 and moisture content varying from 10% to 25 % was used to develop the target values. Several other studies and Pilot projects were dedicated to determining the target value of LWD for use in quality control and assurance (White *et al*.,2007; Schwartz *et al*., 2017) based on similar procedures. In general, all these methods were based either on experience, some form of laboratory test, or test strips. To bridge this gap between design parameter and construction quality control, Mazari *et al*. (2014) put forward a mechanistic quality control method for the determination of the target modulus. Several studies have used radial sensors to obtain the deflection bowl from LWD load and back calculate the moduli of pavement layers (Senseney and Mooney, 2010). Good correlations were obtained for the back calculated moduli for granular layers and subgrade soils with the laboratory resilient modulus at similar stress of state and with back calculated FWD moduli. Further, good correlations of LWD modulus

with laboratory CBR and DCPT was observed by George *et al*. (2009). White *et al*. (2007) attempted to correlate LWD predicted moduli with the with the resilient moduli determined from laboratory testing on the Shelby tube samples. As LWD modulus is a function of total strain and the laboratory resilient modulus is calculated from the resilient strain, both moduli were not considered the same. Instead, a secant modulus was derived from the permanent strain data and the resilient modulus was calculated from the recoverable strain, which was then separately correlated to the LWD modulus. Good correlations were obtained between the secant modulus and LWD modulus. Empirical correlations were developed between the LWD modulus and the resilient modulus. In a recent study, Mousavi *et al*. (2017) evaluated the empirical relationship suggested by White *et al*. (2007) and found that the empirical model underpredicted the laboratory resilient modulus, and therefore more research is needed to use the LWD and resilient modulus interchangeably. Based on the studies carried out, some of the most popular correlations between the LWD modulus and the laboratory resilient modulus is summarized in Table 2.6.

Table 2.6: LWD modulus correlations with resilient modulus

Reference	Model	Remarks
White *et al*. (2007)	$M_r = \frac{(E_{LWD} + 45.3)}{1.24}$	E_{LWD} calculated using an assumed Poisson's ratio of 0.35 and a shape factor of π/2 and 2 for cohesive and cohesionless soils and correlated to resilient modulus at a confining pressure = 41.4 kPa and Deviator stress= 69 kPa
Mohammad *et al*. (2008)	$M_r = 27.75 * E_{LWD}^{0.18}$	E_{LWD} calculated using an assumed Poisson's ratio of 0.4 and a shape factor of π/2 and 2 for cohesive and cohesionless soils and correlated to resilient modulus at a confining pressure = 13.8 kPa and Deviator stress= 41.4 kPa
Mousavi *et al*.(2017)	$k_i = C_1 + C_2(\frac{\sigma}{\delta})$ i = 1,2,3	The ratio of applied stress to deflection (σ/δ) of the LWD was empirically related to the MEPDG constitutive model coefficients k_1,k_2,k_3.

Note: E_{LWD}= LWD Elastic Modulus; M_r= Resilient modulus; σ= Applied Stress applied by the LWD (kPa); δ= Surface deflection.

Although considerable efforts have been put into using the LWD as a quality control tool, little to no efforts have been put into evaluating the LWD modulus for use in mechanistic designs. Puppala (2008) pointed out the need to compare and assess the LWD modulus to laboratory resilient modulus w.r.t a reference stress state representative of field loading conditions. Further research on the interpretation of LWD moduli will help in the implementation of the LWD moduli in pavement design resilient modulus prediction.

Among the intrusive methods, the most widely accepted method for stiffness estimation is the Dynamic Cone Penetrometer (DCP). Many researchers have attempted to correlate the DCP Index (DCPI) with the resilient modulus as specific stress levels. Table 2.7 presents a summary of the empirical models correlating the DCPI with the laboratory resilient modulus.

Table 2.7: DCP index correlated to the resilient modulus

Reference	Model	Suitable soil type
Hassan (1996) *	$M_r = 7013.065 - 2040.783\ ln(DCPI)$	Cohesive
George and Uddin (2000)	$M_r = 235.3(DCPI) - 0.48$	Coarse -grained
Herath *et al*. (2005)	$M_r = 16.25 + \frac{978.24}{DCPI}$	Cohesive
Mohammad *et al*. (2008)	$M_r = \frac{1045.9}{\text{DCPI}^{1.096}}$	Cohesive

*Note: M_r: Resilient Modulus (MPa); DCPI : DCP index in mm/blow; *Mr: Resilient Modulus (Psi); *DCPI: DCP index in Inches/blow.*

2.9 Resilient modulus characterization for mechanistic pavement design

The preceding sections have discussed the functional and operational distinctions between the initial tangent modulus, secant modulus, and resilient modulus. In the context of a typical pavement structure, the resilient modulus is considered to be a more accurate representation of material behavior due to dynamic wheel loading. Resilient Modulus (M_r) is a stress dependent parameter, which varies with the stress state of the subgrade material. A typical soil element within the subgrade is acted upon by the wheel load stresses and the confinement pressure due to the overlying layers as shown in Figure 2.4.

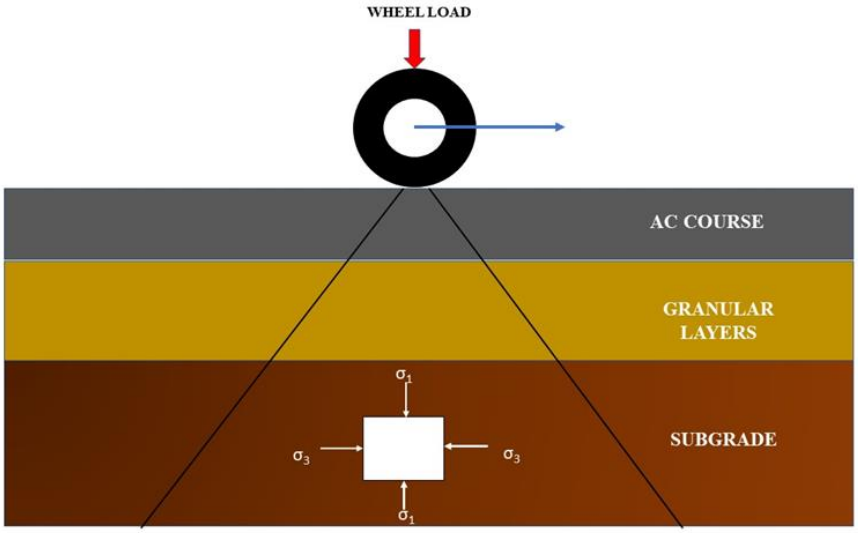

Figure 2.4: State of stress of a subgrade element within the pavement structure

Therefore, the stress state of a soil element within the subgrade varies from point to point, and so does the modulus. However, the Level 2, Level 3 of MEPDG and most mechanistic design methods require a specific representative resilient modulus value as input (Shell Pavement Design Method, 1978; Austroads, 2012; IRC 37,2002; IRC 2012; IRC,2018). The stress-dependent constitutive models used for resilient modulus estimation relies on stress calculation that is determined by the pavement structure, traffic load, and the subgrade's resilient modulus. Therefore, a question arises as to which stress state should be used for calculation of a single representative modulus for pavement design. Different stress combinations have been used by various researchers for such estimations. Using an elastic analysis of a typical pavement structure, various stress states have been recommended in the literature for input in resilient modulus constitutive models for calculation of representative resilient modulus as summarized in Table 2.8.

Table 2.8: Recommended stress levels for resilient modulus calculation

Reference	Stress input recommended
Elliott (1992)	Confining pressure (σ_3) = 0 Deviatoric stress (σ_1) = 41.6 kPa
Huang (1993)	Confining pressure (σ_3) = 14 kPa Deviatoric stress (σ_1) = 37 kPa
Hossain (2008)	Confining pressure (σ_3) = 13.8 kPa Deviatoric stress (σ_1) = 41 kPa
MEPDG (2008)	Bulk stress (θ) = 85 kPa Octahedral stress (τ_{oct}) = 21 kPa

In case of projects which requires widening or rehabilitation of pavements, the design resilient modulus is usually obtained using the DCP, the FWD or the LWD. As the in-situ evaluation of subgrade modulus usually yields the low strain elastic moduli, appropriate empirical correlation as discussed in section 2.7 must be used to obtain the design resilient modulus at the recommended stress level. For MEPDG Level 1 characterization of subgrade soils, the constitutive model parameters k_1, k_2, k_3 are determined using the RLTT apparatus and fed as an input into an FEM model to calculate the pavement responses. Therefore, the subgrade resilient modulus for mechanistic pavement design can be characterized in two ways: (i) Single representative modulus at recommended stress levels (ii) Non-linear stress-based characterization in which the constitutive model parameters k_1, k_2, k_3 are used as inputs.

2.10 Alternate cost-effective methods of subgrade modulus determination

The repeated load triaxial test (RLTT) although widely used, has limitations related to its cost and requirement of skilled man power. This prompted the researchers to explore alternate methods of characterizing the soil resilient modulus using simple test methods like the static triaxial test, the oedometer test and the CBR test. This section provides an overview of the various alternate methods used for the purpose of resilient modulus characterization.

2.10.1 Resilient modulus determination using the static triaxial test apparatus

Kim *et al*. (2001) proposed a methodology to predict the resilient modulus of subgrade soils using a conventional triaxial apparatus. The development of the alternative testing method involved a comprehensive investigation into the influence of strain amplitude, loading frequency, mean effective stress, and number of loading

cycles on the resilient modulus (M_r) of subgrade soils. Deformational characteristics were assessed through various tests, including cyclic M_r, static Triaxial, and resonant column - torsional shear tests. Synthetic specimens with predetermined stiffness values, spanning from soft subgrade soils to subbase materials, were fabricated and the testing systems used in the study were appropriately calibrated. The proposed alternative M_r testing procedures were formulated based on the deformational characteristics specific to subgrade soils. To validate the reliability of the proposed test method, the moduli obtained using the alternative M_r testing approach were compared against those obtained through standard M_r tests.

2.10.2 Resilient modulus determination using the repeated load oedometer test

Nagula *et al*. (2018) used a repeated loading procedure using the conventional oedometer test used to measure the consolidation of the soil. In the conventional oedometer test, incremental axial loads are applied to the sample and the resulting deformations are measured. In contrast, the repeated-load oedometer test involves applying incremental axial loads to achieve a specific maximum load, unloading the sample, and recording the corresponding deformations that are recovered during unloading. Tests were conducted using two modes: Load controlled and deformation controlled. In the load-controlled tests, the material was loaded up to the maximum axial load in incremental steps of 0.2 kN, after which it was unloaded to 10% of the maximum axial load. In the displacement-controlled test, the sample underwent deformation at a constant rate of 0.08 mm/min until the maximum axial load was reached for each sequence. Once the target axial load was attained, the test was halted, and the sample was unloaded at the same rate until the load reached a base load value equivalent to 10% of the maximum axial load. Deformations were measured at 15-second intervals during both the loading and unloading stages. Both tests involved applying two cycles of loading and unloading for each axial stress, and the modulus value was determined by evaluating the second reloading curve in both tests. The calculated modulus was then verified by comparing with the results of a numerical analysis of the test using the hardening soil model.

2.10.3 Repeated Load CBR (RLCBR) test

Although attempts have been made to characterize the resilient behaviour of the subgrade soils using the triaxial and oedometer tests, due to its familiarity among the pavement engineers, the Repeated load CBR(RLCBR) test remains the most widely

researched and explored. The repeated load CBR (RLCBR) test was first utilized in the 1980s by Loach (1987) at Nottingham University to conduct tests on reconstituted soils with known effective stress and stress history. The RLCBR test involves repetitive loading of a conventional CBR test specimen while measuring the corresponding resilient deformation using an LVDT in a data acquisition system. Opiyo(1995) showed that Equation 2.20 can be utilized to determine the surface deflection, *u*, of a quasi-static infinite half-space under a circular load based on elastic theory.

$$u = \frac{f\,(1-\nu^2)\sigma r}{E} \tag{2.20}$$

Where

ν = the Poisson's ratio

σ= the stress at the surface

r = the radius of the circular load

u = Deformation

E = The elastic modulus of the material

f = a factor which is: 2 for a uniformly distributed load,π/2 for a stiff plate stress distribution

u = Deformation

The stress distribution produced by the steel plunger in a CBR test is identical to that of the stiff plate since the deflection at each point beneath the plunger is uniform. Thus, the equation for the RLCBR test is similar to Equation 2.20, except for the factor f, and the Poisson's ratio and displacement exponent. This variation is due to the fact that the CBR test is conducted on limited dimension specimens confined by a stiff steel that imparts high confinement stress to the material (Opiyo 1995). Consequently, Equation 2.20 was modified accordingly to Equation 2.21.

$$E = \frac{k_1\,(1-\nu^{k_2})\sigma_p r}{u^{k_3}} \tag{2.21}$$

Where

k_1, k_2, k_3 = Model constants

ν = The Poisson's ratio

σ_p= The Plunger stress

r = The plunger radius

E = The equivalent resilient modulus

u = Resilient Deformation

Equation 2.21 formed the basis for resilient modulus estimation using the RLCBR test. Araya (2011) termed the RLCBR resilient modulus as the equivalent modulus because being a complex triaxial system, the stiffness of the soil specimen in a CBR mould varies along its depth and the calculated modulus is representative of the entire CBR specimen. Several authors have attempted to calibrate the model parameters k_1, k_2 and k_3 using either numerical modelling or experimental methods (Araya, 2011; Hao and Pabst, 2021; Narzary and Ahamad, 2021). The various proposed models in the literature are summarized in Table 2.9.

Table 2.9: Models for calculating the RLCBR equivalent modulus

Author	Model
Opiyo (1995) (Without friction)	$M_r = \frac{1.797\ (1-\nu^{0.889})\ \sigma_p r}{w^{1.098}}$
Opiyo (1995)/ Molenaar (2007) (With Friction)	$M_r = \frac{1.375\ (1-\nu^{1.286})\ \sigma_p r}{w^{1.086}}$
Araya (2011)	$M_r = \frac{1.513\ (1-\nu^{1.104})\ \sigma_p r}{w^{1.086}}$
Hao and Pabst (2021)	$M_r = \frac{2.432(1-\upsilon^{2.630})\sigma_p.r}{w^{0.766}}$
Narzary and Ahmed (2020)	$M_r = \frac{0.4(1-\upsilon^2)\sigma_p.r}{w}$

Note: Mr= RLCBR Resilient modulus (kPa); ν= Poisson's ratio of the tested material; w= Resilient deformation of the material tested under plunger loading(mm); r= Radius of the CBR plunger in mm; σ_p= Plunger stress in kPa.

Opiyo (1995) introduced two models based on Equation 2.21 that incorporate the effects of soil-mold interaction into the determination of the material's elastic modulus using Finite Element Methods. One model was without considering the friction effects between the mold and soil, and the other one was considering the friction effects. Not much information on its correlation with the resilient modulus is available. Molenaar (2007) used Opiyo's model considering friction to characterize seven

different soils. Molenaar concluded that the RLCBR modulus correlates well with the resilient modulus obtained from triaxial testing at confinement levels of about 24 kPa. Araya (2011) regressed the model parameters for Equation 2.21 using a finite element model of the CBR test considering linear elastic behaviour. A data set was generated using assumed values of Elastic modulus varying from 100 MPa-1000 MPa representative of granular materials, and Poisson's ratio varying from 0.15-0.45. RLCBR tests were conducted on granular material in a larger mould of size 250mm diameter and 200mm height, with and without strain gauges and the RLCBR modulus was correlated to the RLTT resilient modulus over a range of stress levels. The results showed the RLCBR modulus was significantly higher than RLTT resilient modulus and only a relative comparison of trends was made. This was attributed to the different stress states of the soil in two different test set ups. Hao and Pabst (2021) proposed a new model to characterize the resilient behaviour of crushed waste rocks. The specimens were tested using the RLCBR test simulating two in situ conditions: the low stress levels for highways and High stress levels for mining haul roads. The RLCBR modulus was validated with resilient modulus from triaxial testing with bulk stress varying between 100 kPa to 650 kPa for low stress levels and from 135 kPa to 3550 kPa for high stress levels. However, Hao and Pabst (2021) reported almost similar values of the RLTT resilient modulus and the RLCBR modulus for the range of bulk stress considered. Narzary and Ahamad (2020) proposed a new model by calibrating Equation 2.21 using a numerical model with assumed elastic modulus value from 10-120 MPa and Poisson's ratio from 0.10- 0.35 and validated it theoretically using the elastic half space theory. The effect of soil physical state on the equivalent modulus was then studied by carrying out RLCBR tests at various density and moisture contents. It was concluded that the effect of moisture and density on the equivalent modulus was similar to that of the resilient modulus determined using an RLTT. In another study, Narzary and Ahamad (2021) pointed out that the repeated load of the plunger causes stiffening effect on the soil specimen under the plunger which was not considered in the previously developed models. Narzary and Ahamad (2021) postulated that specimens compacted using IS light compaction method undergoes hardening under repeated plunger loading, whereas the specimens compacted using IS heavy compaction method undergoes softening under repeated plunger loading. Numerical analysis of the RLCBR test was performed using an elastoplastic model. Results showed that, although the numerical model could accurately predict the hardening behaviour in specimens

compacted using heavy compaction, it failed to capture the hardening behaviour under specimens compacted using light compaction method. Therefore, the Narzary and Ahamad (2020) model was modified to include the effect of hardening as shown in Equation 2.22:

$$M_e = 3.93\left(\frac{w_1}{w_2}\right)E_{equ} \quad (2.22)$$

Where, M_e= Corrected equivalent modulus, w_1= Elastic deformation estimated from the RLCBR model, w_2= Deformation produced by a load level equal to that applied for the RLCBR model using an elastic half space model.

Once the model constants are calibrated, a RLCBR test can be conducted to obtain the plunger stress and the resilient deformation. The set up used for a RLCBR test is similar to that of a standard CBR test, but repeated loads are applied using the plunger instead of the conventional loading. Under multiple load repetitions at the same rate of deformation, the soil particles undergo permanent and recoverable deformations. After a few repetitions, the permanent deformation ceases, and only stable recoverable or resilient deformation is observed. Due to the complex stress state of a CBR specimen, the resilient modulus of the soil cannot be directly computed as in the case of RLTT. Instead, the resilient deformation and the plunger stress is used in Equation 2.21 to estimate the resilient modulus of the material. A schematic of the RLCBR test setup is shown in Figure 2.5.

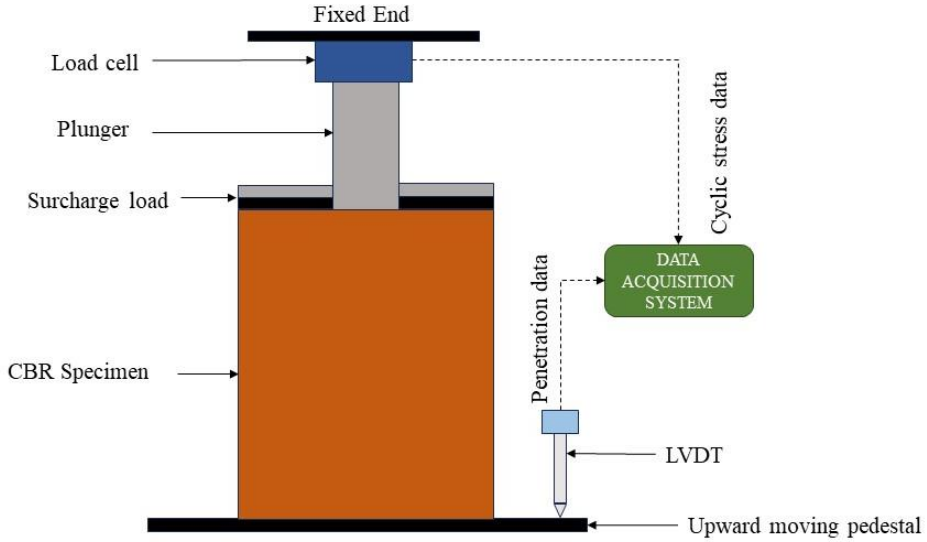

Figure 2.5: Schematic of the RLCBR test

The RLCBR test can be conducted in two modes: (i) Deformation controlled mode (ii) Load controlled mode.

- ***Deformation controlled mode:*** In the deformation-controlled mode, the CBR specimen is loaded at a constant rate to an initial target deformation and the corresponding load is noted. The specimen is unloaded at the same rate to a minimum load (usually 10% of the load sustained at the target deformation) to complete one cycle of loading. The load sustained at the target deformation is taken as the maximum load applied, and 10% of this load is taken as the minimum contact load, that is maintained throughout the test. In the subsequent loading cycles, the load is maintained between the maximum and minimum value of load as obtained from the first cycle. Now, a question arises as to what should be the initial target deformation and how many loading cycles must be applied. Several researchers have used different initial target deformations and number of loading cycles over the years, which are summarized in Table 2.10.

Table 2.10: Initial target deformation and number of loading cycles used in deformation controlled RLCBR tests

Reference	Initial target deformation(mm)	Number of cycles
Araya (2011)	2.54	100
Molenaar (2007)	2.5	100
Haghighi (2018)	2.5	10
Nagula et al., (2018)	2.5	10
Narzary and Ahamad (2020)	1.75, 2.5, 5	100

The majority of researchers commonly utilized an initial target deformation of 2.5 mm and a fixed number of 100 loading cycles, as evident from Table 2.10. It is important to note that the rationale behind selecting this initial target deformation is to ensure that the CBR specimen remains within the elastic range and does not undergo yielding. However, previous studies by Narzary and Ahamad (2020) and Loach (1987) have demonstrated that the material reaches a state of general failure at a deformation of 2.5 mm. Hence, it is recommended to perform the RLCBR test at a deformation below 2.5 mm. Additionally, the number of cycles applied should be chosen in a manner that the resulting deformation after the specified number of loading cycles is completely resilient or recoverable. With the exception of Haghighi *et al*. (2018), there is a general consensus among the authors regarding this aspect, and hence number of loading cycles of 100 is recommended in most cases. The resilient deformation from the last five cycles is averaged out, and along with the plunger stress is used in any of the models summarized in Table 2.9 to obtain the equivalent RLCBR modulus or the resilient modulus of the soil specimen.

- ***Load controlled mode***: In the load-controlled test mode, the RLCBR test is conducted in sequences of predetermined loads. The purpose of conducting the RLCBR test in load-controlled mode is to characterize the stress dependent non-linear elastic behaviour of the geomaterials, similar to that in an RLTT. Several authors have reported studies on the load controlled RLCBR test to characterize geomaterials (Nagula,2018; Hao and Pabst ,2021; Leischner *et al*., 2022) conducted RLCBR test in the load-controlled. The axial load was incrementally increased by 0.2 kN, and the corresponding penetration of the

CBR plunger was measured after a 5-second interval for each load increment. The load was continued to be increased until the plunger achieved a penetration of 2.5 mm. Hao and Pabst (2021) developed an empirical relation between the bulk stress, the plunger stress and the Poisson's ratio in an RLCBR test as shown in Equation 2.23:

$$\theta = (0.707\nu + 0.4356)\sigma_p \qquad (2.23)$$

6 load sequences were applied on the CBR specimen in an RLCBR test with minimum axial stress varying from 100 kPa to 1100 kPa and the resulting data was used to calculate the bulk stress for each stress sequence. The calculated bulk stress was then used to fit the M_r-θ (Seed *et al*., 1967) model and validated against the RLTT modulus. In another study, Leischner *et al*. (2022) proposed a methodology to determine the MEPDG constitutive model constant parameters using the RLCBR test. RLCBR tests were performed in CBR specimens of the UGM materials by applying five load sequences of 100-500 kPa with 100 load repetitions in each cycle. The bulk and the octahedral stresses were calculated using the following empirical relations:

$$\theta = \sigma_1 + 2\frac{\nu\sigma_1}{(1-\nu)} \qquad (2.24)$$

$$\tau_{oct} = \frac{\sqrt{2}}{3}(\sigma_1 - \frac{\nu\sigma_1}{(1-\nu)}) \qquad (2.25)$$

Where, σ_1 is the vertical plunger stress and ν = 0.35 is the Poisson's ratio of the soil. A modified form of the modified universal model or the MEPDG model was proposed for the RLCBR test as under.

$$M_r = ak_1P_a(\frac{\theta}{P_a})^{bk_2}(1+\frac{\tau_{oct}}{P_a})^{k_3} \qquad (2.26)$$

Where, a = 0.72 and b=1.17 are factors.

2.11 Numerical modelling of CBR test

Over the years, traditional experimental CBR tests have provided valuable insights, but they can be time-consuming, costly, and sometimes limited in capturing complex soil behaviour. As a result, researchers have increasingly turned to numerical techniques, particularly Finite Element Modelling (FEM), to simulate and analyse CBR tests efficiently. This literature review explores the recent advancements and challenges

in applying Finite Element Modelling to CBR tests. Various researchers over the years have used numerical modelling of CBR to achieve different objectives. Negi and Singh (2021) utilized a 3D Finite element model to understand the mechanics of using geosynthetics in subgrade soils. Araya (2011) and Narzary and Ahamad (2018) utilized a finite element model to determine the Elastic modulus of granular materials and soils under plunger loading. Mendoza and Caicedo (2019) analysed the material behaviour of the soil under plunger loading by considering pore pressure development by considering drained and undrained conditions.

The geometry of the CBR test can be modelled either in a 3-dimensional domain (Negi and Singh, 2021) or in 2 dimensions using the axisymmetric approach (Araya, 2011; Mendoza and Caicedo,2019). Although 3D models have proven more accurate, 2D axisymmetric models reduce the computational time manifold. The circumferential boundary conditions are usually taken as a roller (Mendoza and Caicedo, 2019; Negi and Singh, 2021; Hights and Stevens,1982) as the rigid mould does not allow the soil to bulge in the lateral direction. However, some researchers have modelled the mould separately by assigning material properties of brass and steel (Narzary and Ahamad, 2018; Araya,2011).The plunger loading is usually assigned by prescribed displacement by indentation of a rigid plunger of 50 mm diameter into the soil specimen.

Additionally, the surcharge load has been modelled as pressure load by most of the authors (Narzary and Ahamad, 2018; Araya, 2011). The researchers have modelled the soil as either elastic or elastoplastic material. Araya (2011) considered the soil material to be completely elastic. Whereas other researchers have used an elastoplastic model. Mohr Coulomb failure criterion is the most commonly used material model due to the ease of determination of its model parameters (Negi and Singh, 2019; Narzary and Ahamad, 2018). However, Mendoza and Caicedo (2019) used a Drucker Pruger model with a cap to understand soil behaviour under plunger loading.

2.12 Summary of literature review

This chapter provided a detailed review of the various methods of subgrade soil characterization in the context of a mechanistic pavement design. This section provides a summary of the literature review carried out.

- Over the years, pavement design methods have undergone significant evolution, transitioning from purely empirical approaches to mechanistic

empirical methods. Adopting mechanistic design methods offers several advantages, including the ability to adapt to changing design conditions such as increased loads, diverse climatic conditions, and incorporating innovative pavement materials. A crucial aspect of any mechanistic design approach is accurately characterizing individual pavement layers: the subgrade, the granular layers and the bituminous layers in terms of their elastic modulus and Poisson's ratio. These material properties are then utilized in layered elastic analysis programs to calculate stresses and strains, which are empirically correlated with pavement performance.

- The elastic modulus of soil in general is a complex topic. The same soil can have numerous resilient moduli values, depending on the test conditions and type of modulus measured. Broadly, the Elastic modulus can be divided into three types: the initial tangent modulus; the secant modulus and the resilient modulus which are discussed in detail in earlier sections. To characterize the non-linear elastic behaviour of a soil, the resilient modulus is widely used across several mechanistic design methods across the world. The resilient modulus, which is representative of the dynamic wheel load stresses is analogous to the Elastic modulus, except that repeated loads are applied in its determination and is defined as the ratio of deviatoric stress to the resilient or recoverable strain.
- Several factors affect the resilient modulus of soils. However, the stress state and moisture are the most prominent factors affecting soil resilient modulus. Therefore, the effect of stress state and moisture content has been explicitly considered in the developed constitutive models for resilient modulus prediction. While reporting the resilient modulus, it is important to specify the stress state at which it has been estimated.
- The resilient modulus can be measured in the laboratory or field using various Non-destructive and intrusive devices. Details of various methods of resilient modulus measurement is presented in sections 2.6 and 2.8 respectively. The most commonly used method for resilient modulus measurement in the laboratory is the RLTT, whereas field measurement of subgrade modulus is carried out using the FWD and the DCP. It is important to understand that various subgrade modulus measurement devices measure the elastic modulus

at different strain levels. The RLTT characterizes the stress dependent non-linear behaviour of the soil, whereas the FWD and the LWD measures the Elastic modulus. Therefore, it becomes essential for a pavement engineer to understand the functional and operation differences among various moduli measuring devices to interpret the moduli value correctly.

- Mathematical modelling of the various factors influencing the resilient modulus of soils is essential to understand the soil resilient behavior. The resilient modulus predictive models can be classified into the following three categories: (i) Empirical relations with soil basic properties, simple tests like CBR, UCS etc. (ii) Resilient modulus constitutive model incorporating stress state (iii) Resilient modulus constitutive model incorporating stress state and effect of moisture content. The empirically correlated predictive equations can predict the resilient modulus at a predefined stress level, if some simple parameters like the CBR, UCS or the soil basic properties are known. On the other hand, the constitutive models can be two or three parameter models and capture the strain hardening and softening behavior of the soils under repeated loading. The field elastic modulus is usually correlated to the laboratory resilient modulus using empirical relations at appropriate stress levels before it can be used in mechanistic design methods.
- The mechanistic-empirical design methods involve two types of subgrade characterization: (i) Single representative modulus at recommended stress levels (ii) Non-linear stress-based characterization in which the constitutive model parameters k_1,k_2,k_3 are used as inputs. In the first type of characterization, a single representative value of the resilient modulus is used in the layered elastic theory at appropriate stress level to calculate the pavement distresses and are used in most mechanistic design methods(IRC 37(2012,2018); Austroads 2012; MEPDG Level 2 and 3).The second type of characterization involves determining the constitutive model parameters k_1, k_2, k_3 using an appropriate laboratory test, which are then used in a FEM model to predict the pavement responses. This type of characterization is usually used in projects of high importance (MEPDG Level 1).
- Due to complexities of cost, time and manpower associated with the RLTT, several alternate methods have been explored to mimic the repeated loading

phenomenon using simple tests like the Triaxial, Oedometer, and CBR tests. Due to its simplicity and familiarity among pavement engineers, the Repeated Load CBR test has attracted considerable research attention in the past decade. The RLCBR test is similar to a conventional CBR test, but employs repeated loading instead of the monotonic loading of the traditional CBR test. Due to the complex stress state of the CBR mould, the resilient modulus cannot be directly calculated from the stress strain curve, but is calculated as an equivalent modulus which is representative of the entire CBR specimen, considering the CBR as quasi-static infinite half-space problem under a circular load based on elastic theory. The RLCBR test can be conducted in two modes: (i) The deformation-controlled mode (ii) The Load controlled mode. The deformation-controlled mode is based on loading the CBR specimen to an initial target deformation at a constant rate and unloading it at the same rate up to a minimum contact load. The load-controlled repeated load CBR test is based on applying incremental predefined loads on the CBR specimen within the elastic range. The deformation-controlled test allows estimating a single resilient modulus value, whereas the load-controlled test characterizes the non-linear stress-dependent behaviour of the geomaterials.

CHAPTER 3

Experimental program and methodology

3.1 General

This chapter presents a detailed description of the materials used and a comprehensive narration of the experimental programme formulated to achieve the study's objectives. The chapter begins with a discussion of various types of soil used in this study, their source and their collection method. Subsequently, a general discussion on the experimental program formulated has been provided. The next section provides a detailed overview of various test protocols used in this study and the basic soil properties obtained from the tests conducted.

3.2 Experimental Methodology

This study involves the testing and characterization of twelve soils predominantly used as subgrade materials in low volume roads (LVR) within the region, specifically Assam and Meghalaya. Among these, ten soil samples were gathered from ten in service low volume roads in Assam and Meghalaya, India. The collection process involved excavating pits with dimensions of 50 cm x 50 cm, digging up to the subgrade layer for material collection as shown in Figure 3.1 (a). The soil#1-soil#8 used in this study for the development of RLCBR model are shown in Figure 3.1 (b). Additionally, two soil samples were sourced from locations within the IIT Guwahati campus roads. The twelve soil specimens in sufficient quantity were transported to the IIT Guwahati laboratory for further testing and characterization. The details of the 12 soils used in the study and their source are detailed in Table 3.1. Table 3.1 also shows the various types of field and laboratory tests conducted on the soils. The detailed procedure of the tests for the current study is however discussed in subsequent sections.

Table 3.1: List of soils used in the study and the its source of collection

Soil ID	Type of Road	Location	Tests conducted					
			UCS	DST	RLCBRD	RLCBRL	LWD	DCP
Soil#1	Low Volume Road	Goalpara, Assam	Yes	Yes	Yes	Yes	Yes	Yes
Soil#2	Low Volume Road	Kamrup (rural), Assam	Yes	Yes	Yes	No	Yes	Yes
Soil#3	Low Volume Road	Kamrup (rural), Assam	Yes	Yes	Yes	Yes	Yes	Yes
Soil#4	Low Volume Road	Darrang, Assam	Yes	Yes	Yes	No	Yes	Yes
Soil#5	Low Volume Road	Kamrup (rural), Assam	Yes	Yes	Yes	Yes	Yes	Yes
Soil#6	Low Volume Road	Kamrup (rural), Assam	Yes	Yes	Yes	Yes	Yes	Yes
Soil#7	Low Volume Road	Darrang, Assam	Yes	Yes	Yes	No	Yes	Yes
Soil#8	Low Volume Road	Kamrup (rural), Assam	Yes	Yes	Yes	No	Yes	Yes
Soil#9	Residential street	IITG, Assam	No	No	Yes	No	No	No
Soil#10	Low Volume Road	Nongpoh, Meghalaya	No	No	Yes	No	No	No
Soil#11	Residential street	IITG,Assam	No	No	Yes	Yes	No	No
Soil#12	Low Volume Road	Kamrup (rural), Assam	No	No	Yes	No	No	No

Note: UCS: Unconfined compressive strength test; DST: Direct shear test; RLCBRD: Repeated load CBR test (Deformation controlled); RLCBRL: Repeated load CBR test (Load controlled); LWD: Light weight deflectometer; DCP: Dynamic cone penetrometer

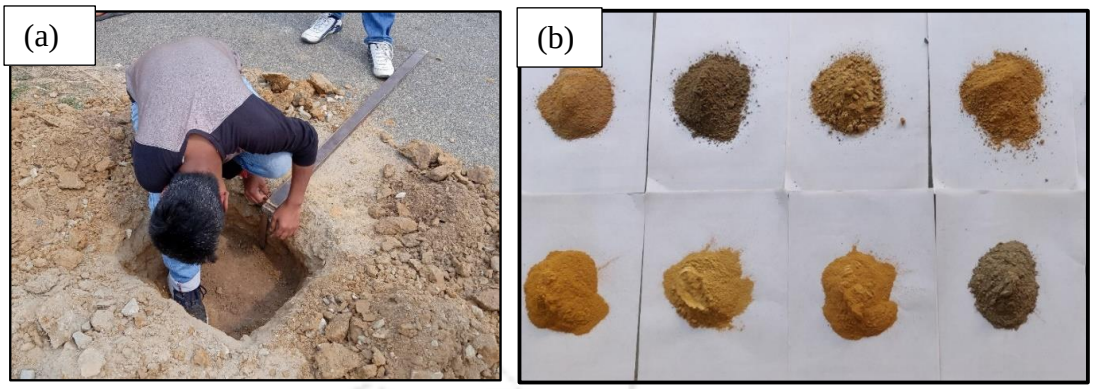

Figure 3.1: (a) Material collection in the field (b) Soil#1-Soil#8 used in the study

3.3 Experimental program

The details of the experimental program adopted to achieve the objectives is shown in Figure 3.2. The various tests carried out to achieve the objectives include basic characterization tests, RLCBR tests for resilient modulus determination and several other tests conducted to determine the input parameters for the numerical model. A detailed description on various tests conducted is presented in section 3.4.

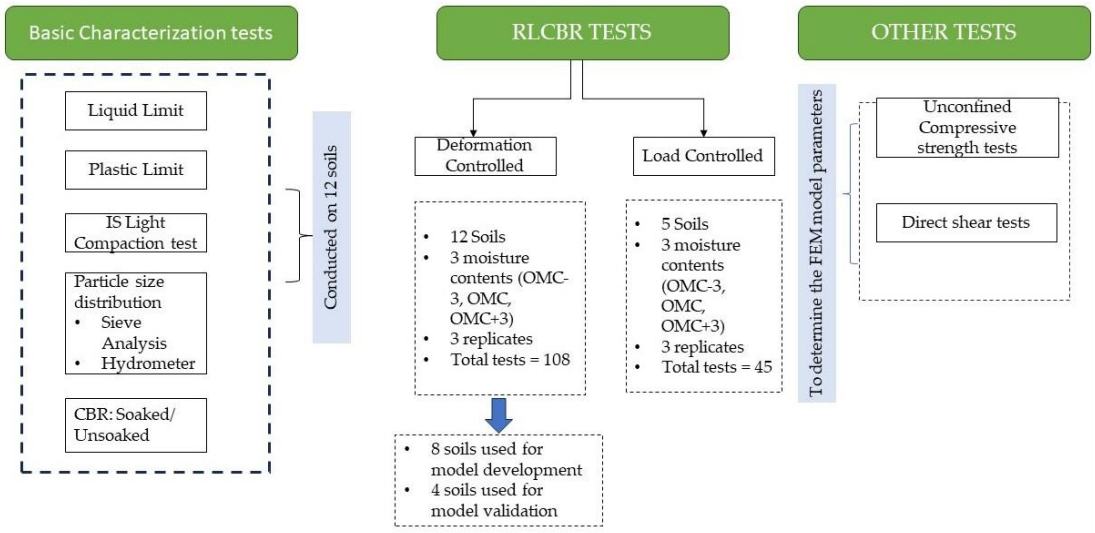

Figure 3.2: Laboratory Experimental Program

3.4 Laboratory Experimental protocols

3.4.1 Determination of basic soil properties

The basic soil properties include the tests which are used for soil identification and classification. Index properties of the soils were determined by conducting Liquid limit and plastic limit tests as per IS 2720 (Part V)-1985. Additionally, IS light compaction tests (Standard Proctor test) as per IS 2720 (Part VII)-1980 was used to determine the compaction characteristics of the soils. Particle size distribution tests including both sieve analysis and hydrometer were performed as per IS 2720 (Part IV)-1985, to classify the soils. Furthermore, both soaked and unsoaked CBR tests were conducted to on statically compacted CBR specimens to analyze the strength characteristics of the soil as per IS 2720 (Part VI) guidelines. A brief description of some important tests carried out is presented here.

- **IS Light compaction test:** The IS light compaction test, as per Indian Standard (IS 2720-Part 8: 1983) was conducted to determine the maximum dry density (MDD) and the optimum moisture content (OMC) of a soil sample under controlled compaction conditions. The IS light compaction test was selected to determine the compaction characteristics of the subgrade soil depending on the type of road from which the material was procured. The test was selected considering that the IS light compaction test is used for determination of low volume road compaction characteristics. A typical OMC-MDD graph for soil#1 is shown in Figure 3.3. Figure 3.3 shows the variation of the dry density with the moisture content for soil#1. The dry density increases with increase in moisture, reaches a maximum and then reduces with further increase in moisture content. To mathematically model this behaviour, a polynomial model was fitted to the data points, with an R^2 value> .9. Three replicates were tested for each soil, and the average OMC and MDD were reported for further use.

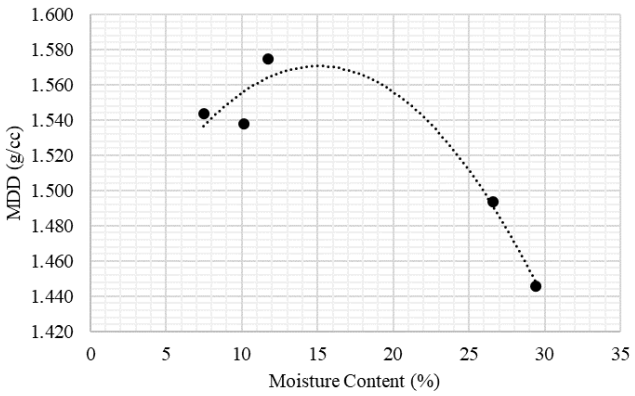

Figure 3.3: A typical OMC-MDD graph for soil#1

- **California Bearing Ratio (CBR) test:** Both unsoaked and soaked California Bearing Ratio (CBR) tests, in accordance with the Indian Standard (IS 2720-Part 16: 1987) was conducted to evaluate the strength characteristics of the soils. The specimens were statically compacted at target moisture content and density. For unsoaked CBR, the specimens were tested immediately after compaction. Whereas, the soaked CBR tests were conducted after soaking for a period of 96 hours. The specimens were penetrated by a standard plunger of 50 mm diameter at a constant penetration rate of 1.25 mm/min. The CBR value was reported as the higher of the ratio of loads sustained at 2.5 mm and 5 mm to the standard loads, expressed as ratio. Three replicates were tested at OMC-MDD and the average expressed as CBR value of the soil. The results of the CBR tests for the 12 soils are provided in Table 3.2. A typical graph for soaked CBR of Soil#1 is shown in Figure 3.4. Three replicates were tested for each soil, in both soaked and unsoaked conditions and the average CBR was reported

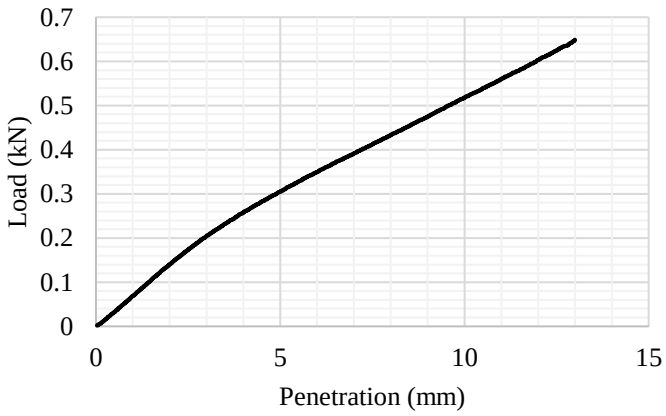

Figure 3.4: A typical load v/s penetration curve from soaked CBR test (Soil#1)

Table 3.2: Results of soil basic properties test

Soil ID	LL	PL	PI	OMC	MDD	IS Classification	Coarse (%)	Fines (%)	CBR (Soaked) (%)	CBR (Unsoaked) (%)
Soil#1	33.0	21.9	11.1	16.4	1.651	CL	11.54	88.46	4	14.5
Soil#2	27.0	16.0	11	17.7	1.752	CL	39.44	60.56	5.6	9.5
Soil#3	40.8	25.5	15.3	23.8	1.516	CI	3.58	96.42	5.3	10.1
Soil#4	27.0	13.3	13.7	16.8	1.699	CL	43.50	56.50	3.5	8.5
Soil#5	28.2	19.1	9.1	14.1	1.853	CL	33.24	66.76	4.2	12.6
Soil#6	30.3	18.7	11.6	15.3	1.717	CL	19.58	80.42	4.1	10
Soil#7	34.3	17.8	16.5	12.1	1.943	CL	35.80	64.20	3.5	8.7
Soil#8	27.3	16.8	10.5	16.4	1.767	CL	12.48	87.52	3.6	9.5
Soil#9	37.0	27.7	9.3	18.7	1.701	CI	7.48	92.52	4.1	8.4
Soil#10	46.3	34.2	12.1	23.5	1.402	MI	20.58	79.42	6.9	10.7
Soil#11	42.2	28.0	14.2	20.4	1.601	MI	10.26	89.74	7.8	12.2
Soil#12	41.3	23.0	18.3	18.6	1.734	CI	37.30	62.70	3.4	7.8

3.4.2 Repeated Load CBR (RLCBR) tests

The repeated load CBR test is a cost-effective way to determine the resilient modulus of geomaterials using the routine CBR test. The test can be conducted in two modes, which are discussed in details as under:

- **Specimen preparation:**

Specimens were prepared in the CBR mould of 150 mm diameter and 175 mm height by means of static compaction in which a pre-weighed amount of soil mixed with water is gradually pushed into a specific volume by means of static weight to achieve the required density. The pre-weighed amount of dry soil is thoroughly mixed with the required amount of water. The CBR mould along with the spacer disc and collar is fitted with the base plate and weighed. The soil water mixture is filled in 5 layers by tamping each layer 25 times using a steel rod. The mold assembly is put in the static compression loading machine, a spacer disk is placed at the top and a gradual load is applied until spacer disk is completely flushed into the mold-collar assembly. The compacted specimen is then weighed to ensure that the required density is achieved. Figure 3.5 shows the method of specimen preparation for the RLCBR test.

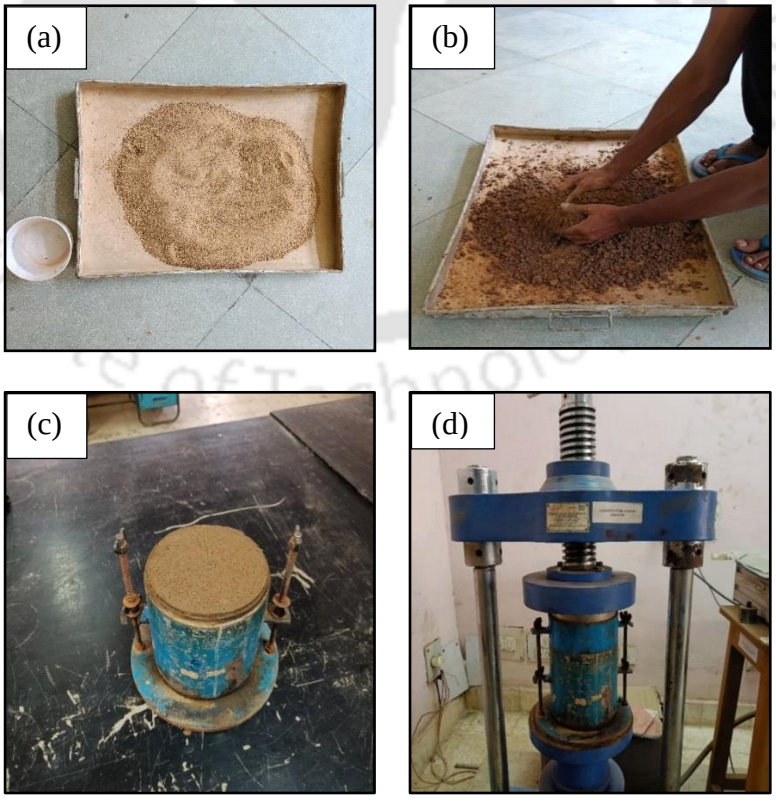

Figure 3.5: Specimen preparation: (a) Pre-weighed amount of pulverized soil and water (b) Hand mixing of soil (c) static compaction (d) Compacted CBR specimen

- **Deformation controlled RLCBR test**

The RLCBR test in deformation-controlled mode involves repetitive loading of a conventional CBR test specimen while recording the corresponding resilient deformation using an LVDT in a data acquisition system. A digital CBR apparatus with a data acquisition system was used to conduct the RLCBR tests. The digital CBR apparatus consists of a load cell, an LVDT, and a data acquisition system to record load and penetration data (Figure 3.6). The test was conducted in a deformation-controlled mode with a fixed load based on a target deformation of 1.5 mm, which was selected to avoid yielding of the CBR specimen (Narzary and Ahamad, 2018).

Figure 3.6: Digital CBR apparatus for conducting RLCBR test

The specimen was manually loaded at a constant rate of 1.25 mm/min until 1.5 mm penetration is reached, and the corresponding load was noted. It was then unloaded at the same rate to a load of 0.1 kN, completing one cycle of load. For the subsequent loading cycles, the specimen was loaded to the load sustained at 1.5 mm penetration in the first cycle and then unloaded to 0.1 kN. As the upper bound of the load is determined based on an initial target deformation, the test is called a deformation-controlled test (Nagula *et al*., 2018). A minimum contact load needs to be maintained to ensure proper contact between the soil surface and the plunger. Review of literature shows that the

contact load in most of the studies for unbound granular materials was kept at 10% of the peak load. However, for fine grained soils which usually has a much lower peak load, unloading manually to 10% of the peak load without losing contact proved challenging. As a result, a contact load of 0.1 kN was maintained for all soil types and test conditions. A typical load penetration curve for the RLCBR test is shown in Figure 3.7, indicating that after a certain number of load cycles, the resulting penetration becomes entirely resilient. The stabilization of the resilient deformation with the number of cycles can be seen in Figure 3.8. The test is repeated for 100 loading cycles, and the resilient deformation is estimated as the average of the last five cycles. At a given test condition, three replicates were tested and the modulus was reported as the average of the three values.

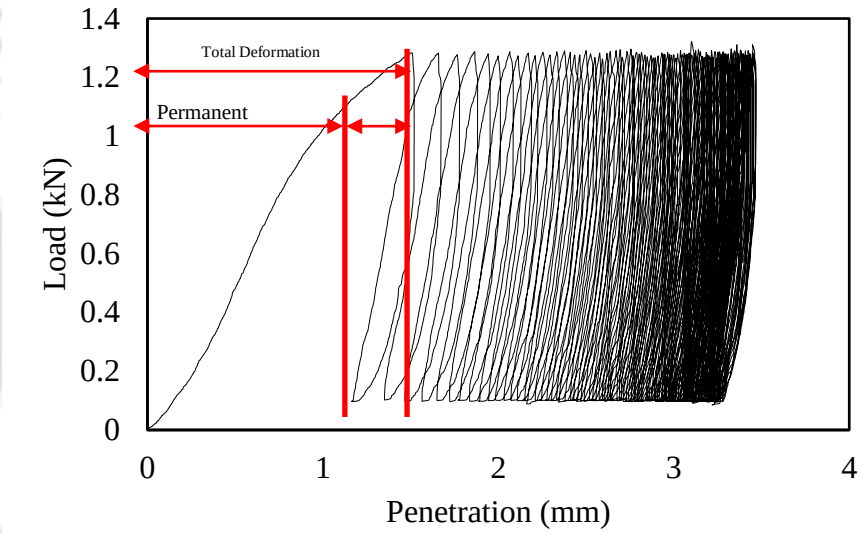

Figure 3.7: Typical load penetration graph from deformation controlled RLCBR test

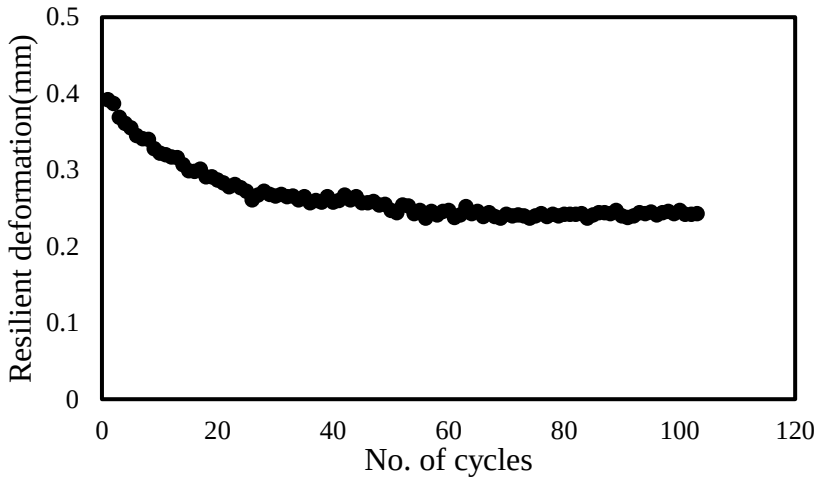

Figure 3.8: Resilient deformation v/s No. of cycles plot

- **RLCBR test in Load controlled mode**

The repeated load CBR test in load-controlled mode involves conducting the tests at predetermined loads instead of target deformation. A total of eight sequences were selected at each test condition to complete one RLCBR test. Detailed description on the procedure for determination of loading sequences are described in Chapter 6. Specimens compacted at target density and moisture content were mounted into the digital CBR apparatus and loaded to the target load level at a constant penetration rate of 1.25 mm/min. Once the target load level was reached, the specimen was unloaded to the contact load of 0.1 kN at the same rate to complete one cycle of loading. In the first load level, 100 load cycles were applied for the preconditioning of the specimen. Subsequently, in the next load levels, 25 loading cycles were applied, before proceeding to the next target load level. 25 load cycles were selected based on recommendations from the literature (Nagula *et al*., 2018; Haghighi *et al*., 2018) and trials carried out in the laboratory prior to carrying out the actual test. Further, for simplification the deformation can be assumed to be entirely resilient after 25 load cycles, because of the initial preconditioning cycles applied. Most of the accumulation of deformation have already been taken place during the applied preconditioning cycles A typical load penetration graph resulting from the RLCBR test in load-controlled mode is shown in Figure 3.9. A single replicate was tested in load-controlled mode, at each test condition.

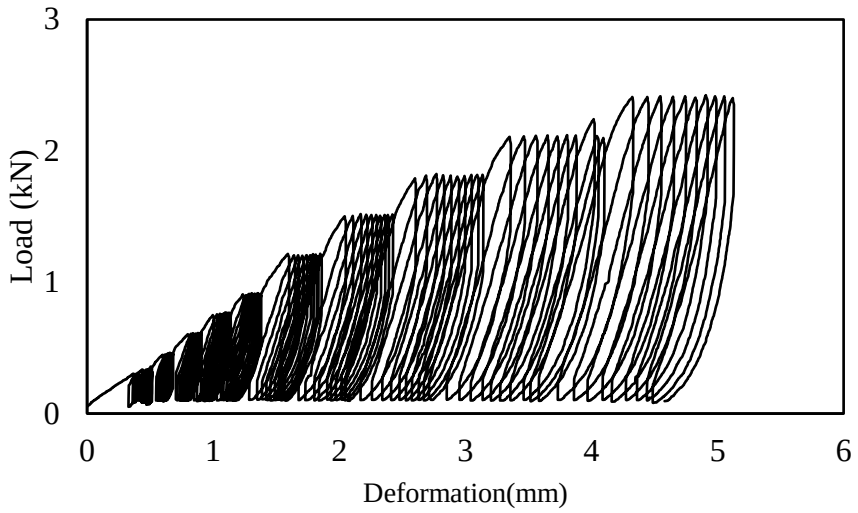

Figure 3.9: Typical load v/s deformation curve from load controlled RLCBR test

3.4.3 Tests for determination of inputs into the numerical model

The inputs for the Mohr Coulomb Elastoplastic model which has been used to model the soil behaviour in the numerical model can be determined from simple laboratory tests like the Unconfined Compressive strength tests and the Direct shear tests. It must be noted that the tests were conducted on soil#1-soil#8 because experimental validation was carried out for the 8 soils only. A brief description of the methodology used to conduct the tests has been presented in this section.

- **Unconfined compressive strength tests**

  Unconfined compressive strength (UCS) tests were conducted to determine the elastic modulus of the soil, as input for the Mohr Coulomb Elastoplastic model. UCS tests were conducted on soil#1-soil#8 as described in per recommendations of IS 2720 Part X at OMC and MDD. The initial tangent moduli for each soil were determined from the load-deformation graphs obtained from the UCS tests. A single replicate was tested at each test condition. The unconfined compressive strength test apparatus used in the study is shown in Figure 3.10 (a).

- **Direct Shear Tests (DST)**

  Direct shear tests were used to determine the Cohesion (c) and angle of internal friction (φ) of soil samples as per the guidelines outlined in the Indian Standard IS: 2720 (Part XIII) –1986. Direct shear tests were conducted on eight soils outlined in **Table *3.1***at optimum moisture content and dry density for

soil#1-Soil#8. The required amount of water and dry soil was calculated to achieve the desired dry densities, and the soil was mixed and compacted in the direct shear mould. A static vertical load was applied to the soil sample, followed by a horizontal force at a constant rate of 1.27 mm/min. The shear load and deformation were measured using a proving ring and dial gauge. This procedure was repeated on three different soil samples for each soil with the same dry density, subjected to static vertical loads of 0.5, 1.0, and 1.5 kg/cm^2, respectively. The shear stress values at failure were plotted against the normal stress for each test to determine the shear strength parameters Cohesion (*c*) and Angle of internal resistance (*φ*). The direct shear test apparatus is shown in Figure 3.10 (b). A typical UCS and a direct shear test graph are shown in Figure 3.11 and Figure 3.12, respectively. In addition, the Elastic modulus (*E*) and the shear strength parameter of each soil#1-soil#8 is presented in Table 3.3.

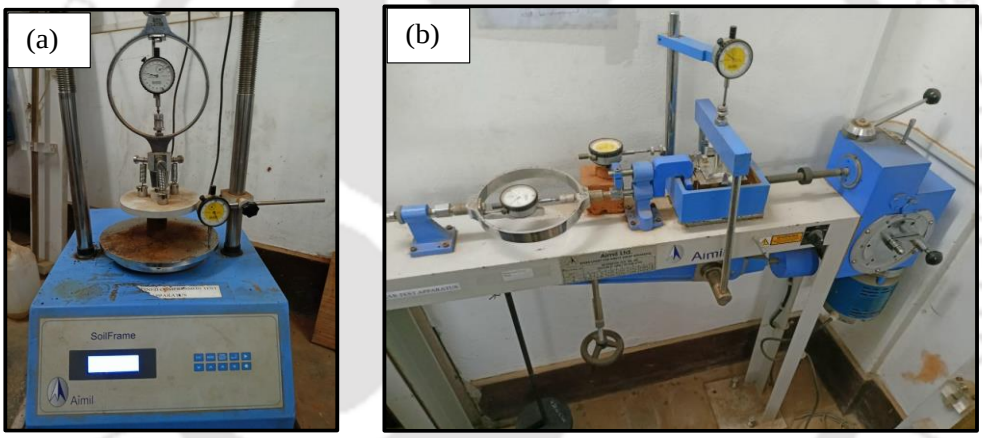

Figure 3.10: (a) Unconfined compressive strength test (b) Direct shear test

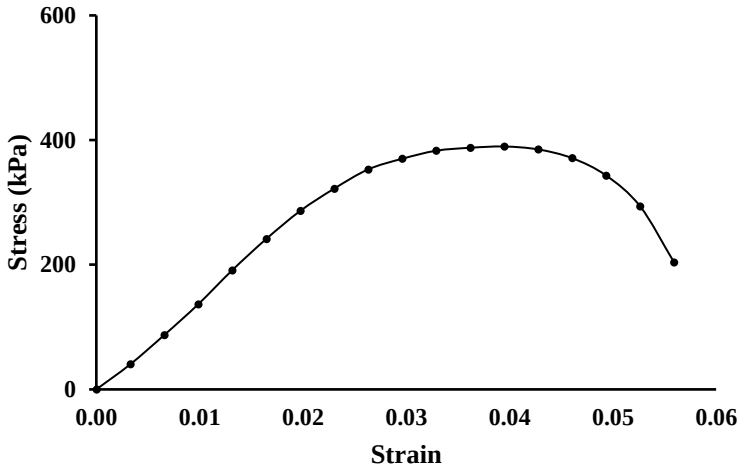

Figure 3.11: A typical UCS stress v/s strain curve

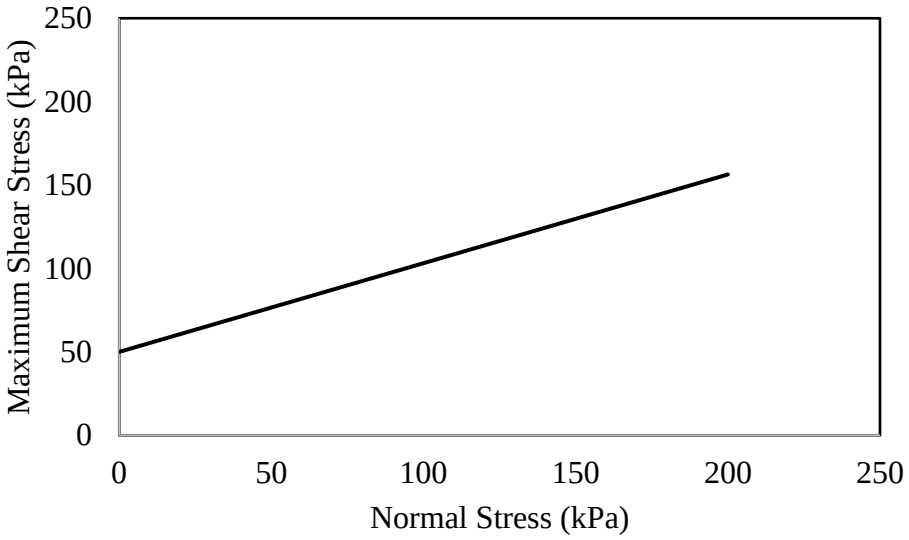

Figure 3.12: A typical Direct shear test graph

Table 3.3: Results of Elastic modulus and shear strength parameters

Soil ID	E (MPa)	C (kPa)	Φ in degrees
Soil#1	39.23	50	28
Soil#2	32.21	45	32
Soil#3	35.08	45	29
Soil#4	27.85	40	27
Soil#5	32.50	42	27.5
Soil#6	38.26	45	30
Soil#7	40.06	52	28
Soil#8	35.27	35	25

3.5 Field Tests

3.5.1 Dynamic Cone Penetration (DCPT) test

The Dynamic Cone Penetrometer (DCP) is portable equipment used in pavement applications to determine the in-situ subsoil characteristics like shear strength and stiffness. The DCP test is standardized by the ASTM D6951-09 and consists of an 8 kg sliding hammer with a 57.5 cm drop height and a 60° conical tip at the bottom end, attached to a 111 cm driving shaft. During the test, the hammer can fall freely from a height of 57.5 cm, which drives the conical tip at the bottom of the hammer into the ground. The penetration depth per blow is recorded in a vertical scale next to the DCP rod, known as the DCP index (DCPI). Therefore, the DCPI is a measure of the penetration resistance of the soil and is expressed in either mm/blow or inch/blow.

The DCPI is correlated empirically to the soil's strength or stiffness characteristics. Several researchers have tried to correlate the DCPI with the resilient modulus of the soil (Hassan, 1996; Herath *et al*., 2005; Mohammad *et al*., 2007). Table 2.7 summarizes the various available correlations in the literature which relates the DCPI to the soil resilient modulus. It should be noted that although the soil resilient modulus varies with the stress state, the available models give a single representative value of the resilient modulus at a confining pressure of 13.79 kPa and deviatoric stress of 41.37 kPa (Puppala,2008).

3.5.2 Light Weight Deflectometer (LWD)

The Light Weight Deflectometer (LWD) or the Portable Falling Weight Deflectometer (PFWD) is a portable Non-Destructive Testing device used to evaluate the in-situ modulus of pavement layers.

Working Principle

The Light weight deflectometer (LWD) is a plate-bearing test that uses a dynamic force to create a load pulse on a buffer system that transmits it through a plate resting on the material to be tested. The plate's resulting velocity or acceleration measurements under the application of the load pulse are measured either by a velocity transducer or an accelerometer. These measurements are then converted to elastic stiffness of the base or subgrade system by employing equations that assume the underlying layers as homogenous elastic half space. The modulus obtained through an LWD is equivalent to the homogenous Young's Modulus of the combined granular and subgrade layers.

Equipment Description

The LWD consists of the following parts:

- Force-Generating Device (falling mass): It should be capable of being raised with negligible friction or resistance, using a guide system, to a predetermined fixed height and dropped onto a steel-spring subassembly. The falling mass should produce a half-sine or haversine-shaped load pulse, with a loading time between 10 and 30 msec.
- Load Plate: The loading plate transfers the load into the testing material. The plate should be rigid and capable of transferring the applied load to the underlying surface.
- Deflection sensors capable of measuring the maximum vertical plate movement.

Test Procedure

The instrument should be stationed over the desired test point. It should be ensured that the testing surface is kept clean and smooth as far as possible so that uniform contact between the load plate and the surface is maintained throughout the test. The test is then conducted by following the underlying steps:

I. The loading plate and the sensors are placed to ensure they are resting on a firm and stable test surface.

II. The weight is dropped from a predetermined height set by the manufacturer and allowed to fall freely to create the desired load pulse. The device is calibrated to a predetermined drop height by the manufacturer and should not be changed by the user.

III. Initially, three preconditioning load pulses are applied, after which the test data are recorded for the subsequent three tests.

IV. The peak plate deflection resulting from each load pulse is recorded and the dynamic Elastic modulus of the tested material is calculated using Equation 3.1.

$$E = \frac{A.P.r(1-\nu^2)}{d} \tag{3.1}$$

where,

E= Stiffness Modulus/ Elastic Modulus (MPa)

A = Plate rigidity factor, default = 2 for a flexible plate, π/2 for a rigid plate.

P = maximum contact pressure (kPa)

r = plate radius (m)

ν = Poisson's ratio (usually in the range 0.3-0.45 depending on test material type)

d = peak deflection (mm)

Figure 3.13 (a) and (b) shows the Light Weight Deflectometer and Dynamic Cone Penetrometer test. The LWD and DCP tests were performed for each of the LVR sections before the procurement of soil from the field at field moisture content and density. The LWD results were taken as the average of three readings, whereas a single DCP test was conducted after conducting the LWD tests.

Figure 3.13: (a) Dynamic Cone Penetration test (b) Light Weight Deflectometer

3.6 Summary

This chapter provided a detailed description on the various test protocols, methodologies and material used in the research. The results of the basic laboratory characterization showed that the soils used in this study are fined grained soils with IS/USCS classification of CL, CI and MI. Furthermore, the plasticity index of the soils was 9-18.1%, and therefore can be classified as low to medium plastic in nature. Additionally, Cohesion was observed to vary in the range of 35-50 kPa, whereas the angle of internal friction varied 25°C to 30°C. The initial tangent modulus determined from the UCS tests ranged within of 27-40 MPa was obtained for the eight soils (Soil#1-Soil#8). Furthermore, CBR tests in unsoaked conditions ranged in the range of 8.5-14.5%. A drastic decrease in CBR values were observed for soaked CBR tests, which ranged within 3.5-7.8 %.

CHAPTER 4

Numerical Simulation of the CBR Test

4.1 General

The CBR is a complex triaxial stress system, where the soil mass is subjected to deviatoric stress by the penetrating plunger and the confining stress by the rigid steel mould. Whereas in the RLTT, the stress state of the soil element can be ascertained by simple arithmetic, the same cannot be said for the CBR specimen under repeated loading. Although the deviatoric or plunger stress can be measured during the experiment, direct measurement of the confining stress during laboratory experimentation is not straightforward. However, a thorough understanding of the stress state of the soil mass in a CBR mould is essential to infer the results of the RLCBR test. This can be achieved through numerical modelling of the CBR using the Finite Element approach. The objective of numerical modelling of the CBR test was to understand the stress state within the CBR test and establish mathematical relationships of the bulk stress and the octahedral shear stress with the plunger stress.

4.2 Details of the numerical model

4.2.1 Model Geometry

The CBR test was numerically modelled using the finite element approach in the commercially available software LS-DYNA®. The computational domain comprised of the soil specimen of 150 mm diameter, 125 mm height and CBR plunger of diameter 50 mm. The model attributes are described in Table 4.1.

Table 4.1: Model attributes of FE based CBR test

Sl. No.	CBR Part	Element Type	No. of Nodes	No. of Elements	Deformable/ Rigid	ELFORM
1	Plunger	SOLID	3707	3200	Rigid	TYPE 1
2	Soil	SOLID	71631	69440	Deformable	TYPE 1

4.2.2 Loads and Boundary conditions

Explicit modelling of the CBR mould, surcharge weight, and their contact with the soil will increase the computational time as this will require modelling their

interaction with the soil using a suitable contact algorithm. The contact algorithms govern the required timestep in the computations as additional equations are required to be solved at the interfaces, thereby increasing the computational time requirement. Therefore, instead of explicitly modelling plunger load, surcharge weight and the mould, the model was simplified by assuming appropriate boundary and loading conditions at the soil-surcharge interface and soil-mould-wall interface. This led to a significant increase in the computational efficacy of the current modelling approach. Subsequently at later stages it will be shown that these assumptions do not affect the results as compared to experimental results. Figure 4.1 (a) shows a schematic of the CBR test, and the simplified numerical model of the same is shown in Figure 4.1 (b). The details of boundary conditions and loads are summarized in Table 4.2.

Table 4.2: Boundary condition and load details

Sl. No.	Interface (As in Figure 4.1(b))	Boundary Condition/ Load
1	Surface load interface B	5 kg surcharge simulated as pressure around the rigid plunger
2	Circumferential interface C	Horizontal fixity to simulate mould rigidity
3	Bottom interface D	Fixed boundary condition
4	CBR plunger	Prescribed displacement @1.25 mm/min as per BIS standards

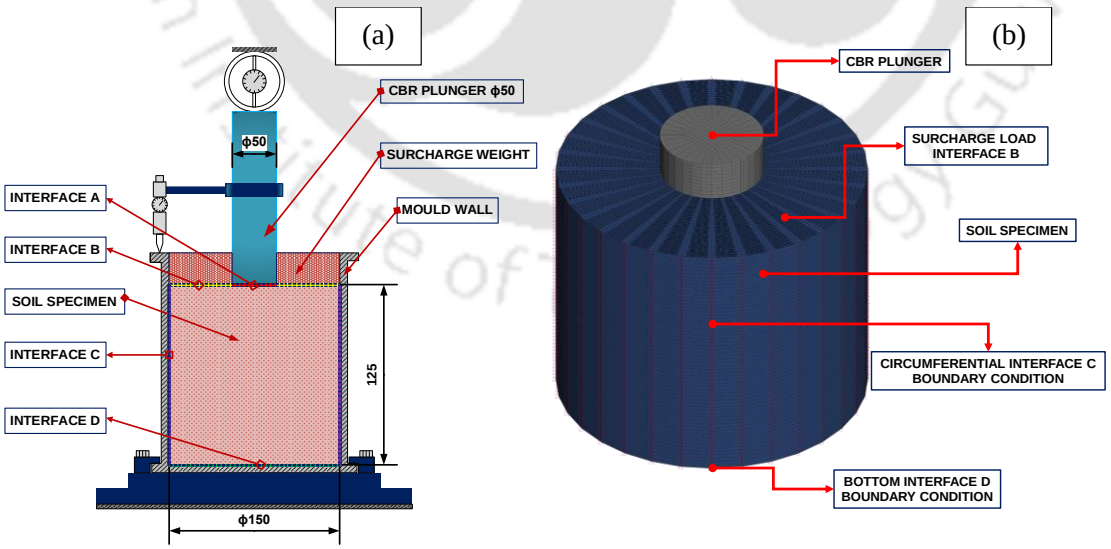

Figure 4.1: (a) Schematic of the laboratory CBR test (b) Finite element model of California bearing test used in this study

4.2.3 Material Model

The soil material was modelled using the Mohr Coulomb Elasto plastic model. In a typical stress state, the stress-strain behavior of the model exhibits linearity within the elastic range, governed by two fundamental parameters derived from Hooke's law: Elastic modulus (E) and Poisson's ratio (ν). Additionally, the failure criteria are determined by two parameters, namely the friction angle (ϕ) and cohesion (c). Moreover, the model incorporates a parameter to describe the flow rule, known as the Dilatancy angle (ψ). For the purpose of model validation, the Elastic modulus of the soils described in Table 3.3 was determined by conducting Unconfined compressive strength tests as per IS 2720 (Part X) at the optimum moisture content and maximum dry density. Further, Direct shear tests were conducted on the soils to determine the Cohesion (c) and angle of internal resistance (φ). The Poisson's ratio of a particular soil is not constant but depends on the physical soil state in terms of density and moisture content. Bowles reported Poisson's ratio values in the range of 0.1-03 for soils (Bowles, 1978). Narzary and Ahamad (2018) reported values ranging from 0.2-0.5 for subgrade soils. IRC 37: 2018 suggests a Poisson's ratio value of 0.35 to be used for subgrade soils in pavement design. Therefore, typical Poisson's ratio values can be expected to vary in the range of 0.1-0.35. For the validation, the Poisson's ratio was varied in the range of 0.10-0.20 based on the soil density (Narzary and Ahamad, 2018). However, the simulations were carried out with Poisson's ratio values of 0.1-0.35.

4.2.4 Meshing and Mesh sensitivity analysis

Appropriate grid and grid-independent solution strategy is the primary requirement of any mesh based computational technique such as the finite element method (FEM), finite difference method (FDM), or the finite volume method (FVM). In this present study, a hexahedral mesh-based grid was prepared for approximation of CBR results. Several solid elements are available to discretize the domain of a finite element model, such as the hexahedron or brick element, the tetrahedron, and the pentahedron. Chosing the type of element for discretization of the domain primarily depends upon the complexity of the geometry, the nature of the problem, and the desired level of accuracy within and at the boundary of the domain. Based on the recommendations of the LS-DYNA® theory manual, tetrahedron and pentahedron elements should be avoided due to the possibility of degenerate elements, which tend

to produce unstable solutions. Furthermore, the hexahedral elements fail when there is a need to discretize a complex domain as the mesh quality in terms of aspect ratio, orthogonality etc. gets significantly compromised. However, when discretizing a simple geometry like the CBR test, the hexahedral elements have been found to give the best solutions due to their uniform aspect ratio and orthogonality (Mendoza and Caicedo, 2019; Narzary and Ahamad,2018). Based on the CBR test domain and the recommendation from the LS-DYNA® theory manual, hexahedral element was used for meshing the domain.

Further, the solution obtained from FEM should be grid independent. For this purpose, a mesh sensitivity analysis was carried out in the present study. The mesh sensitivity analysis is the evaluation of the computational strategy for different grid sizes of the domain. A computational strategy will be grid-independent when the solution obtained does not change abruptly on changing the mesh size. In this regard, the main objective of mesh sensitivity analysis was to obtain the optimal size of the mesh. The computational domain having different mesh sizes and model attributes for mesh sensitivity analysis is described in Table 4.3.

Table 4.3: Model attributes of FE based CBR test

Sl. No.	CBR Part	Element Type	Mesh Size (mm)	No. of Nodes	No. of Elements	Deformable/ Rigid	ELFORM
1	Plunger	SOLID	1.25	3707	3200	Rigid	TYPE 1
2	Soil	SOLID	10	1694	1456	Deformable	TYPE 1
3	Soil	SOLID	7.5	3528	3145	Deformable	TYPE 1
4	Soil	SOLID	5	12090	11200	Deformable	TYPE 1
5	Soil	SOLID	2.5	89760	86400	Deformable	TYPE 1
6	Soil	SOLID	1.25	186951	181900	Deformable	TYPE 1

Figure 4.2 shows various mesh sizes used for the sensitivity analysis. The test case having serial number 1 in Table 4.7 was used for the mesh sensitivity analysis. The load penetration curve from the CBR model using the above grids was obtained and shown in Figure 4.3. Further, the CBR values using different mesh sizes were computed and graphically compared in Figure 4.4. Figure 4.3 shows that at higher grid sizes (10 mm) the load carrying capacity is slightly lower than the finer grid sizes, indicated by a lower load-penetration graph. Similarly, in Figure 4.4, an inverted U shape can be

observed when the CBRs are compared for the different grid sizes considered, indicating that the lowest load was sustained at the highest grid size. The probable reason for this trend is the geometric discontinuity between the plunger and the soil specimen and the presence of singularity at the edge of the plunger, which results in very high stress concentrations. The FEM fails to find a feasible solution for such a case as stress tends to infinity, leading to erroneous results. Whenever a finer mesh is used, this error can be localized, meaning that the error can be confined to within the few elements in the vicinity of the point of singularity, without getting propagated to the other elements of the model, This can be observed in Figure 4.3 and Figure 4.4, where the percentage error decreases as a refined mesh is used.The solutions obtained from these grids depict that the grid size is important when the soil is at the verge of failure. The higher size of grids resulted into over stiff behaviour of the soil which is not true. Further, the reduction in grid sizes reduces the stiffness in the solutions and accurately matches with the experimental results. Although all grid sizes provide closer results but if we consider the nearest solution as compared to experimental results and mesh independent solution then it is evident that the 2.5 mm mesh size is the optimum mesh for the prediction of CBR values. Therefore, the adopted mesh size for further investigation is 2.5 mm.

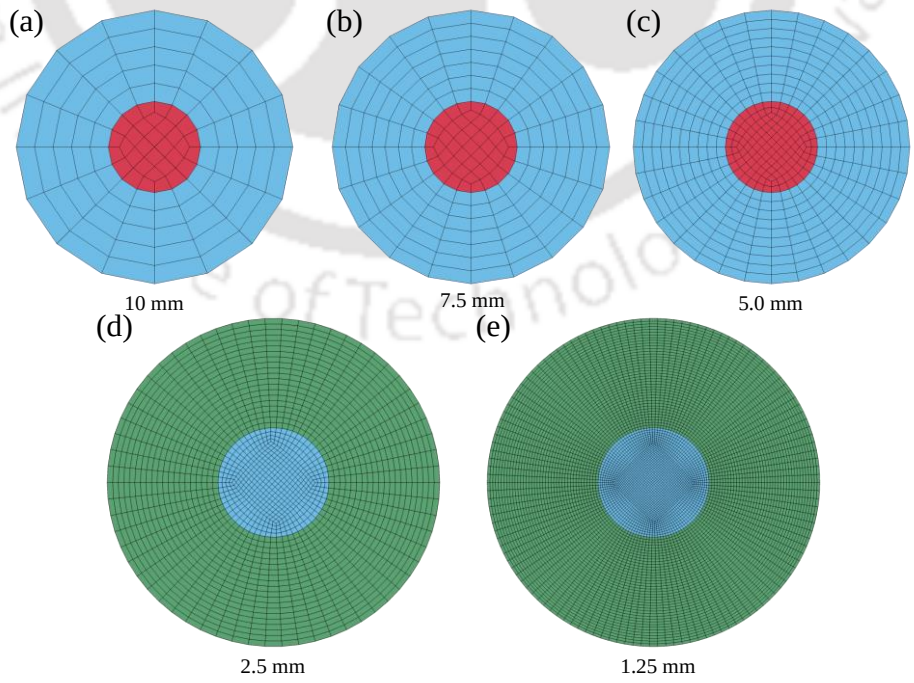

Figure 4.2: Mesh sizes used for sensitivity analysis of numerical model

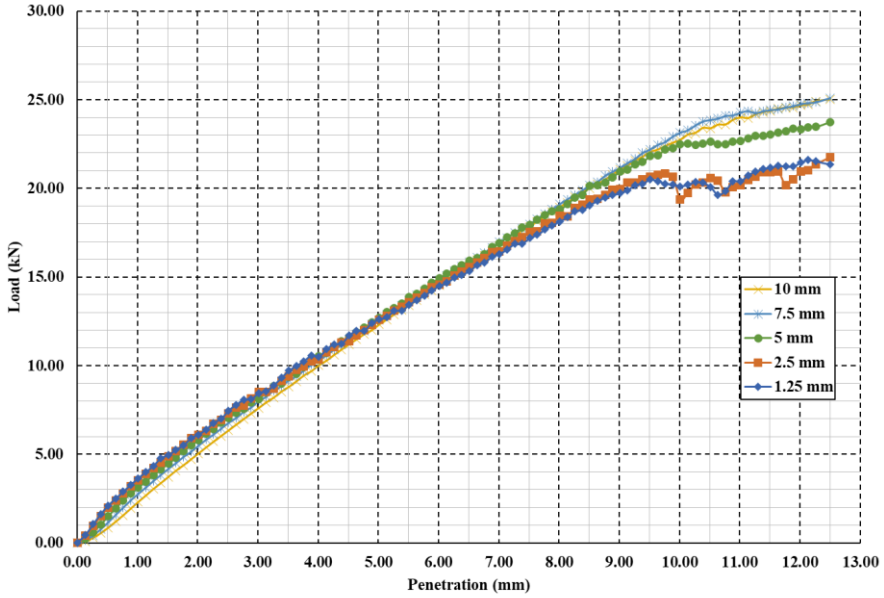

Figure 4.3: The load penetration curve obtained using different grid size

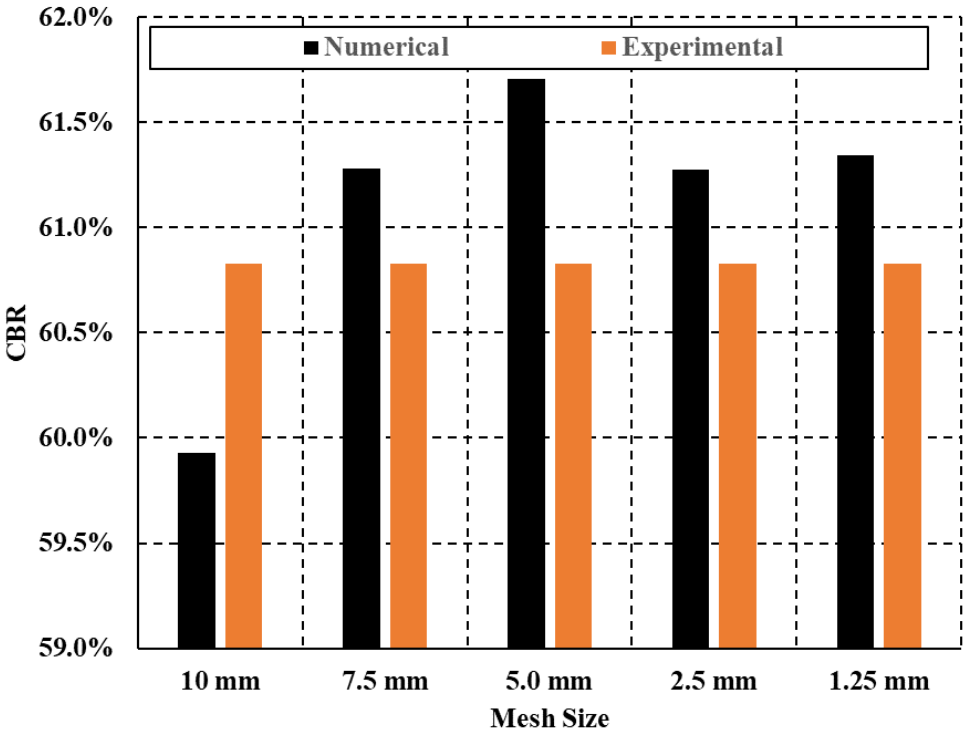

Figure 4.4: Predicted CBR for different mesh size

4.3 Validation of Numerical model

The validation of the numerical model was carried out in two stages: (i) Validation with data from literature (ii) Validation using laboratory experimental data

for the eight soils reported (Soil#1-Soil#8) in Table 3.1. For the stage 1 validation, data reported in Narzary and Ahamad (2018), was used to validate the CBR model. The reason for selecting the particular research work for validation is that the complete set of inputs for a Mohr Coulomb material model was available. The CBR values and the Load sustained by the specimen at 12.5 mm penetration data from laboratory experiments as reported in the research paper were compared with the same parameters from the current model, using material model parameters as reported in Table 4.4. An error analysis was conducted as shown in Table 4.5, which showed that mostly all the CBR values predicted by the numerical model is within 5% of the experimental values reported. The comparison with the load sustained by the specimen at 12.5 mm from the Load penetration graph (F_{FEM}) shows good agreement as well, however the percentage error ranged within 10-30%. Considering that RLCBR testing is mostly confined in the elastic regime of the material behaviour, this error range was considered acceptable. To understand the effect of the dilatancy angle (ψ) on the load penetration behaviour in the CBR tests, trial simulations were carried out at ψ=0°, ψ=(φ-30°)/n, where n= 2,4,6,8. It was observed that for the soils considered in this study, which were fine grained cohesive soils, better results were observed at lower dilatancy angles. Similar observations were also observed by Narzary and Ahamad (2018), and therefore the dilatancy angle was set as zero in all the simulations.

In case of validation with the laboratory data, the load penetration curves from the experimental CBR tests and simulated CBR tests were compared for the eight soils (Soil#1-Soil#8) reported in Table 3.1. Good agreement was observed between both sets of data. A typical load penetration graph for soil#6 obtained from the FEM and compared with the laboratory data is shown in Figure 4.5**Error! Reference source not found.**. Additionally, the error analysis pertaining to CBR and the load sustained at 12.5 mm are presented in Table 4.6. It can be observed that the FEM predicted CBR were within 10% of the experimental values. On the other hand, the F_{FEM} values could be seen to be deviating more than 20% in certain cases. However, as the application of the model is within the elastic regime of the load penetration curve, the model can be rendered adequate for application.

Table 4.4: Properties used for numerical model validation (Narzary and Ahamad (2018))

Sl. No.	CE (%)	Compaction Type	MC (%)	Dry Density (g/cm^3)	Poisson's Ratio (ν)	c (kPa)	φ (°)	E (MPa)	G (MPa)	Experimental Results	
										CBR %	F_{LAB}(kN)
1	100	Heavy	14.0	1.81	0.2	123.12	36.50	101.77	42.40	60.83	21.8
2	75	Heavy	14.0	1.78	0.2	116.30	37.60	86.24	35.93	52.41	19.72
3	50	Heavy	14.0	1.74	0.15	109.00	38.31	76.82	33.40	45.53	16.59
4	25	Heavy	14.0	1.67	0.15	92.27	42.92	27.68	12.03	24.65	8.74
5	100	Light	16.5	1.72	0.15	91.81	41.70	19.36	8.42	19.18	7.11
6	75	Light	16.5	1.66	0.15	76.37	39.40	13.43	5.84	15.40	5.03
7	50	Light	16.5	1.61	0.10	61.46	38.70	10.36	4.71	11.79	3.62
8	25	Light	16.5	1.53	0.10	55.37	37.20	4.97	2.26	6.86	2.23
9	100	Heavy	12.0	1.78	0.20	104.83	36.50	110.66	46.11	63.75	24.03
10	100	Heavy	13.0	1.80	0.20	121.24	36.50	110.61	46.08	62.73	23.43
11	100	Heavy	15.0	1.80	0.20	108.90	39.00	65.67	27.36	43.60	15.61
12	100	Heavy	16.0	1.78	0.20	92.60	43.23	30.56	12.73	27.15	10.71
13	100	Light	14.5	1.68	0.15	84.11	43.53	20.62	8.97	22.40	7.53
14	100	Light	15.5	1.70	0.15	88.34	43.23	18.18	7.90	19.03	7.05
15	100	Light	17.5	1.70	0.15	67.76	40.70	19.34	8.41	17.23	6.24
16	100	Light	18.5	1.69	0.15	61.61	39.00	15.66	6.81	14.29	5.02

**Note*: CE*: Compaction energy;* MC*: Moisture Content;* F_{LAB}*: Load sustained at 12.5 mm in the laboratory test*

Table 4.5: FE based model results and error analysis (Narzary and Ahamad, (2018))

Sl. No.	CE (%)	Compaction type	Experimental Results (Narzary and Ahamad, 2018)		FE Results (Present study)		% Error in CBR	$\frac{F_{FEM}}{F_{LAB}}$	% Error in F_{LAB}
			CBR (%)	F_{LAB}(kN)	CBR %	F_{FEM}(kN)			
1	100	Heavy	60.83	21.26	62.53	21.35	-2.79	1.00	-0.42
2	75	Heavy	52.41	18.6	52.25	19.03	0.31	0.98	-2.31
3	50	Heavy	45.53	16.56	45.74	18.83	-0.46	0.88	-13.71
4	25	Heavy	24.65	8.11	23.63	10.30	4.14	0.79	-27.00
5	100	Heavy	63.75	22.98	64.45	18.63	-1.10	1.23	18.93
6	75	Heavy	62.73	22.95	65.86	21.82	-4.99	1.05	4.92
7	50	Heavy	60.83	21.26	62.53	21.35	-2.79	1.00	-0.42
8	25	Heavy	43.6	14.54	44.66	18.58	-2.43	0.78	-27.79
9	100	Light	19.18	6.57	18.92	7.16	1.36	0.92	-8.98
10	75	Light	15.40	4.79	16.10	4.79	-4.55	1.00	0.00
11	50	Light	11.79	3.61	10.91	3.42	7.46	1.06	5.26
12	25	Light	6.86	2.21	6.72	1.86	2.04	1.19	15.84
13	100	Light	22.4	7.4	21.82	6.97	2.59	1.06	5.81
14	100	Light	19.03	6.83	19.00	6.36	0.16	1.07	6.88
15	100	Light	17.23	6.32	19.1	7.16	-10.85	0.88	-13.29
16	100	Light	14.29	5.15	13.81	4.74	3.36	1.09	7.96

Note: CE: Compaction energy; F_{LAB}: Load sustained at 12.5 mm in the laboratory test; F_{FEM}: Load sustained at 12.5 mm from the FEM model; $\%\ Error\ in\ CBR = \frac{Experimental\ CBR - FEM\ CBR}{Experimental\ CBR} * 100$; $\%\ Error\ in\ F_{LAB} = \frac{F_{LAB} - F_{FEM}}{F_{LAB}}$

Table 4.6: Validation of numerical model with laboratory test data

Soil ID	Experimental results		Numerical results		% Error	
	CBR (%)	F_{Lab} (kN)	CBR (%)	F_{FEM}	CBR (%)	F_{FEM}
Soil#1	14.5	4.7	14.3	5.5	1.38	-17.02
Soil#2	9.5	2.8	10.1	3.4	-6.32	-21.43
Soil#3	10.1	3.0	10.8	3.2	-6.93	-6.67
Soil#4	8.5	2.4	9.1	2.7	-7.06	-12.50
Soil#5	12.6	3.8	13.2	4.3	-4.76	-13.16
Soil#6	10	3.2	10.2	3.3	-2.00	3.12
Soil#7	8.7	2.5	8.7	3.1	0.00	-24.00
Soil#8	9.5	2.9	10.4	3.2	-9.47	-10.34

Note *; F_{LAB}: Load sustained at 12.5 mm in the laboratory test; F_{FEM}: Load sustained at 12.5 mm from the FEM model; ;*$\%\ Error\ in\ CBR = \frac{Experimental\ CBR - FEM\ CBR}{Experimental\ CBR} * 100$ *; $\%\ Error\ in\ F_{LAB} = \frac{F_{LAB} - F_{FEM}}{F_{LAB}}$*

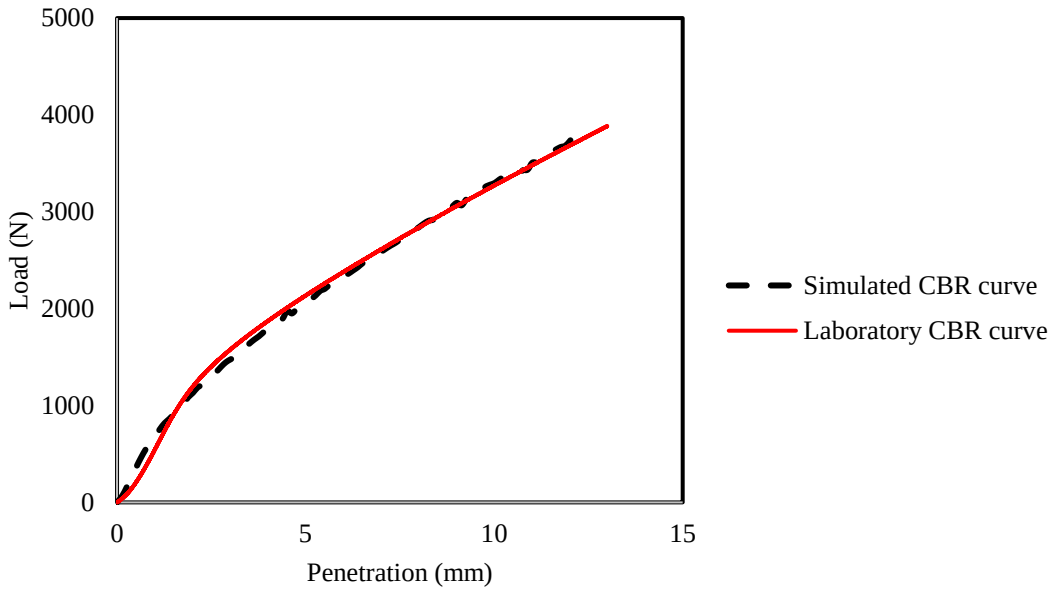

Figure 4.5: Validation of numerical model with laboratory data (Soil#6)

4.4 Results of numerical analysis

The validated numerical model was used to establish possible mathematical relationships between the bulk and octahedral shear stress with the plunger stress. The plunger stress determined during laboratory CBR tests can then be used to estimate the bulk and octahedral shear stress within the CBR specimen under plunger loading. Figure 4.6 shows the stress contours of the compressive (z stress), bulk stress (θ), and Von mises stress. It can be observed that the stress bulb in each of the three cases is mostly confined within the area under the plunger load. Therefore, a representative average bulk and Von Mises stress can be obtained by averaging the stress in all the elements within this bulb. The region under the plunger (50 mm diameter) and a representative depth of 2/3rd of the specimen height was considered appropriate, and the average bulk and Von Mises stress were calculated as the average of stresses in all the elements within this volume. The Von Mises stress was converted into the Octahedral shear stress, as shown in Equation 4.1.

$$Octahedral\ shear\ stress = \frac{\sqrt{2}}{3}\ x\ Von\ Mises\ stress \tag{4.1}$$

Simulations were performed at various combinations of Elastic modulus and Poisson's ratio for the type of soil considered, as summarized in Table 4.7. Elastic moduli and Poisson's ratios were selected based on the possible range for typical fine-grained soil, factoring in the effect of moisture fluctuations and soil compaction level in the field. A higher Poisson's ratio is representative of lower moisture contents, whereas a lower Poisson's ratio is representative of high moisture content within the soil matrix (Hicks, 1970; Monismith, 1971). Therefore, the possible field moisture variations in the soil were mimicked by varying the Poisson's ratio (0.1-0.35) and the Elastic modulus (10 MPa-100 MPa) of the soil in the FE simulations. This increased the applicability of the developed regression equations from the FEM and as well as the final predictive model for the RLCBR test. The plunger stress, bulk stress and the Von mises stress data were then extracted at three different penetration levels of 1 mm, 2 mm and 3 mm, which was mostly within the elastic range of the soil. Under these conditions, a simple linear relationship was observed between the average bulk and octahedral shear stress, as expressed in Equations 4.2 and 4.3.

$$\theta_{avg} = 0.2882\sigma_p, \text{ R}^2 = 0.996 \quad (4.2)$$

$$\tau_{avg} = 0.1787\sigma_p + 1.167, \text{ R}^2 = 0.997 \quad (4.3)$$

Where

θ_{avg}= Average bulk stress in the CBR specimen under plunger loading (MPa)

σ_p = Plunger stress (MPa)

τ_{avg}= Average octahedral shear stress in the CBR specimen under plunger loading (MPa).

Table 4.7: Elastic Modulus and Poisson's ratio combinations used in simulations

Elastic Modulus (MPa)	Poisson's ratio	Penetration
10	0.10,0.15,0.20,0.25,0.30,0.35	1 mm, 2 mm, 3 mm
20	0.10,0.15,0.20,0.25,0.30,0.35	1 mm, 2 mm, 3 mm
30	0.10,0.15,0.20,0.25,0.30,0.35	1 mm, 2 mm, 3 mm
40	0.10,0.15,0.20,0.25,0.30,0.35	1 mm, 2 mm, 3 mm
50	0.10,0.15,0.20,0.25,0.30,0.35	1 mm, 2 mm, 3 mm
60	0.10,0.15,0.20,0.25,0.30,0.35	1 mm, 2 mm, 3 mm
70	0.10,0.15,0.20,0.25,0.30,0.35	1 mm, 2 mm, 3 mm
80	0.10,0.15,0.20,0.25,0.30,0.35	1 mm, 2 mm, 3 mm
90	0.10,0.15,0.20,0.25,0.30,0.35	1 mm, 2 mm, 3 mm
100	0.10,0.15,0.20,0.25,0.30,0.35	1 mm, 2 mm, 3 mm

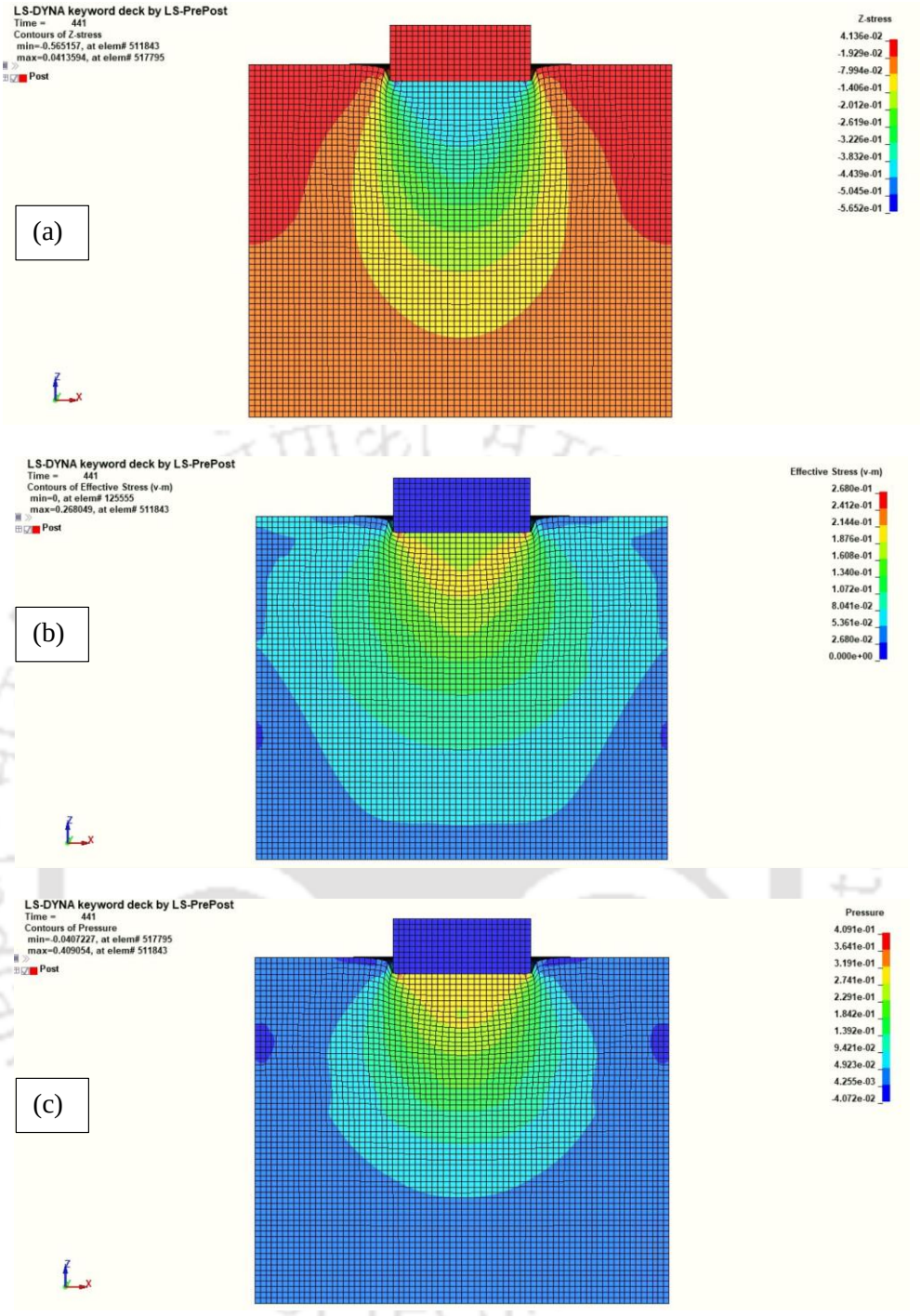

Figure 4.6: Stress contours of (a) z-stress (b) Effective stress or the Von Mises stress (c) Bulk stress within the CBR specimen under the plunger loading for E = 50 MPa, ν = 0.35 and penetration = 2 mm

4.5 Summary

This chapter presented the details of the numerical model formulated using the FEM approach to simulate the CBR test. The objective of conducting the numerical modelling was to obtain a simple mathematical relationship between the bulk stress, octahedral shear stress and the plunger stress, which can be measured experimentally. The model was formulated in 3D workspace with the commercial package LS-DYNA®. A mesh sensitivity analysis was conducted to select the optimum mesh size, which was finalized to be 2.5 mm. Further, the model was validated using data from the literature, as well as laboratory measured data for eight soils (Soil#1-Soil#8). It was observed that for the given range of cohesion (c) and angle of internal friction (φ), the specimen yielded after 3 mm penetration. Therefore, simulations were conducted for several assumed combinations of Elastic modulus (E) (10-100 MPa) and Poisson's ratio (ν) (0.1-0.35) for typical fine-grained soils considered in this study. The bulk stress, octahedral shear stress and the plunger stress data were extracted at three different penetrations: 1 mm, 2 mm and 3 mm, resulting in 180 total simulations. Octahedral shear stress and bulk stress were taken as average of the stresses of each element within the stress bulb. A simple linear relationship was established between the bulk stress and the plunger stress, octahedral shear stress and the plunger stress. For a given plunger stress, the average bulk stress and octahedral shear stress can be estimated using the proposed Equation 4.2 and 4.3, respectively.

CHAPTER 5

Deformation Controlled RLCBR Test and Predictive Modelling

5.1 General

This chapter presents a methodology and predictive model for determination of the resilient modulus of subgrade soils using the RLCBR test. Despite extensive research in the last decade, previous studies on RLCBR (Repeated Load California Bearing Ratio) test protocols and models relied on assumed combinations of elastic modulus and Poisson's ratio values for regressing the model parameters, which may not accurately represent the actual properties of the soil. Additionally, the stress state of the subgrade soil has a significant impact on its resilient behavior, making it crucial to use a representative resilient modulus that considers the in-situ stress conditions of in-service pavements (George& Uddin,2000; Puppala,2008). Therefore, this chapter proposes a novel methodology and a predictive model that provides a more comprehensive characterization of subgrade soil modulus using the RLCBR test. This methodology considers the state of stress within the soil under the complex triaxial loading of the CBR test and relates it to the stress state of a typical stress element within an in-service pavement, aiming to provide more realistic estimates of the resilient modulus.

5.2 Methodology

Opiyo (1995) postulated that the elastic modulus of a soil specimen under repeated plunger loading can be estimated using a modified model based on the deflection of an elastic half space under a rigid plate (Equation 2.21). The model shows that the resilient modulus for an assumed Poisson's ratio depends on the plunger stress encountered and the resulting resilient deformation, with three unknown model coefficients. Now, to estimate the resilient modulus for subgrade soils, a testing protocol and a corresponding predictive model can be proposed which estimates the resilient modulus at the recommended stress levels of θ = 85 kPa and τ_{oct}= 21 kPa as per MEPDG recommendations(Mazari *et al*.,2013;MEPDG, 2004). For this, the model parameters a_1, a_2, a_3 have to be regressed using appropriate values of resilient modulus (M_r), Plunger stress (σ_p) and resilient deformation (u). Of the 12 soils considered in this

study, 8 were used for the RLCBR model development. Figure 5.1 presents the proposed framework for the RLCBR model.

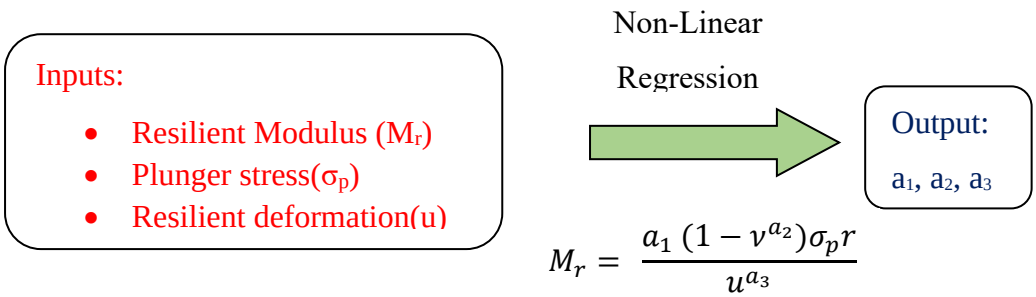

Figure 5.1: Framework for RLCBR model development

STEP 1: Determination of plunger stress (σ_p) and resilient deformation (u)

The plunger stress and resilient deformations were determined by conducting RLCBR tests in deformation-controlled mode (as described in Chapter 3) on 8 soils: Soil#1-Soil#8. Tests were conducted at three moisture contents (OMC-3, OMC and OMC+3) resulting in 24 test combinations. Three replicates were tested at each test condition and the average of the three were reported as the average resilient deformation and plunger stress for that particular test condition.

STEP 2: Determination of resilient modulus for model fitting

The MEPDG constitutive model as described in Chapter 2, Table 2.4 was used to determine the resilient modulus. The model considers stress state variation within the pavement structure based on the octahedral shear stress and the bulk stress as shown in Equation 5.3.

$$M_r = k_1 P_a \left(\frac{\theta}{P_a}\right)^{k_2} \left(\frac{\tau_{oct}}{P_a} + 1\right)^{k_3} \quad (5.1)$$

Where

M_r = Resilient Modulus; P_a = Atmospheric pressure; θ = Bulk stress; τ_{oct} = Octahedral Shear stress (√2/3 x Von Mises stress); k_1, k_2, k_3 are model coefficients, which were determined in this study using LTPP empirical correlations as described in Equations 2.13 to 2.18.

To calculate the resilient modulus using the MEPDG model, an estimate of the soil specimen's bulk stress and octahedral shear stress is required. As the bulk stress and the

octahedral shear stress cannot be directly calculated in case of an RLCBR test, a numerical model using the FEM approach was used to establish simple mathematical relationships between the plunger stress which can be measured during the RLCBR test with the average bulk and octahedral shear stress of the soil under plunger loading as described in Chapter 4 as follows:

$$\theta_{avg} = 0.2882\sigma_p, \text{ R}^2 = 0.996$$

$$\tau_{avg} = 0.1787\sigma_p + 1.167, \text{ R}^2 = 0.997$$

The experimentally obtained plunger stress was used to compute the bulk stress and octahedral shear stress of the soil under the CBR plunger loading using the relations obtained from the FEM analysis. The estimated bulk stress and the octahedral shear stress, along with empirically determined coefficients from were used in the Mechanistic Empirical Pavement Design Guide (MEPDG) constitutive model to estimate the resilient modulus.

STEP 3: Non-linear least square regression to obtain a_1, a_2, a_3

The resilient modulus calculated along with the plunger stress and resilient deformation was used to fit Equation 2.21 by carrying out a non-linear least square regression to obtain parameters a_1, a_2, a_3. The proposed model was then validated with RLCBR test data for four independent subgrade soils over a range of moisture contents. The detailed research methodology is described in Figure 5.2.

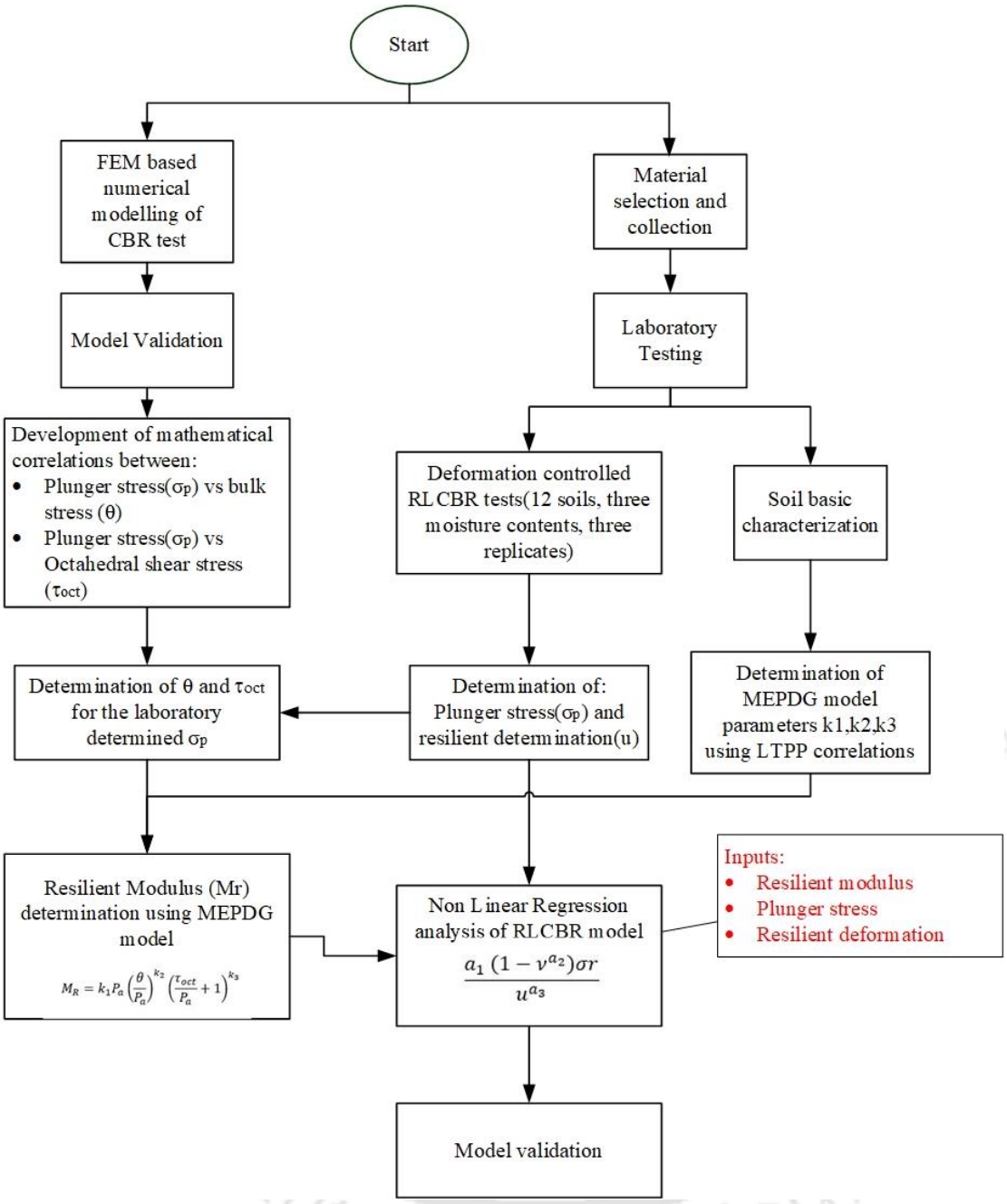

Figure 5.2: Research Methodology

5.3 RLCBR test results

RLCBR tests were carried out on the twelve soils reported in

Table ***3.1*** in displacement-controlled mode, as described in chapter 3. Tests were carried out at MDD at three different moisture contents to account for moisture variability in the field. The plunger stresses for the various soils used in the study are presented in Figure 5.3. The plunger stress was observed to vary in the range of 185-960 kPa for the twelve soils tested. A significant effect of moisture was observed on the plunger load for each soil. A clear declining trend was observed in an increase in moisture content, as expected. When the moisture content increased from OMC-3 to OMC+3, a decrease of 69% in plunger stress was observed for Soil#1, whereas a decrease of 25% was observed for Soil#9 and Soil#11, respectively. An increase in water content reduces the plunger stress due to two reasons: (i) Lubricating effect of water: As the moisture content increases, the residual water in the pores creates a thin water film around the soil particles. This decreases the load taking capacity of the soil as the soil particles get easily reoriented under the plunger load. (ii) Development of pore water pressure within the voids: At high saturation levels, pore pressure develops under plunger loading. As pore water pressure develops, the effective stress in the soil decreases, resulting in decrease in both strength and stiffness of the soil.

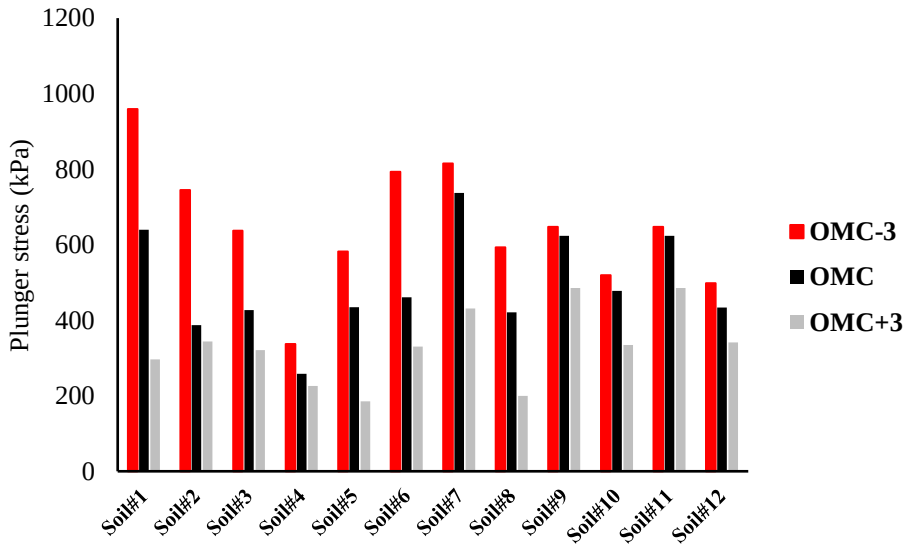

Figure 5.3: Effect of moisture content on plunger stress

5.4 Average bulk and octahedral shear stress calculation from the plunger stress

In order to achieve meaningful estimates of the resilient modulus, it is essential to ensure that the bulk stress under the CBR plunger within the specimen remains consistent with the stress levels experienced by the subgrade layer in a pavement under actual in-service conditions. An appropriate reference for comparison of the bulk and octahedral shear stress is the AASHTO T307 (2003), which provides standard specifications for conducting the RLTT. The AASHTO T307 recommends 15 confining and deviatoric stress sequences, representing the typical stress encountered by a subgrade element within its service life. Figure 5.4 presents a comparison of the stresses within the CBR specimen with the stresses encountered by the subgrade soil in a typical pavement structure. Results revealed that the bulk stress, computed for the specified elastic modulus and Poisson's ratio, exhibited a range between 30.2 kPa to 654 kPa. Similarly, the octahedral shear stress demonstrated variations within the 37.5 kPa to 391 kPa range. Analysis of the stress sequences from AASHTO T307, however show that the bulk stress within a typical subgrade element range within 69-234 kPa, whereas the octahedral shear stress varies from 13-52 kPa. Therefore, there is a need for introduction of a correction factor into the computed bulk and octahedral stresses. Araya (2011) and Leischner (2022) introduced correction factors into the model to account for this. However, another approach is to rescale the data within the required range (Miradi *et al*., 2009; Ghorbani *et al*.,2020). Rescaling of the data was carried out using Equations 5.1 and 5.2, so that the data is re adjusted within the range of stresses encountered by a typical subgrade (Miradi *et al*.,2009). Such a scaling does not alter the statistics of the model, while predicting data over the required range.

$$\theta_{corrected} = \theta_s(\min) + \frac{(\theta_s(max) - \theta_s(\min))(\theta_{avg} - \theta_{avg}(\min))}{(\theta_{avg}(max) - \theta_{avg}(\min))} \quad (5.2)$$

$$\tau_{corrected} = \tau_s(\min) + \frac{(\tau_s(max) - \tau_s(\min))(\tau_{avg} - \tau_{avg}(\min))}{(\tau_{avg}(max) - \tau_{avg}(\min))} \quad (5.3)$$

Where

$\theta_{corrected}/\tau_{corrected}$ = Corrected bulk/Octahedral stress

$\theta_s(\min)/\tau_s(\min)$ = Minimum bulk/Octahedral stress on a subgrade soil element from AASHTO T307

$\theta_s(max)/\ \tau_s(\max)$ = Maximum bulk/ octahedral shear stress on a subgrade soil element from AASHTO T307

$\theta_{avg}(\min)$ / $\tau_{avg}(\min)$ = Minimum average bulk/octahedral shear stress under plunger loading obtained from the FEM

$\theta_{avg}(max)$ / $\tau_{avg}(\max)$ = Maximum average bulk/octahedral shear stress under plunger loading obtained from the FEM

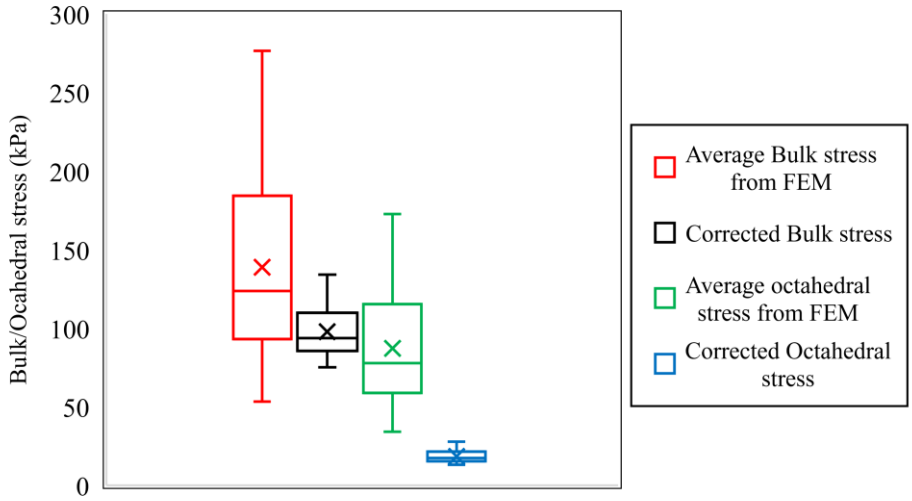

Figure 5.4: Average and corrected bulk and octahedral shear stresses obtained from FEM

5.5 Resilient modulus calculation using the MEPDG constitutive model

Once the average bulk and octahedral shear stresses are computed for a particular test condition, it can be used in the MEPDG constitutive model to evaluate the resilient modulus for the soil specimen, once the model coefficients k_1, k_2, k_3 are known. The bulk and octahedral shear stresses for the RLCBR specimens under plunger load were determined following the methodology outlined in section 5.4. Additionally, the model coefficients k_1, k_2, and k_3 were derived using the empirical correlations from the Long-Term Pavement Performance (LTPP) database (Amber and Von Quintos,2002). The LTPP empirical correlations offer various equations to estimate the MEPDG model parameters based on fundamental soil properties. Due to the extensive dataset used in developing these empirical correlations, they have demonstrated significant potential in predicting the resilient modulus (M_r) of subgrade soils (George, 2004). Furthermore,

the LTPP correlations account for the impact of moisture and density variations. Equations 2.13 to 2.18 represent the LTPP correlations applicable to fine-grained silty and clayey soils.

The method of points estimate was used to evaluate the impact of the inherent material variability on the resilient modulus (M_r) computed using LTPP correlations. Instead of directly calculating the model coefficients, the soil's basic properties were treated as random variables, with mean values obtained from laboratory test results and the coefficient of variation (COV) taken from literature. Subsequently, the resilient modulus was estimated as a dependent random variable. Point estimate method was employed to determine the first and second moments (mean and variance) of the dependent random variable (George,2004).

Let Y be a function of four random variables x_1, x_2, x_3 and x_4, then

$$Y = f(x_1, x_2, x_3, x_4)$$

Then, the mean and variance of Y are given by,

Mean, $\mu_Y = P_{++}Y_{++} + P_{+-}Y_{+-} + P_{-+}Y_{-+} + P_{--}Y_{--}$

Variance, $\sigma_Y^2 = P_{++}Y_{++} + P_{+-}Y_{+-} + P_{-+}Y_{-+} + P_{--}Y_{--} - \mu_Y^2$

Where

$Y_{++} = Y(x_{1+}, x_{2+}, x_{3+}, x_{4+})$;

$Y_{--} = Y(x_{1+}, x_{2-}, x_{3+}, x_{4-})$;

$Y_{-+} = Y(x_{1-}, x_{2+}, x_{3-}, x_{4+})$;

$Y_{--} = Y(x_{1-}, x_{2-}, x_{3-}, x_{4-})$;

$x_+ = \mu_x + \sigma_x$;

$x_- = \mu_x + \sigma_x$;

$P_{++} = P_{--} = 0.25(1 + r_{x1,x2} + r_{x2,x3} + r_{x3,x4} + r_{x4,x1}$;

$P_{+-} = P_{-+} = 0.25(1 - r_{x1,x2} - r_{x2,x3} - r_{x3,x4} - r_{x4,x1}$; and

$r_{x1,x2}$, $r_{x2,x3}$, $r_{x3,x4}$, $r_{x1,x4}$ are the correlation coefficient between x_1,x_2,x_3 and x_4. If x_1, x_2, x_3 and x_4 are independent, then $r_{x1,x2} = r_{x2,x3} = r_{x3,x4} = r_{x1,x4} = 0$.

Varying all the independent variables at a time renders the method to be excessively complex. Therefore, at a time, four independent variables were varied by a unit standard

deviation, and the resultant expected variation on the resilient modulus was quantified. George (2004) conducted a sensitivity analysis on the LTPP model response variables and ranked them in the order of higher to lower sensitivity. Based on the results of the sensitivity study, the response variables selected for variation and their coefficient of variations (COVs) are summarized in Table 5.1.

Table 5.1: COVs for basic soil properties used in the point estimate method (George, 2004)

Soil type	Rank	Soil property	Coefficient of variation (COV)
Clay	1	w_c	15
	2	P_{200} %	15
	3	%Clay	25
	4	% Silt	25
Silt	1	w_c	15
	2	PI%	30
	3	%Clay	25
	4	%Silt	25

The resilient moduli for the eight soils in various moisture contents were calculated utilizing the MEPDG constitutive model, represented by Equation 5.1. The results of the model coefficients obtained using LTPP empirical correlations and corresponding resilient modulus for the computed average bulk and octahedral shear stress for the eight soils used for development of the RLCBR model (Soil#1-Soil#8) are summarized Table 5.2. Further, Table 5.3 presents the model coefficients for soil#9-Soil#12, which were used for validation of the proposed model.

Table 5.2: MEPDG model coefficients and resilient modulus at average bulk and octahedral shear stress of the CBR specimen (Soil#1-Soil#8)

Soil ID	OMC-3				OMC				OMC+3			
	k_1	k_2	k_3	M_r	k_1	k_2	k_3	M_r	k_1	k_2	k_3	M_r
Soil#1	1.299	0.28	-2.157	95.93	1.167	0.28	-2.268	82.18	1.036	0.28	-2.379	46.44
Soil#2	1.053	0.203	-1.52	85.99	0.922	0.203	-1.623	77.77	0.791	0.203	-1.726	45.46
Soil#3	1.055	0.37	-1.409	85.91	0.924	0.37	-1.511	61.39	0.793	0.37	-1.614	45.92
Soil#4	0.966	0.23	-2.38	73.62	0.835	0.23	-2.456	44.37	0.704	0.23	-2.532	35.86
Soil#5	0.948	0.257	-1.252	79.47	0.817	0.257	-1.36	62.3	0.686	0.257	-1.468	47.07
Soil#6	1.128	0.251	-1.426	93.06	0.997	0.251	-1.555	73.79	0.866	0.251	-1.684	47.61
Soil#7	1.284	0.301	-1.936	99.05	1.153	0.301	-2.055	91.05	1.022	0.301	-2.173	56.35
Soil#8	1.123	0.27	-2.777	69.37	0.992	0.27	-2.887	57.79	0.861	0.255	-3.089	26.56

Table 5.3: MEPDG model coefficients for Soil#9-Soil#12(Used for model validation)

Soil ID	OMC-3			OMC			OMC+3		
	k_1	k_2	k_3	k_1	k_2	k_3	k_1	k_2	k_3
Soil#9	1.032	0.216	-2.073	0.921	0.216	-2.493	0.81	0.216	-2.913
Soil#10	1.221	0.164	-1.482	1.11	0.164	-1.902	0.999	0.164	-2.321
Soil#11	1.118	0.197	-2.565	0.987	0.197	-2.663	0.899	0.197	-2.728
Soil#12	1.203	0.259	-2.327	1.072	0.259	-2.425	0.984	0.259	-2.489

5.6 Model development: Non-linear least square regression

Once the resilient modulus was estimated as shown in section 5.5, the parameters a_1, a_2, a_3 of Equation 2.21 were obtained by conducting a non-linear least square analysis. The least square regression requires three parameters as input: the resilient modulus (M_r), the plunger stress (σ_p) and the resilient deformation(u), as already discussed. Using a non-linear least square regression, the model coefficients a_1, a_2, a_3 of Equation 2.21 were determined and the resulting Equation 5.4 can be expressed as follows:

$$Mr = \frac{1.888(1-\mu^{1.616})\sigma_p r}{u^{0.908}} \quad (5.4)$$

Equation 5.4 provides an estimation of the resilient modulus for the stress state that a subgrade soil element is likely to experience throughout its service life. However, MEPDG recommends the resilient modulus to be predicted specifically at θ = 85 kPa and τ_{oct} = 21 kPa. Therefore, Equation 5.4 needs to be standardized to the recommended stress level by multiplying with an appropriate correction factor. **Figure *5.5*** shows a graph plotted with RLCBR modulus obtained using Equation 5.4 in the x-axis, and the representative resilient modulus at the recommended stress level in the y axis for the eight soils at various test conditions. If a trendline is fitted to the obtained data with the intercept set to zero, it can be observed that on an average, the representative resilient modulus are 0.844 times the RLCBR modulus determined using Equation 5.4.Therefore, a correction factor of α= 0.844 was multiplied with Equation 5.4, and the modified equation can be presented as in Equation 5.5.

$$Mr = \frac{1.593(1-\mu^{1.616})\sigma_p r}{u^{0.908}}, \; R^2 = 0.95 \quad (5.5)$$

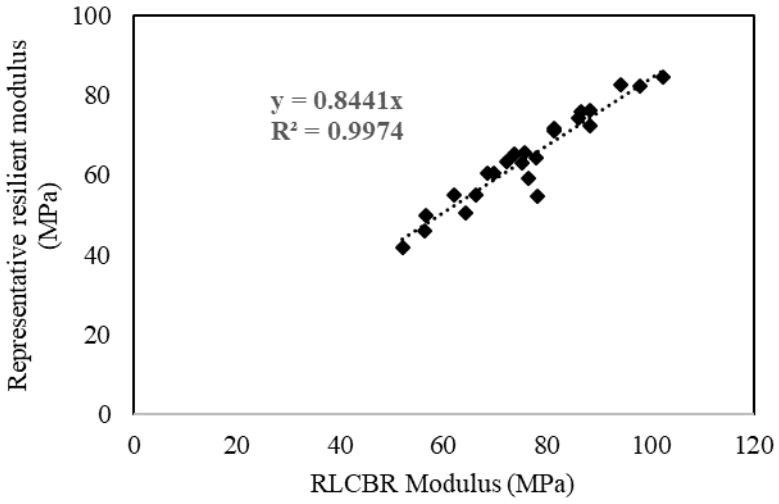

Figure 5.5: Determination of correction factor

5.7 Validation of developed model and performance assessment

To validate the proposed model, RLCBR tests were conducted on four independent fine-grained soils (Soil#9-Soil#12) at three moisture contents. The RLCBR modulus estimated using Equation 5.5 was compared with the resilient modulus calculated from the MEPDG constitutive model at recommended stress levels of θ= 85 kPa and τoct= 21 kPa, with the model coefficients determined from the LTPP empirical correlations. The resilient modulus thus calculated is herein called the representative resilient modulus, which is representative of the stress state of the subgrade. The representative resilient modulus was calculated using a bulk stress (θ) of 12.4 psi (85 kPa) and an octahedral stress (τ_{oct}) of 3 psi (21 kPa) in the MEPDG model, with model parameters estimated using the LTPP correlations. The representative resilient modulus at three moisture content (OMC-3, OMC and OMC+3) of the 4 soils used for validation of the proposed model is shown in Figure 5.6.

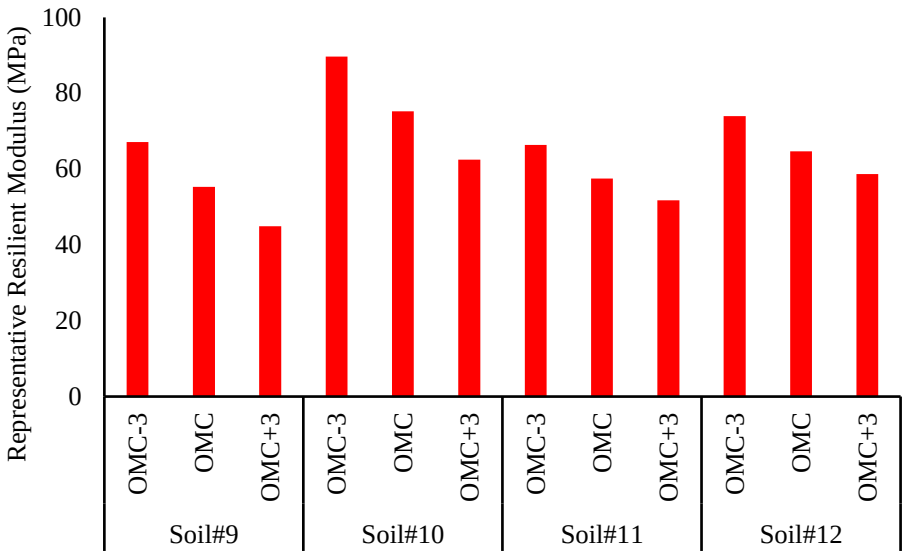

Figure 5.6: Representative resilient modulus for soil#9-soil#12

Figure *5.7* compares the representative resilient modulus with the RLCBR modulus calculated using the proposed model. The RLCBR modulus estimated using the proposed RLCBR model is almost equal to the representative modulus calculated using the MEPDG constitutive model with an R^2 of 0.99. Figure *5.8* through Figure 5.11 shows the comparison of RLCBR modulus calculated using various RLCBR models proposed in the literature with the representative resilient modulus calculated using the MEPDG constitutive model. It can be observed that the previous models over predicted the representative resilient modulus by 4-13% in general. However, Hao and Pabst (2021) model overpredicted the resilient modulus by about 41%. This is reasonable considering that the model was developed considering the high stress levels encountered by haul crushed waste rocks, and therefore may not be suitable for subgrade soils.

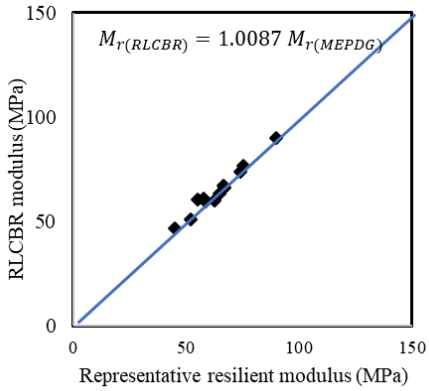

Figure 5.7: Comparison of RLCBR modulus of the proposed model with representative resilient modulus

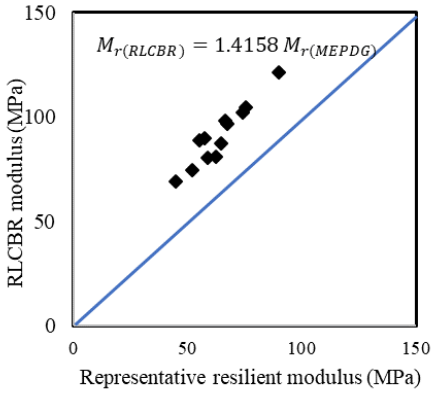

Figure 5.8: Comparison of RLCBR modulus from Hao and Pabst (2021) model with representative resilient modulus

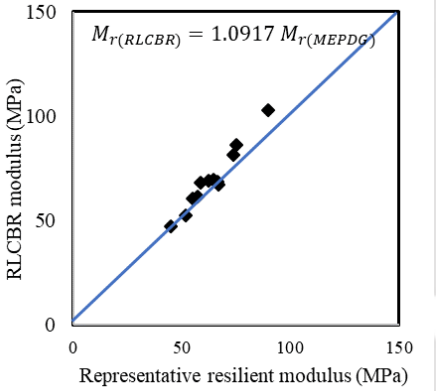

Figure 5.9: Comparison of RLCBR modulus from Araya (2011) model with representative resilient modulus

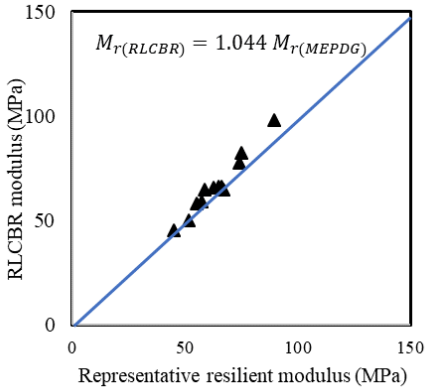

Figure 5.10: Comparison of RLCBR modulus from Molenaar (2007) model with representative resilient modulus

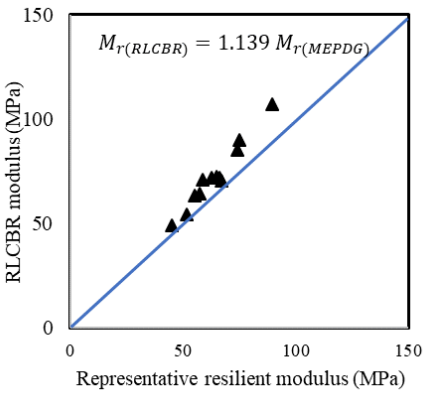

Figure 5.11: Comparison of RLCBR modulus from Opiyo (1995) model with representative resilient modulus

The performance and prediction capability of the models were further analysed by three metrics: the Mean absolute error (MAE); the Mean square error (MSE) and the root mean square error (RMSE). In technical terms, RMSE (Root Mean Square Error) represents the square root of the mean of the squared errors, whereas MAE (Mean Absolute Error) is the mean of the absolute values of errors. In this context, errors signify the difference between the predicted values (those generated by the regression model) and the actual values of a specific variable (Representative resilient modulus). Mathematically, The MAE, MSE and the RMSE can be represented by Equations 5.6 to 5.8.

$$MAE = \frac{\sum_{i=1}^{n}|y_i - x_i|}{n} \tag{5.6}$$

$$MSE = \frac{\sum_{i=1}^{n}(y_i - x_i)^2}{n} \tag{5.7}$$

$$RMSE = \sqrt{\frac{\sum_{i=1}^{n}(y_i - x_i)^2}{n}} \tag{5.8}$$

here

y_i= Model predicted resilient modulus

x_i = True value of resilient modulus (At recommended stress state)

N = Total number of data points

It can be observed from Table 5.4 that the MAE, MSE and the RMSE was significantly lower than the RLCBR models proposed earlier, when compared to the representative resilient modulus, implying a better prediction capability of the proposed model.

Table 5.4: Performance assessment of the proposed model

Parameter	Present model	Opiyo (NF)* (1995)	Molenaar (2007)	Araya (2011)	Hao and Pabst (2021)
MAE	1.66	8.61	3.31	5.58	27.15
MSE	4.41	93.66	17.11	46.70	760.79
RMSE	2.10	9.68	4.14	6.83	27.58

**Note: MAE: Mean absolute error; MSE: Mean square error; RMSE: Root mean square error*NF: No friction between mould and soil*

5.8 Statistical analysis of RLCBR modulus

Significance testing by student's t-test was used to analyze the effect of moisture on the subgrade resilient modulus determined using the proposed RLCBR model at α= 5%. In other words, whether the proposed model is capable of capturing the variation in moisture content was analyzed and the results are summarized in Table 5.5. The analysis was made separately for OMC-3 and OMC+3 specimens. The effect of moisture on the RLCBR modulus was found to be significant with a P-value <0.05, indicating that the proposed model can capture the effect of moisture on the soil modulus.

Table 5.5: t-test results for the proposed RLCBR model

Test Condition	P-value	Significant
OMC-3	0.0001	Yes
OMC+3	0.000	Yes

5.9 Comparison with field modulus

The laboratory RLCBR modulus using the deformation-controlled mode was compared with the Dynamic cone penetration and Light weight deflectometer modulus. Field tests were conducted on ten in service as per the procedures outlined in Chapter 3. Further, empirical correlations were used to calculate the a DCP modulus from the DCP index, whereas the LWD modulus was directly obtained from the device.

5.9.1 Field evaluation of pavements

Field evaluation was carried out by conducting Dynamic Cone Penetration test (DCPT) and Light Weight Deflectometer (LWD) test with test protocol as discussed in Chapter 3. The LVR sections comprised a granular subbase layer and a granular base layer topped by 20 mm of Open Graded Premix carpet (OGPC). Test pits of 50 cm x 50 cm were excavated upto the subgrade level. This was followed by conducting three LWD tests at subgrade level, followed by a DCP test as per ASTM D6951 guidelines. A solitary DCP test was performed at the subgrade level at each road section. The DCP index for the subgrade layer was computed as the average of the DCP indices for the entire subgrade layer. The average DCPI was then used to calculate the field modulus using Mohammad *et al*.(2008) empirical relation. Lastly, field moisture content was measured and density was assessed using the core cutter method/Sand replacement method.

5.9.2 Comparison of field and laboratory modulus

A comparison of the field and laboratory modulus is presented in Table 5.6. A direct correlation analysis would not be meaningful as the RLCBR modulus was estimated at OMC MDD at stress level of θ= 85 kPa and τ_{oct}= 21 kPa. It must be noted that, the laboratory tests were conducted at OMC-MDD state in controlled laboratory conditions. However, the field modulus was obtained in field conditions at moisture contents and density much different than that in the lab. Further, the operational differences between the LWD, DCP and the RLCBR modulus, contribute to the differences in modulus values of the soil. Furthermore, it can be observed that the DCP modulus was higher than the LWD modulus for all the cases. Considerable difference between the field modulus and the laboratory modulus was observed for soil#1, soil#2, soil#4, and #7. This can be explained by the much higher field moisture content for the soils. The laboratory RLCBR modulus was generally higher than the field-calculated modulus. Further, a relatively closer value was observed between the LWD modulus for Soil#5 and Soil# 8. The moisture and density conditions in the field can explain this. A lower field moisture content and higher field density (>90% of MDD) in both cases was observed, suggesting the significant influence of the density and moisture on subgrade resilient modulus. The comparison assessment of the field and RLCBR test results suggest that a reference modulus from the laboratory RLCBR test can be used to evaluate the construction quality in the field in terms of modulus in addition to

traditional density checking. Hence the resilient modulus prediction model developed using RLCBR, a quick and simple test, could provide more inputs to quality control characteristics in the field for the construction of subgrade soils.

Table 5.6: **Comparison of laboratory RLCBR modulus with field modulus**

Soil ID	FDD	FMC	Avg DCP modulus	LWD Modulus		RLCBR modulus
				Avg.	Std.Dev	
Soil#1	1.421	22.22	37.8	22.22	1.21	87.00
Soil#2	1.531	24.21	41.0	24.55	0.49	75.30
Soil#3	1.710	19.13	55.2	50.44	1.58	72.68
Soil#4	1.531	22.39	30.2	22.39	0.57	63.65
Soil#5	1.621	17.21	60.5	54.5	2.36	67.27
Soil#6	1.501	20.10	42.1	36.07	0.86	80.86
Soil#7	1.532	21.45	29.8	21.99	0.48	87.33
Soil#8	1.521	17.85	57.5	52.38	1.11	81.11

5.10 Summary

A novel methodology and predictive model for the RLCBR test has been proposed in this chapter. The model can be used by practicing engineers to obtain the resilient modulus values of subgrade soils, while gathering important information like the load deformation data. For any resilient modulus predictive model, it is important to correlate with the stress levels that is expected for a subgrade element in a in service pavement. To address this issue, a novel methodology was used for model development with due consideration of state of stress of the soil within the CBR mould under plunger loading. Eight soils predominantly used as subgrades were used to develop the model. Deformation controlled RLCBR tests were conducted at three different moisture contents to take in to account the probable moisture variations in the field.

A nonlinear regression analysis was carried out to obtain the model coefficients. The model was validated with RLCBR experimental data from four independent subgrade soils, by comparing the RLCBR modulus using the proposed model with the resilient modulus obtained using the MEPDG model at recommended stress states of θ= 85 kPa and τ_{oct} = 21 kPa, which showed very good agreement. Further, the predictive capacity of the model was assessed using the mean absolute error (MAE), mean square error (MSE) and the root mean square error (RMSE).

Comparison with models from the literature showed that the proposed model significantly reduced the error parameters, thus exhibiting better prediction capabilities for subgrade soils. In addition, statistical analysis shows the effect of moisture on RLCBR modulus to be significant at α = 0.05, indicating that the proposed model could capture the effect of moisture on the resilient modulus.

To sum up, if RLCBR tests are conducted on fine grained subgrade soils in deformation-controlled mode with a target deformation of 1.5 mm, the resilient modulus at the recommended stress levels of θ= 85 kPa and τ_{oct} = 21 kPa can be obtained with the following model.

$$Mr = \frac{1.593(1-\mu^{1.616})\sigma_p r}{u^{0.908}}$$

CHAPTER 6

Load Controlled RLCBR Results

6.1 General

Subgrade soils are stress dependent non-linear elastic materials (Seed *et al*.,1967; Dunlap, 1963). For pavements of high importance as in the case of MEPDG Level 1, the stress dependent behaviour of the soil needs to be characterized appropriately. It is commonly done by using a resilient modulus constitutive model, either a two parameter or a three-parameter model. For Level 2 analysis of the MEPDG, the subgrade resilient modulus is calculated as a single representative value considering a recommended stress state for a typical pavement structure in the MEPDG model. The model coefficients are obtained through empirical correlations with simple soil properties. However, in Level 1 analysis of the MEPDG, the model parameters (k_1, k_2, k_3) are directly used as input in the MEPDG AASHTOWARE software. In this case, k_1, k_2, k_3 is estimated using a laboratory test to determine the model coefficients. Usually, for such characterization, the Repeated load triaxial test (RLTT) is conducted as per AASHTO T307 (2003) over fifteen stress sequences to obtain the model coefficients for a particular test condition. To address the need for a more cost-effective and simpler alternative to the RLTT, this chapter proposes a novel methodology using the Repeated Load CBR test (RLCBR) in load-controlled mode to determine the MEPDG constitutive model coefficients. The proposed model was then employed to describe the stress-dependent behavior of five subgrade soils across a range of moisture contents.

6.2 Determination of stress sequences for load controlled RLCBR test

To characterize the stress dependent behaviour of the subgrade soils, it is essential to apply repeated loading on the soil specimen which is representative of the ones experienced in the field. For an RLTT test, the stress states have been defined and recommended by the AASHTO T307 (2003). However, the same stress levels are not applicable to the RLCBR test as it is an indentation test, and the soil is subjected to higher stress levels. Furthermore, due to the indentation of a rigid plunger onto the soil specimen, it is difficult to apply a predefined load in a RLCBR test as the load sustained by the soil at a particular penetration depends on the soil strength.

The behaviour of a soil sample under CBR plunger loading changes from the elastic to plastic regime as the penetration increases. To determine the resilient modulus, it is important to ensure that the applied loads are within the elastic limit of the soil (AASHTO T307,2003; Araya, 2011). Therefore, before conducting an RLCBR test in the stress-controlled mode, it is essential to determine the peak load which can be sustained by the soil sample before it tends towards failure. This was determined by conducting unsoaked CBR tests on each soil at three different moisture contents (OMC-3, OMC and OMC+3). The curve can be idealised to be consisting of two limbs, one corresponding to the elastic behaviour and the other the plastic regime of the soil. A tangent was drawn coinciding with each limb of the soil and extended to intersect. The point of intersection, extended to the Y-axis gives the peak load that can be applied to a particular soil (P), as shown in Figure 6.1.

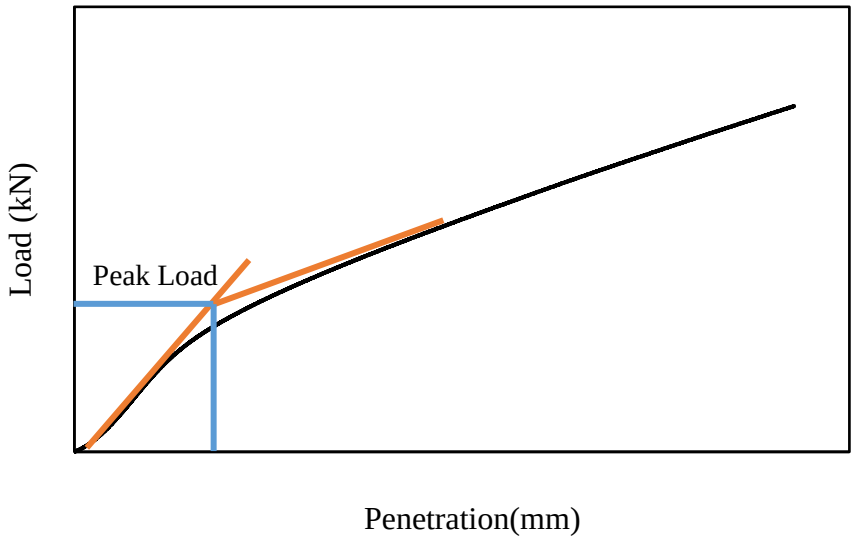

Figure 6.1: Determination of peak load for fixing of stress levels

It has to be noted that the value of peak load is different for different soils, depending on the strength of the soil. After obtaining the peak load (P), the stress sequences for the RLCBR test were fixed in terms of proportion of the peak load as shown in Table 6.1.

Table 6.1: Stress sequences applied in RLCBR test

Sl. No.	Load (kN)	Number of cycles	Remarks
1	0.20P	100	Conditioning Phase
2	0.25P	25	Testing Phase
3	0.30P	25	Testing Phase
4	0.40P	25	Testing Phase
5	0.50P	25	Testing Phase
6	0.60P	25	Testing Phase
7	0.70P	25	Testing Phase
8	0.80P	25	Testing Phase
9	0.90P	25	Testing Phase

A conditioning phase comprising of 100 load cycles were applied to the soil, post which eight stress sequences of 25 cycles each were applied at each stress sequence. A total of 25 load sequences were selected based on engineering judgement, as post 100 preconditioning cycles, the deformation was observed to be entirely resilient after 25 loading cycles for each stress sequence. Stress controlled RLCBR tests were conducted on five soils (Soil#1, Soil#3, Soil#5, Soil#6 and Soil#11) at three different moisture contents as per the procedure outlined in section 3.4.2. The peak loads at three moisture contents for the five soils as obtained from unsoaked CBR tests is presented in Figure 6.2. For the five soils used in this study, highest peak load was observed for Soil#11, whereas the lowest peak load was observed Soil#6. As expected, a decrease in peak load was observed when the moisture content changed from OMC-3 to OMC+3.

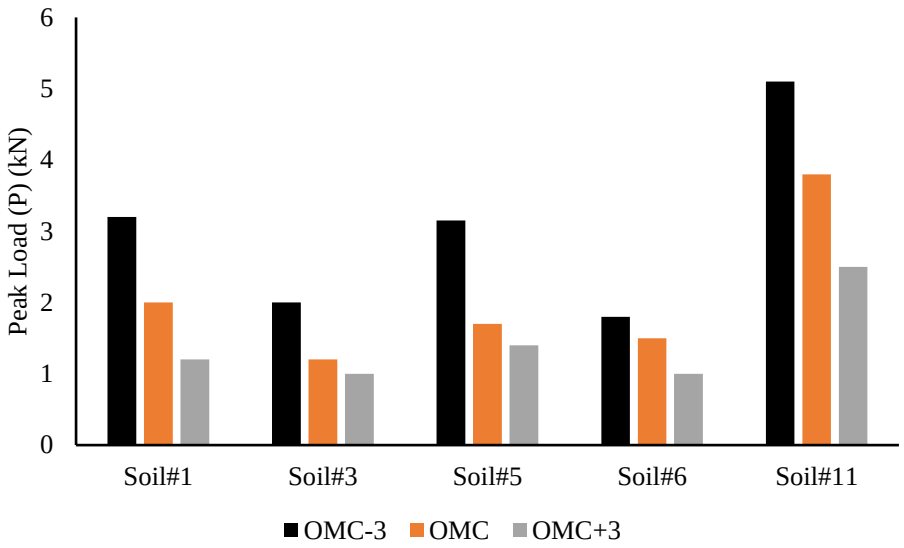

Figure 6.2: Peak load determined from unsoaked CBR tests

Now, once the peak load was obtained for each test condition, the applicable load for each stress sequence was determined and is summarized in Table 6.2. It must be noted that only five stress sequences were applied for the specimens at OMC+3. This was because the peak load being very low on the wet side of optimum, loads lower than 40% were difficult to apply manually.

Table 6.2 : Target loads for various stress sequences considered

Stress sequence (Load in kN)	Soil Name														
	Soil#1			Soil#3			Soil#5			Soil#6			Soil#11		
	OMC-3	OMC	OMC+3	OMC-3	OMC	OMC+3	OMC-3	OMC	OMC+3	OMC-3	OMC	OMC+3	OMC-3	OMC	OMC+3
S1= 0.20 P	0.64	0.40	---	0.40	0.24	---	0.63	0.34	---	0.36	0.30	---	1.02	0.76	---
S2= 0.25 P	0.80	0.50	---	0.50	0.30	---	0.79	0.43	---	0.45	0.38	---	1.28	0.95	---
S3 = 0.30 P	0.96	0.60	---	0.60	0.36	---	0.95	0.51	---	0.54	0.45	---	1.53	1.14	---
S4 =0.40 P	1.28	0.80	0.48	0.80	0.48	0.40	1.26	0.68	0.56	0.72	0.60	0.40	2.04	1.52	1.00
S5 =0.50 P	1.60	1.00	0.60	1.00	0.60	0.50	1.58	0.85	0.70	0.90	0.75	0.50	2.55	1.90	1.25
S6 = 0.60 P	1.92	1.20	0.72	1.20	0.72	0.60	1.89	1.02	0.84	1.08	0.90	0.60	3.06	2.28	1.50
S7 = 0.70 P	1.26	1.40	0.84	1.40	0.84	0.70	2.21	1.19	0.98	1.26	1.05	0.70	3.57	2.66	1.75
S8 = 0.80 P	1.44	1.60	0.96	1.60	0.96	0.80	2.52	1.36	1.12	1.44	1.20	0.80	4.08	3.04	2.00

6.3 Determination of MEPDG model coefficients (k_1, k_2, k_3)

The MEPDG constitutive model has been discussed in detail in previous sections. The model incorporates the effect of state of stress on the resilient behaviour of subgrade soils based on the bulk stress and the octahedral shear stress. Therefore, to obtain the model coefficients, corresponding to each stress sequence described in Table 6.2., the octahedral shear stress, the bulk stress and the resilient modulus needs to be known.

Calculation of θ and τ_{oct}

In case of the RLTT, the bulk and octahedral shear stress can be obtained using simple arithmetic. However, the same cannot be done in the case of the RLCBR test. The average octahedral shear stress and the average bulk stress were evaluated for each stress sequence using Equations 4.2 and 4.3 developed from the numerical model of the CBR test using Finite element approach. As already explained in previous chapters, the stress experienced by a CBR specimen under plunger loading is much larger than that experienced by a typical subgrade element in an in-service pavement, and therefore needs to be corrected (Araya, 2011; Leischner *et al.*,2022). Therefore, the bulk stress and octahedral shear stress used were corrected using Equations 5.1 and 5.2**.**

Calculation of resilient modulus (M_r)

In case of RLTT, the resilient modulus for each stress sequence can be easily computed as the ratio of the deviatoric stress to the resilient strain. However, the same cannot be done using the RLCBR test. The resilient modulus in this case can be calculated using Equation 5.4 described in section 5.6, with the equation as follows:

$$M_r = \frac{1.888(1-\mu^{1.616})\sigma_p r}{u^{0.908}}$$

This equation was developed considering the possible range of stress that an in-service subgrade element may encounter.

Non-Linear least square regression

The resilient modulus, the corrected average bulk and octahedral shear stress of the CBR specimen were used to carry out a non-linear least square regression analysis in

a solver platform. The framework for the non-linear regression analysis is shown in Figure 6.3.

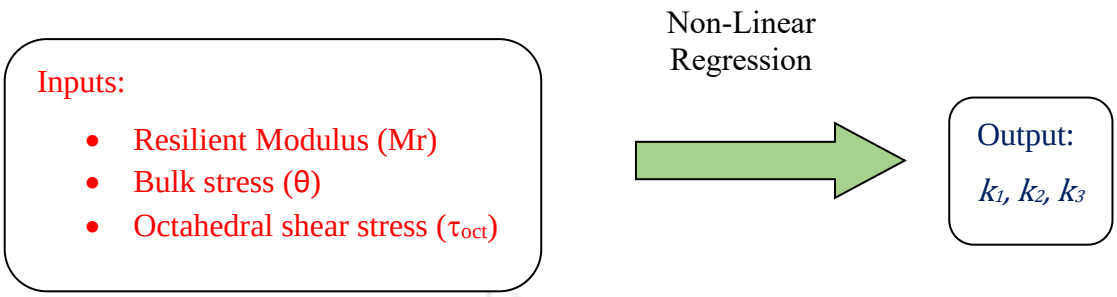

Figure 6.3: Framework for nonlinear regression analysis of MEPDG model with RLCBR data

Table 6.3 to Table 6.5 summarizes the MEPDG model coefficients obtained from the RLCBR tests conducted in load-controlled mode for the three moisture contents considered. It can be observed from Table 6.3 to Table 6.5 that the coefficients k_1, k_2 are positive, whereas the coefficient k_3 is negative. The positive values of the k_1 and k_2 coefficients depict the hardening effect on the soil for the increasing bulk stress. Whereas, the negative values of coefficient k_3 indicates the softening behaviour of the soil with an increase in octahedral shear stress. The behaviour of the soil in a particular state of stress can only be explained by putting appropriate values of stresses into the MEPDG constitutive model. Further, R^2 values of the model fit were observed to be greater than 0.80 in all the cases.

Table 6.3: MEPDG model coefficients from RLCBR test at OMC-3

Soil ID	k_1	k_2	k_3	R^2
Soil#1	1.1821	0.3050	-2.231	0.93
Soil#3	1.0210	0.3428	-1.481	0.85
Soil#5	0.9821	0.2821	-1.181	0.89
Soil#6	1.1201	0.2418	-1.532	0.92
Soil#11	1.3210	0.1721	-2.021	0.81

Table 6.4: MEPDG model coefficients from the RLCBR test at OMC

Soil ID	k_1	k_2	k_3	R^2
Soil#1	1.1591	0.2921	-2.281	0.94
Soil#3	0.9531	0.3321	-1.535	0.91
Soil#5	0.8341	0.2635	-1.292	0.87
Soil#6	1.0090	0.2389	-1.671	0.82
Soil#11	1.2105	0.1689	-2.029	0.82

Table 6.5: MEPDG model coefficients from the RLCBR test at OMC+3

Soil ID	k_1	k_2	k_3	R^2
Soil#1	1.0521	0.2601	-2.301	0.91
Soil#3	0.8051	0.3289	-1.682	0.89
Soil#5	0.6751	0.2481	-1.491	0.87
Soil#6	0.8691	0.2321	-1.732	0.83
Soil#11	0.9827	0.1521	-2.121	0.80

6.4 Validation of MEPDG model coefficients obtained from RLCBR test

The model coefficients obtained from RLCBR test data was validated using the model coefficients empirically obtained using the LTPP correlations. It was established by George (2004) that developed using a vast database of soils, the LTPP correlations are most potent in estimating the MEPDG model coefficients, yielding values closer to those obtained using the RLTT experimental data. The validation although an abstract one, provides promising results while pursuing a MEPDG Level 1 design. The validation of the model coefficients is presented in Figure 6.4, Figure 6.5 and Figure 6.6, respectively. As can be seen from the Figures, the coefficients

determined using RLCBR test shows promising correlations with the empirically determined model coefficients.

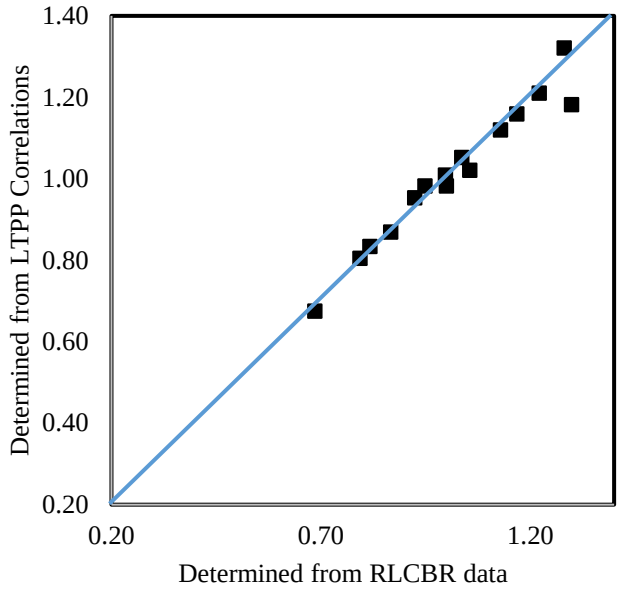

Figure 6.4: Validation of MEPDG model coefficient k_1

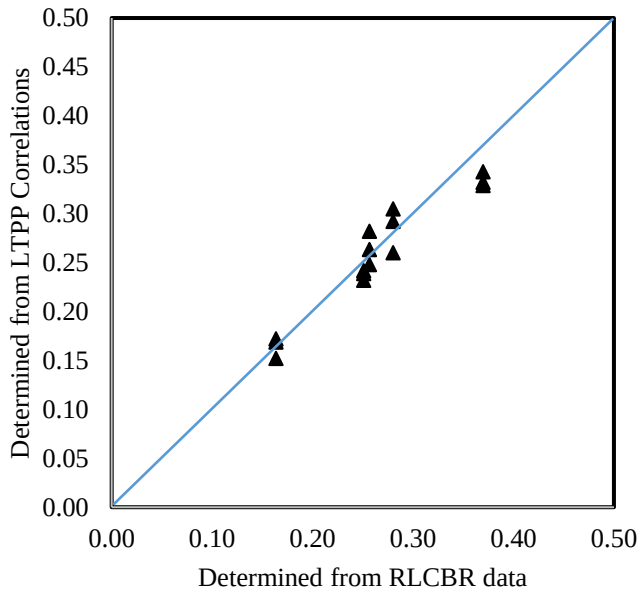

Figure 6.5: Validation of MEPDG model coefficient k_2

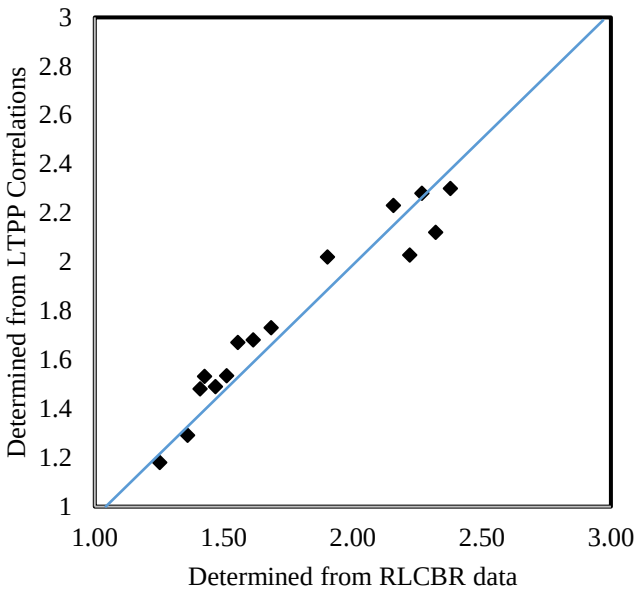

Figure 6.6: Validation of MEPDG model coefficient k_3

6.5 Effect of stress on soil behaviour

The effect of stress on the behaviour of the soil was analysed using the model coefficients determined using the RLCBR test results and the MEPDG constitutive model. Figure 6.7 through Figure 6.9 presents the results of effect of variation of stress on the resilient behaviour of soil#6 at different confining pressures (CF). It can be observed that with increase in axial or deviatoric stress a decrease in resilient modulus was observed, a phenomenon known as strain softening. As moisture content increased, the degradation with deviatoric stress becomes more rapid. Further, the effect of confining pressure was less pronounced as compared to the effect of deviatoric stress. At higher moisture contents, the effect of confining pressure becomes almost negligible as can be seen from Figure 6.9. Similar observations were made for the other four soils (Seed and McNeill,1958; Zhou and Gong, 2000; Narzary and Ahamad, 2021).

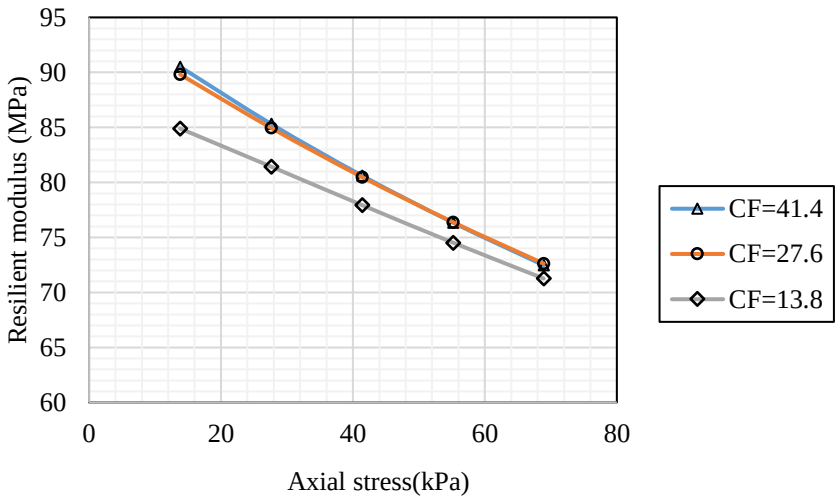

Figure 6.7: Variation of resilient modulus with axial stress (OMC-3)

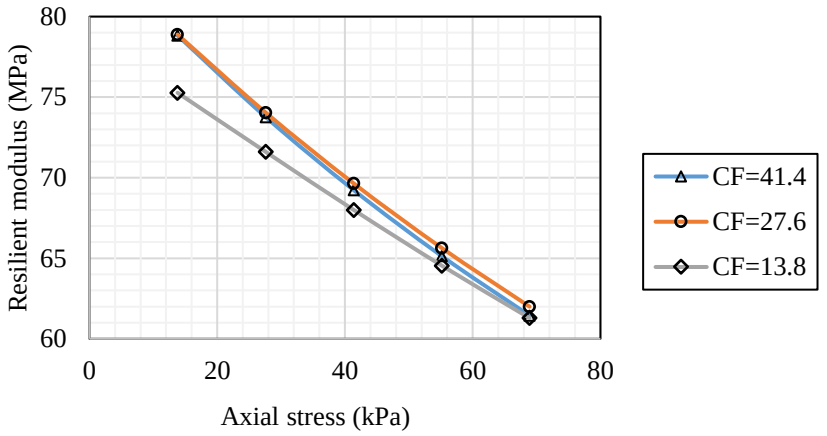

Figure 6.8: Variation of resilient modulus with axial stress (OMC)

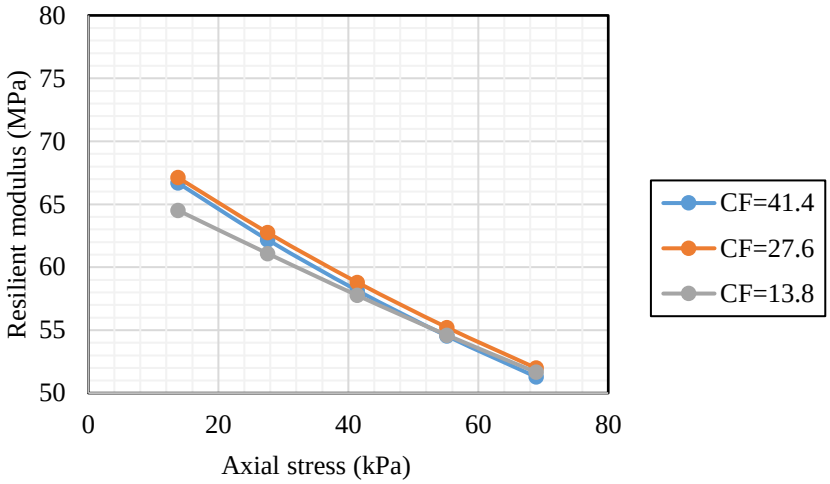

Figure 6.9: Variation of resilient modulus with axial stress (OMC+3)

6.6 Summary

This chapter presented the results of the RLCBR tests conducted in Load controlled mode. The nonlinear stress dependent characterization of soils is essential for pavements of high importance, usually the MEPDG Level 1. Conventionally it is done by carrying out a nonlinear least square regression analysis using the RLTT data. Alternately, a novel cost-effective methodology using the RLCBR test was proposed in this section to fit the MEPDG model parameters using the RLCBR test data. RLCBR tests were conducted in Load-controlled mode on five soils and three moisture contents, with eight stress sequences. The stress sequences were applied as percentages of the peak load within the elastic regime obtained from the unsoaked CBR tests. The bulk and octahedral shear stress corresponding to each stress sequence was then computed using correlations developed using the FEM analysis. The resilient modulus at each stress sequence was obtained using Equation 5.4. A nonlinear least square regression analysis was carried out for the eight load sequences in a solver platform and the MEPDG model coefficients were obtained for the five soils at three different moisture contents. The determined coefficients were validated by comparing with the model coefficients computed using the LTPP correlations. Although only a generalized comparison can be made using empirical correlations, promising results were observed towards utilizing the RLCBR test for MEPDG Level 1 characterization. Statistical analysis of the model coefficients showed that the effect of moisture on the coefficients were not significant. Further, the MEPDG model was used to evaluate the effect of

deviatoric stress and confining pressure on the soil resilient modulus. Results showed a strain softening behaviour of the soils under increasing deviatoric stress.

CHAPTER 7

Conclusions and Recommendations

7.1 General

Based on the extensive numerical, laboratory and field studies conducted, the following findings and contributions are highlighted:

7.1.1 Finite element modelling of the CBR test

A 3D Finite element model was formulated to study the CBR specimen's stress state. The significant findings from the numerical model of the CBR test were as under:

- Mesh sensitivity analysis showed that the 2.5 mm mesh size is optimum for FEM analysis. Model validation showed that the FEM model formulated has a relative error of less than 10% in all the cases considered.
- Analysis of the load v/s penetration curve showed that for the type of soils considered in this study, soil yielding takes place after 3 mm in all the cases, and therefore below 3 mm, the soil can be considered elastic.
- The analysis of stress contours within the specimen shows that the development of stresses within the specimen is mainly confined to the area below the plunger in the form of a bulb. Therefore, the bulk and octahedral stresses within the CBR specimen can be considered the average of stresses within this bulb.
- The specimen's average bulk and octahedral stress were 30-654 kPa and 38-391 kPa, respectively. Therefore, a correction factor must be applied when using the stresses for resilient modulus calculation for subgrade soils concerning what is encountered in the field.

  Contribution from the task:

- Under elastic conditions, a linear relationship was developed between the octahedral stress, bulk stress and the applied plunger stress.

$$\theta_{avg} = 0.2882\sigma_p, \text{ R}^2 = 0.996$$

$$\tau_{avg} = 0.1787\sigma_p + 1.167, \text{ R}^2 = 0.997$$

The developed relations can compute the specimen's average bulk and octahedral shear stress once the plunger stress is known.

7.1.2 Repeated Load CBR test in deformation-controlled mode

The RLCBR modulus depends on the plunger stress and the resilient deformation. The plunger stress in the deformation-controlled RLCBR test for the twelve soils varied in the 185-960 kPa range over the three moisture contents. A decrease in the range of 25%-69% was observed in the plunger stress when the moisture was increased from OMC-3 to OMC+3. Additionally, the resilient deformations varied in the range of 0.1 mm-0.35 mm.

***Contribution from the task*:**

- A new RLCBR predictive model was proposed using a novel methodology that considers the specimen's stress under plunger loading.

$$Mr = \frac{1.593(1-\mu^{1.616})\sigma_p r}{u^{0.908}}$$

- Validation of the proposed model with the resilient modulus calculated at θ= 85 kPa and τ_{oct}= 21 kPa using the MEPDG constitutive equations showed good agreement. Comparison with previously proposed models showed superior prediction capability of the model indicated by the lower mean absolute error, mean square error and root mean square error.
- The effect of moisture on the resilient modulus was significant when analysed using a student's t-test carried out at a significance level of α= 5%. Hence, the model could capture the effect of moisture variations on the resilient modulus of the soils.

7.1.3 Repeated Load CBR test in Load-controlled mode

The repeated load CBR test in load-controlled mode was used to characterize the stress-dependent behaviour of the subgrade soil. A methodology was proposed to use the RLCBR test to determine MEPDG model coefficients.

Contribution from the task:

A methodology to estimate the model coefficients from the RLCBR test was proposed as follows:

- *Step 1*: *Determination of peak load from unsoaked CBR tests*.
- *Step 2*: *Fixing the stress sequences.*
- *Step 3*: *Conducting load-controlled RLCBR tests on the soils at various test conditions*.
- *Step 4*: *Determination of average bulk and octahedral shear stress*.
- *Step 5*: *Calculation the resilient modulus at each stress sequence*.
- *Step 6*: *Determine* k_1, k_2, k_3 *using non-linear regression analysis or solver tools.*

The model coefficients were validated by comparing the model coefficients with that calculated using the LTPP empirical relations. The results show promising results towards utilising the RLCBR test for Level 1 MEPDG characterization.

The effect of deviatoric and bulk stress on the resilient modulus was analysed using the MEPDG constitutive model. A decrease in resilient modulus with deviatoric stress was observed for all the soils. However, the confining pressure's effect was less prominent than deviatoric stresses.

7.1.4 Comparison of laboratory and field modulus

A general range comparison was made between the field-determined elastic modulus and the laboratory-determined RLCBR modulus. Among the field moduli, the moduli calculated using DCP was higher than the LWD modulus in all cases. Further, comparison with laboratory modulus showed a significant difference exists between the field and laboratory moduli, especially for tests where the field moisture conditions were much different than the laboratory conditions. The differences can be attributed to the different physical states in the field and laboratory conditions and different operational differences between the devices.

7.2 Future scope

Based on the findings of the study, the following future works are proposed:

- The behaviour of the soil under repeated plunger load has not been considered while developing the models. Future work may focus on this area in delineating the softening and hardening behaviour of the soil under plunger loading.

- Responses from the RLTT test for varying materials and production conditions should be used to enhance the model predicting capacity.
- The proposed methodology and models can be extended for unbound granular materials, which would be useful for practicing engineers.
- Many experiments are required to consider the effects of soil physical states like moisture and compaction on the RLCBR modulus. Different compaction methods, compaction energy, and moisture variations must be evaluated to consider the effect of soil physical states on the RLCBR modulus.
- More field and laboratory testing must be conducted to establish meaningful correlations between the field and laboratory resilient modulus, which can be used for quality control and assurance of subgrades.

Publications

International conference

1. Kaushik, S.; S, Anjan Kumar. (2020). Characterization of resilient modulus of a clayey soil using the Repeated Load CBR (RLCBR) test, *Second ASCE India Conference on "Challenges of Resilient and. Sustainable Infrastructure Development in Emerging Economies*", March *2020*

2. Kaushik, S.; S, Anjan Kumar.; Ryntathiang, T.L. (2022). A study on the association between RLCBR and DCP subgrade moduli for Low Volume Road evaluation. *The 9th symposium on pavement surface characteristics (SURF,2022)*, September 12-14, 2022, Milan, Italy.

3. Kaushik, S., Kumar,S. and Siddagangaiah, A. K., *Estimation of subgrade resilient modulus using the Repeated Load CBR(RLCBR) test, 103rd Annual meeting of the Transportation Research Board/Record, Washington D.C, U.S.A.* **(Accepted)**

References

AASHTO Interim Guide for Design of Pavement Structures. 1961. American Association of State Highway and Transportation Officials,Washington D.C.

AASHTO Interim Guide for Design of Pavement Structures. 1972. American Association of State Highway and Transportation Officials,Washington D.C.

AASHTO Interim Guide for Design of Flexible Pavements. 1986. American Association of State Highway and Transportation Officials,Washington D.C.

AASHTO Guide for Design of Pavement Structures. 1993. American Association of State Highway and Transportation Officials, Washington, D.C.

AASHTO Mechanistic-Empirical Pavement Design Guide (MEPDG), Interim Edition: A Manual of Practice. 2008. American Association of State Highway and Transportation Officials, Washington, D.C.

AASHTO T307:Standard Method of Test for Determining the Resilient Modulus of Soils and Aggregate Materials. 2003. American Association of State Highway and Transportation Officials,Washington D.C.

Abu-Farsakh, M. Y., Alshibli, K., Nazzal, M., & Seyman, E. 2004. Assessment of in-situ test technology for construction control of base courses and embankments (Report No. FHWA/LA. 04/389). Louisiana Transportation Research Center.

Araya, A.A. 2011.Characterization of Unbound Granular Materials for Pavements (PhD. Thesis). IHE/TU Delft, The Netherlands.

Austroads.2012.Technical Basis of Austroads Guide to Pavement Technology, Part 2: Pavement Structural Design, Edited by G. Jameson. Sydney, Australia.

Ayres, M. 1997. Development of a Rational Probabilistic Approach for Flexible Pavements Analysis. Thesis (PhD).University of Maryland.

Barksdale, R. D., Lago Alba, J. A., Khosla, N. P., Kim, R., Lambe, P. C., & Rahman, M. S. 1997."Laboratory Determination of Resilient Modulus for Flexible

Pavement Design (NCHRP Project 1-28,)."

Barksdale, R.D. 1971."Compressive Stress Pulse Times in Flexible Pavements for Use in Dynamic Testing."*Highway Research Record 345,Highway Research Board, Washington, D.C.*: 32–44.

Barksdale, R.D. and Itani, S.Y. 1989. "Influence of Aggregate Shape on Base Behaviour." *Transportation Research Record 1227,Transportation Research Board, National Research Council, Washington D.C*: 173–82.

Barksdale, R.D. 1972. "Laboratory Evaluation of Rutting in Base Course Materials." In *Proc., 3rd International Conference on Asphalt Pavements,University of Michigan,Ann Arbor*,161–174.

Bhattacharjee, S. and Bandyopadhyay, K. 2015. "Evaluation of Elastic Modulus of Fly Ash Embankment by Repeated Load CBR Test." In *ICE Proceedings of the XVI ECSMGE Geotechnical Engineering for Infrastructure and Development*, , 793–98.

Bilodeau, J. P., & Doré, G. 2014. "Stress distribution experienced under a portable light-weight deflectometer loading plate. "*International Journal of Pavement Engineering*, *15*(6), 564-575.

Borden, R. H., Lowder, W. M., & Khosla, N. P. 1986."*Evaluation of pavement subgrade support characteristics by dilatometer test*." North Carolina State University, Center for Transportation Engineering Studies.

Bowles, J.E. 1996. "*Foundation Analysis and Design, Fifth Ed*." Singapore: The McGraw-Hill Companies, Inc, Singapore.

Briaud, J.-L. 2001. Geotechnic *Introduction to Soil Moduli.*

Zapata, C. E., Andrei, D., Witczak, M. W., & Houston, W. N. 2007. "Incorporation of environmental effects in pavement design. "*Road Materials and Pavement Design*, *8*(4), 667-693

.Cary, C. E., and Zapata, C. E. 2011. "Resilient Modulus for Unsaturated Unbound Materials." *Road Materials and Pavement Design*, 12(3): 615–38.

Choubane, B. and McNamara, R.L. 2000. "*Flexible Pavement Embankment Moduli Using Falling Weight Deflectometer (FWD) Data*" Research Report FL/DOT/SMO/00- 442. Florida Department of Transportation, State Materials Office, Tallahassee.

Dai, S., & Zollars, J. 2002. "Resilient modulus of Minnesota road research project subgrade soil." *Transportation Research Record 1786*(1),*Transportation Research Board, National Research Council, Washington D.C* : 20-28.

Dawson, A. R., Thom, N. H., and Paute, J. L. 1996. "Mechanical Characteristics of Unbound Granular Materials as a Function of Condition." In *Flexible Pavements, Proceedings, European Symposium*, Rotterdam, The Netherlands, 35–44.

Drumm, E. C., Boateng-Poku, Y., & Johnson Pierce, T. 1990. "Estimation of subgrade resilient modulus from standard tests. "*Journal of geotechnical engineering*, *116*(5), 774-789.

Dunlap,W.S.1963."*A Report on a Mathematical Model Describing the Deformation Characteristics of Granular Materials, Technical Report 1.Project 2-8-62-27*." Texas
Transportation Institute, Texas A&M University, College Station.

Elliott, Robert P. 1992. "Selection of Subgrade Modulus for AASHTO Flexible Pavement Design." *Transportation Research Record* 1354, *Transportation Research Board, National Research Council, Washington D.C :*39–44.

Engineers, U.S. Army Corps of. 1945. *The California Bearing Ratio Test as Applied to the Design of Flexible Pavements for Airports. Technical Memory. Number 213-1.* Vicksburg.

Farrar, M. J.;Turner, J. P. 1991. *Resilient Modulus of Wyoming Subgrade Soils (No. MPC Report No. 91-1.* Mountain Plains Consortium. Fargo.

Figueroa, J. L., and Thompson, M. R. 1980. "Simplified Structural Analysis of Flexible Pavements for Secondary Roads Based on ILLI-PAVE." *Transportation Research*

Record 776,Transportation Research Board, National Research Council,Washington,D.C:5–10.

Fleming, P. R., Frost, M. W., & Lambert, J. P. 2007. “Review of Lightweight Deflectometer for Routine in Situ Assessment of Pavement Material Stiffness.” *Transportation Research Record* 2004(1),*Transportation Research Board, National Research Council,Washington, D.C*: 80–87.

Fleming, P.R. and Rogers, C.D.F.1995. “Assessment of Pavement Foundations during Construction.” In *Proceedings of the Institution of Civil Engineers-Transport, 111 (2),* , 105– 115.

Fredlund, D. G., Bergan, A. T., and Wong, P. K. 1977. “Relation between Resilient Modulus and Stress Research Conditions for Cohesive Subgrade Soils.” *Transportation Research Record 642, Transportation Research Board,Washington, DC*: 73–81.

George, K. P., & Uddin, W. 2000. "*Subgrade Characterization for Highway Pavement Design (No.FHWA/MS-DOT-RD-00-131)."*Final Report, University of Mississippi, in cooperation with the Mississippi Department of Transportation, U.S Department of Transportation, and Federal Highway Administration, Oxford.

George, K. P. 2004."*Prediction of Resilient Modulus from Soil Index Properties.(No. FHWA/MS-DOT-RD-04-172)."* University of Mississippi. Mississippi.

George, V., Rao, N. C., & Shivashankar, R. 2009. "PFWD, DCP and CBR correlations for evaluation of lateritic subgrades."*International Journal of Pavement Engineering*, *10*(3), 189-199.

Ghorbani, B., Arulrajah, A., Narsilio, G., Horpibulsuk, S., & Bo, M. W. 2020. "Development of genetic-based models for predicting the resilient modulus of cohesive pavement subgrade soils." *Soils and Foundations*, *60*(2), 398-412.

Green, J.L. and Hall, J.W. 1975. "*Non Destructive Vibratory Testing of Airport Pavements: Experimental Test Results and Development of Evaluation Methodology and Procedure."* Washington DC.

Gudishala, R. 2004. “Development of Resilient Modulus Prediction Models for Base and Subgrade Pavement Layers from In Situ Devices Test Results.” Master’s thesis, Louisiana State University,Baton Rouge,.

Haghighi, H., Arulrajah, A., Mohammadinia, A., & Horpibulsuk, S. 2018. "A new approach for determining resilient moduli of marginal pavement base materials using the staged repeated load CBR test method."*Road Materials and Pavement Design*, *19*(8), 1848-1867.

Han, Z., and Vanapalli, S. K. 2015. “Model for Predicting the Resilient Modulus of Unsaturated Subgrade Soil Using the Soil-Water Characteristic Curve.” *Canadian Geotechnical Journal*, 52(10): 1605–19.

Han, Z., & Vanapalli, S. K. 2016. "State-of-the-art: Prediction of resilient modulus of unsaturated subgrade soils." *International Journal of Geomechanics*, *16*(4), 1-15

Hao, S., & Pabst, T. 2021. "Estimation of resilient behavior of crushed waste rocks using repeated load CBR tests." *Transportation Geotechnics*, *28*, 100525.

Hassan, A. B. 1996. “The Effects of Material Parameters on Dynamic Cone Penetrometer Results for Fine-Grained Soils and Granular Materials.” Oklahoma State University.

Herath, A., Mohammad, L. N., Gaspard, K., Gudishala, R., & Abu-Farsakh, M. Y. 2005. "The use of dynamic cone penetrometer to predict resilient modulus of subgrade soils." In *Advances in pavement engineering* (pp. 1-16).

Heukelom, W., & Klomp, A. 1962. “Dynamic Testing as a Means of Controlling Pavements during and after Construction.” In *In International Conference on the Structural Design of Asphalt Pavements*, University of Michigan, Ann Arbor.

Heydinger, A. G., Xie, Q., Randolph, B. W., & Gupta, J. D. 1996. “Analysis of Resilient Modulus of Dense- and Open-Graded Aggregates.” *Transportation Research Record 1547(1), Transportation Research Board, National Research Council,Washington, DC*: 1–6.

Hicks, R.G. and C.L. Monismith. 1971.*“Factors Influencing the Resilient Response of*

Granular Materials." Institute of Transportation and Traffic Engineering, University of California, Berkeley Washington, D.C.

Hight, D. W., & Stevens, M. G. H. (1982). An analysis of the California Bearing Ratio test in saturated clays. *Geotechnique*, *32*(4), 315-322.

Highway Research Board (HRB). 1952. "*Final Report on Road Test on Maryland. Special Report 4*." Washington,D.C.

Highway Research Board (HRB). 1962."*The AASHO Road Test, Report 7. Special Report 61-G*." Washington,D.C.

Hogentogler,C. and Terzaghi, K. 1929. "Interrelationship of Load, Road and Subgrade." *Public Roads* 10: 37–64.

Hossain, M. S. 2008. "*Characterization of Subgrade Resilient Modulus for Virginia Soils and Its Correlation with the Results of Other Soil Tests. VTRC 09-R4."* Virginia Transportation Research Council, Charlottesville,.

Hossain, M. Shabbir, and Wan Soo Kim. 2015. "Estimation of Subgrade Resilient Modulus for Fine-Grained Soil from Unconfined Compression Test." *Transportation Research Record* 2473(1), *Transportation Research Board, National Research Council,Washington, D.C*: 126–35.

Highway Research Board (HRB). 1945. "Report of Commitee on Classification of Materials for Subgrades and Granular Type Roads." *Proceedings, Highway Research Board* 25: 376–84.

Huang, Y.H. 1993. "*Pavement Analysis and Design*. First Edition. Pearson Education Inc.

Institute, Asphalt. 1970. *Thickness Design: Asphalt Pavements for Highways and Streets (Manual Series No. 1)*. The Asphalt Institute,Lexington.

IRC:37:1984:Guidelines for the Design of Flexible Pavements (First Revision). 1984. Indian Roads Congress, New Delhi, India.

IRC:37:2002:Guidelines for the Design of Flexible Pavements (Second Revision). 2002.

Indian Roads Congress, New Delhi, India.

IRC:37:2012:Guidelines for the Design of Flexible Pavements (Third Revision). 2012. Indian Roads Congress, New Delhi, India.

IRC 37:2018: Guidelines for Design of Flexible Pavements (Fourth Revision). 2018. Indian Roads Congress, New Delhi, India.

Kalcheff, I.V. and Hicks, R.G. 1973. "A Test Procedure for Determining Resilient Properties of Granular Materials." *ASTM Journal of Testing and Material Evaluation,* 1(6): 472–79.

Kardani, N., Aminpour, M., Raja, M. N. A., Kumar, G., Bardhan, A., & Nazem, M. 2022. "Prediction of the resilient modulus of compacted subgrade soils using ensemble machine learning methods." *Transportation Geotechnics*, *36*, 100827.

Khasawneh, M. A., & Al-jamal, N. F. 2019. "Modeling resilient modulus of fine-grained materials using different statistical techniques." *Transportation Geotechnics*, *21*, 100263.

Khoury, N. N., & Zaman, M. M. 2004."Correlation between resilient modulus, moisture variation, and soil suction for subgrade soils." *Transportation research record*, *1874*(1), *Transportation Research Board, National Research Council,Washington, D.C:* 99-107.

Kim, D. S., Kweon, G. C., & Lee, K. H. 2001. "Alternative method of determining resilient modulus of subgrade soils using a static triaxial test." *Canadian Geotechnical Journal*, *38*(1), 107-116.

Kolisoja, P. 1997. "Resilient Deformation Characteristics of Granular Materials, PhD Thesis." Tampere University of Technology, Publ. No. 223, Tampere, Finland.

Laboratoire Central Des Ponts et Chaussees (LCPC)Conception et Dimensionnement Des Structures de Chaussee e Guide Technique. Laboratoire Central Des Ponts et Chaussees. 1981. Paris.

Lee,W., Bohra, N.C. , Altschaeffl, A.G. and White, T.D. 1997. "Resilient Modulus of Cohesive Soils 36." *Journal of Geotechnical and Geoenvironmental Engineering*

123(2): 131–36.

Leischner, S., Spanier, T. and Canon Falla, G. 2022. “Effective Experimental Characterization of the Non-Linear Elastic Deformation Behavior of Unbound Granular Materials.” In *Eleventh International Conference on the Bearing Capacity of Roads, Railways and Airfields, Volume 2*,435–44.

Lekarp, F., Isacsson, U., & Dawson, A. (2000). State of the art. I: Resilient response of unbound aggregates. *Journal of transportation engineering*, *126*(1), 66-75.

Lenke, L.R., McKeen, R.G. and Grush, M. "*Evaluation of a Mechanical Stiffness Gauge for Compaction Control of Granular Media*."Report NM99MSC-07.2. New Mexico State Highway and Transportation Department, Albuquerque.

Lenke, L. R., McKeen, R. G., & Grush, M. P. (2003). Laboratory evaluation of GeoGauge for compaction control. *Transportation research record*, *1849*(1), *Transportation Research Board, National Research Council, Washington, D.C:* 20-30.

Liang, R. Y., Rabab’ah, S., & Khasawneh, M. 2008. “Predicting Moisture-Dependent Resilient Modulus of Cohesive Soils Using Soil Suction Concept.” *Journal of Transportation Engineering* 134(1): 34–40.

Lister, N.W. & Powell, D. 1987. “Design Practices for Pavements in the United Kingdom.” In *Proceedings of the 6th International Conference on the Structural Design of Asphalt Pavements,* Ann Arbor.

Loach, S.C. 1987. "Repeated Loading of Fine Grained Soils for Pavement Design.PhD Thesis", University of Nottingham.

Malla, R. B., & Joshi, S. (2006). *Establish subgrade support values for typical soils in New England* (No. NETCR 57).

Mazari, M., Garcia, G., Garibay, J., Abdallah, I., & Nazarian, S. 2013. *Impact of modulus based device variability on quality control of compacted geomaterials using measurement system analysis* (No. 13-3192).

Mazari, M., Navarro, E., Abdallah, I., & Nazarian, S. 2014. “Comparison of Numerical

and Experimental Responses of Pavement Systems Using Various Resilient Modulus Models." *Soils and Foundations* 54(1): 36–44.

Mendoza, C., & Caicedo, B. 2019. "Elastoplastic framework of relationships between CBR and Young's modulus for fine grained materials."*Transportation Geotechnics*, *21*, 100280.

Miradi, M., Molenaar, A. A. A., & Van de Ven, M. F. C. 2009. "Performance modelling of porous asphalt concrete using artificial intelligence." *Road Materials and Pavement Design*, *10*(sup1), 263-280.

Mohammad, L. N., Huang, B., Puppala, A. J., & Allen, A.1999. "Regression model for resilient modulus of subgrade soils." *Transportation Research Record*, *1687*(1), *Transportation Research Board, National Research Council, Washington, D.C:* 47-54.

Mohammad, L. N., Herath, A., Abu-Farsakh, M. Y., Gaspard, K., & Gudishala, R. 2007. Prediction of resilient modulus of cohesive subgrade soils from dynamic cone penetrometer test parameters. *Journal of Materials in Civil Engineering*, *19*(11), 986-992.

Molenaar, A.A.A. 2007. "Characterization of Some Tropical Soils for Road Pavements." *Transportation Research Record* 2(1989) *Transportation Research Board, National Research Council, Washington, D.C*: 186–93.

Mooney, M. A., & Miller, P. K. 2009. "Analysis of lightweight deflectometer test based on in situ stress and strain response." *Journal of geotechnical and geoenvironmental engineering*, *135*(2), 199-208.

Moossazadeh, J. and Witczak, M.W. 1981. "Prediction of Subgrade Moduli for Soil That Exhibits Nonlinear Behaviour." *Transportation Research Record 810, Transportation Research Board, National Research Council, Washington DC,*: 9–17.

Mousavi, S. H., Gabr, M. A., & Borden, R. H. 2017. "Subgrade resilient modulus prediction using light-weight deflectometer data." *Canadian Geotechnical Journal*, *54*(3), 304-312.

MS-2 Asphalt Mix Design Methods. 2015. Seventh Edition. Asphalt Institute,Lexington, Kentucky, USA.

Nagula, S. S., Robinson, R. G., & Krishnan, J. M. 2018. "Mechanical characterization of pavement granular materials using hardening soil model." *International Journal of Geomechanics*, *18*(12), 04018157.

Narzary, B. K., & Ahamad, K. U. 2018."Estimating elastic modulus of California bearing ratio test sample using finite element model."*Construction and Building Materials*, *175*, 601-609.

Narzary, B. K., & Ahamad, K. U. 2020. "Equivalent modulus for fine-grained subgrade soil. "*Journal of Transportation Engineering, Part B: Pavements*, *146*(2), 04020004.

Narzary, B. K., & Ahamad, K. U. 2021. "Estimation of Equivalent Modulus of Fine-Grained Subgrade Soil from Numerical Model." *Journal of Transportation Engineering, Part B: Pavements*, *147*(1), 04020084.

Nazarian, S., Baker, M. and Crain, K. 1995. "Use of Seismic Pavement Analyzer in Pavement Evaluation." *Transportation Research Record 1505,Transportation Research Board, National Research Council, Washington, D.C*: 1–8.

Nazarian, S., Pezo, R. and Picronell, M. 1996. "*Testing Methodology for Resilient Modulus of Base Materials,Research Report 1336-1*."Center for Geotechnical and Highway Materials Research, University of Texas at El Paso.

Nazarian, S., Yuan, D., Tandon, V. and Arrellano, M. 2003. "*Quality Management of Flexible Pavement Layers with Seismic Methods, Research Report 1735-3F*. "Center for Highway Materials Research, University of Texas at El Paso.

Nazarian, S., Yuan, D., Tandon, V., & Arellano, M. 2005. *Quality management of flexible pavement layers with seismic methods*. Center for Transportation Infrastructure Systems, University of Texas at El Paso.

Nazzal, M., Abu-Farsakh, M., Alshibli, K., & Mohammad, L. 2004. "Evaluating the

Potential Use of a Portable LFWD for Characterizing Pavement Layers and Subgrades." In *Geotechnical Engineering for Transportation Projects*, 915–24.

Negi, M.S., & Singh, S.K. 2021."Experimental and Numerical Studies on Geotextile Reinforced Subgrade Soil." *International Journal of Geotechnical Engineering* 15(9): 1106–17.

Ni, B., Hopkins, T. C., Sun, L., & Beckham, T. L. 2002. "Modeling the Resilient Modulus of Soils." In *Proceedings of the 6th International Conference on the Bearing Capacity of Roads, Railways, and Airfields, Vol. 2,* (pp. 1131-1142). CRC Press.

Ooi, P. S., Sandefur, K. G., & Archilla, A. R. 2006. "*Correlation of resilient modulus of fine-grained soils with common soil parameters for use in design of flexible pavements* (No. HWY-L-2000-06)."

Ooi, P. S., Archilla, A. R., & Sandefur, K. G. (2004). Resilient modulus models for compacted cohesive soils. *Transportation research record, 1874*(1),*Transportation Research Board, National Research Council, Washington, D.C:* 115-124.

Vennapusa, P., & White, D .2009. "Comparison of Light Weight Deflectometer Measurements for Pavement Foundation Materials." *Geotechnical Testing Journal* 32(3): 239–51.

Parreira, A. B., and Gonçalves, R. F. 2000. "The Influence of Moisture Content and Soil Suction on the Resilient Modulus of a Lateritic Subgrade Soil." In *GeoEng Int. Conf. on Geotechnical and Geological Engineering*, Melbourne, Australia.

Pereira, P., and Pais,J. 2017. "Main Flexible Pavement and Mix Design Methods in Europe and Challenges for the Development of an European Method." *Journal of Traffic and Transportation Engineering (English Edition)* 4(4): 316–46.

Pezo, R.F. and Hudson,W.R. 1994. "Prediction Models of Resilient Modulus for Nongranular Materials,." *Geotechnical Testing Journal* Vol. 17(3): 349–355.

Ping, W. V., Yang, Z., & Gao, Z. 2002." Field and laboratory determination of granular

subgrade moduli. "*Journal of Performance of Constructed Facilities*, *16*(4), 149-159.

Porter, O. J. 1938. The preparation of subgrades.

Porter, O. J.1950. "Development of the original method for highway design." *Transactions of the American Society of Civil Engineers*, *115*(1), 461-467.

Powell, W.D., Potter, J.F., Mayhew, H.C.1984. *The Structural Design of Bituminous Roads. LR 1132.*

Puppala, A. J. (2008). "*Estimating stiffness of subgrade and unbound materials for pavement design* (Vol. 382)."Transportation Research Board.

Von Quintus, H., and Killingsworth, B. 1998. "*Analyses Relating to Pavement Material Characterizations and Their Effects on Pavement Performance," Report No. FHWARD-97-085. Washington, D.C.*

Rada, G.;Witczak, M. W. 1981. "Comprehensive Evaluation of Laboratory Resilient Moduli Results for Granular Material." *Transportation Tesearch Record 810,Transportation Research Board, National Research Council, Washington, D.C*: 23–33.

Rahim, A.A., and George. K.P.2003. "Falling Weight Deflectometer for Estimating Subgrade Elastic Moduli." *Journal of Transportation Engineering* 129(1): 100–107.

Rahim,A.M. 2005. "Subgrade Soil Index Properties to Estimate Resilient Modulus for Pavement Design." *International Journal of Pavement Engineering* 6(3): 163–69.

Rahim, A.M., and George, K. P. 2004. "Subgrade Soil Index Properties to Estimate Resilient Modulus",." *Paper Presented at 83rd Annual Meeting of Transportation Research Board*, Washington D C.

Robinson, R. G. 1974. "Measurement of the Elastic Properties of Granular Materials Using a Resonance Method." *TRRL Supplementary Rep. No. 111UC, TRRL*.

Santha, B.L. 1994. “Resilient Modulus of Subgrade Soils: Comparison of Two Constitutive Equations." *Transportation Research Record 1462,Transportation Research Board, National Research Council*,Washington D.C:79–90.

Sas, W., Gluchowski, A., & Szymanski, A. 2012."Determination of the Resilient modulus MR for the lime stabilized clay obtained from the repeated loading CBR tests." *Annals of Warsaw University of Life Sciences-SGGW. Land Reclamation*, *44*(2).

Sawangsuriya, A., Edil, T. B., and Benson, C. H. “Effect of Suction on Resilient Modulus of Compacted Fine-Grained Subgrade Soils.”*Transportation Research Record 1462, Transportation Research Board, National Research Council*,Washington D.C:82–87.

Schwartz,C.W., Afsharikia,Z., & Khosravifar, S. 2017. "*Standardizing Lightweight Deflectometer Modulus Measurements for Compaction Quality Assurance (No. MD-17-SHA-UM-3-20)."*

Seed,H. B., Mitry, F. G., Monismith, C. L., Chan, C. K. 1967. "*Prediction of Flexible Pavement Deflections from Laboratory Repeated-Load Tests. NCHRP Report,(35)*."

Seed, H. B., Chan, C. K., & Lee, C. E. 1962. "Resilience characteristics of subgrade soils and their relation to fatigue failures in asphalt pavements." In *International Conference on the Structural Design of Asphalt Pavements. SupplementUniversity of Michigan, Ann Arbor*.

Seed, H. B., & McNeill, R. L. 1957. "*Soil deformations under repeated stress applications*.” *ASTM Special Technical Publication, No. 32*: 177–197.

Senseney, C. T., & Mooney, M. A. 2010. "Characterization of two-layer soil system using a lightweight deflectometer with radial sensors." *Transportation research record 2186*(1), *Transportation Research Board, National Research Council*,Washington D.C:21-28.

Shell Pavement Design Manual: Asphalt Pavements and Overlays for Road Traffic. 1978. Shell International Petroleum Company.London.

Shook, J. F. 1982. “Thickness Design of Asphalt Pavements-the Asphalt Institute Method.” In *In Proceedings of 5th International Conference on the Structural Design of Asphalt Pavement*,17–44.

Siddharthan, R., Sebaaly, P. E., & Javaregowda, M. 1992. "Influence of statistical variation in falling weight deflectometers on pavement analysis." *Transportation research record 1377, Transportation Research Board, National Research Council*,Washington D.C: 57.

Siekmeier, J. A., Young, D., and Beberg, D. 2000. “Comparison of the Dynamic Cone Penetrometer with Other Tests During Subgrade and Granular Base Characterization in Minnesota.” In *Symp. Nondestructive Testing of Pavements and Backcalculation of Moduli: Third Volume, ASTM STP 1375*,175–188.

Steele, D.J. 1945. *Application of the Classification and Group Index in Estimating Desirable Subbase and Total Pavement Thickness (A Discussion).*

Sukumaran, B., Kyatham, V., Shah, A., & Sheth, D.2002. "Suitability of using california bearing ratio test to predict resilient modulus."In *Proceedings:Federal aviation administration airport technology transfer conference* (p. 9).

Opiyo,T. 1995. “A Mechanistic Approach to Laterite-Based Pavements in Transport and Road Engineering. (MSc Thesis).” International Institute for Infrastructure. Hydraulics and Environment Engineering, Delft, the Netherlands.

Tamrakar, P., & Nazarian, S. 2016. "*Impact of gradation and moisture content on stiffness parameters of base materials"* (No. CAIT-UTC-054). Rutgers University. Center for Advanced Infrastructure & Transportation.

Terrel, R. L., Awad, I. S., & Foss, L. R. 1974. "Techniques for characterizing bituminous materials using a versatile triaxial testing system." In *Fatigue and Dynamic Testing of Bituminous Mixtures*. ASTM International.

Thom, N. H., and Brown, S. F. 1987. “Effect of Moisture on the Structural Performance of a Crushed-Limestone Road Base.”*Transportation Research Record No. 1121, Transportation Research Board, National Research Council*,Washington D.C: 50–56.

Thompson, M.R. and Q.L. Robnett. 1976. "*Resilient Properties of Subgrade Soils. Final Report-Data Summary.*"Transportation Engineering Series 14, Illinois Cooperative Highway Research and Transportation Program Series, University of Illinois,Urbana Champaign.

Elliott, R.P., & Thornton,S.I.1988."Simplification of subgrade resilient modulus testing." *Transportation Research Record, 1192, Transportation Research Board, National Research Council,Washington D.C*:1-7.

Uzan, J. 1985. "Characterization of granular material." *Transportation research record 1022*(1), *Transportation Research Board, National Research Council,Washington D.C*:52-59.

Vanapalli, S. K., Fredlund, D. G., and Pufahl, D. E. 1999. "The Influence of Soil Structure and Stress History on the Soil-Water Characteristics of a Compacted Till." *Geotechnique* 49(2): 143–59.

White, D., Vennapusa, P., & Thompson, M. (2007). Field validation of intelligent compaction monitoring technology for unbound materials.

Witczak, M.W. 2003."*Project No. 1-28A Final Report: Harmonized Test Methods for Laboratory Determination of Resilient Modulus for Flexible Pavement Design (Volume I: Unbound Granular Material)*."

Witczak, M.W. and J. Uzan. 1988. "*The Universal Airport Pavement Design System, Report 1 of 4, Granular Material Characterization*."

Wolfe, W.E. and T.S. Butalia. 2004. "*Seasonal Instrumentation of SHRP Pavements, Final Report for Ohio Department of Transportation*."

Yang, S. R., Huang, W. H., & Tai, Y. T. 2005. "Variation of resilient modulus with soil suction for compacted subgrade soils." *Transportation Research Record 1913*(1), *Transportation Research Board, National Research Council,Washington D.C*:99-106.

Yau, A., & Von Quintus, H. L. 2002. "*Study of LTPP laboratory resilient modulus test data and response characteristics* "(No. FHWA-RD-02-051; 3032.1). Turner-

Fairbank Highway Research Center.

Yoder, E. J., & Witczak, M. W. 1975. *Principles of Pavement Design.* John Wiley & Sons.

Zhou, J. and Xiaonan G. 2001. “Strain Degradation of Saturated Clay under Cyclic Loading.” *Canadian Geotechnical Journal* 38(1): 208–12.

APPENDIX-I

Bulk and octahedral shear stresses used for regression

E	ν	Penetration (mm)	Plunger stress (kPa)	Average Bulk stress(kPa)	Octahedral shear stress(kPa)
10	0.1	1	224.78	30.18	38.53
10	0.1	2	372.62	66.67	71.53
10	0.1	3	485.37	100.54	95.38
10	0.15	1	231.79	32.89	37.98
10	0.15	2	390.30	72.74	72.77
10	0.15	3	509.81	110.62	100.22
10	0.2	1	240.76	36.30	37.66
10	0.2	2	413.56	80.17	73.86
10	0.2	3	546.50	122.32	104.62
10	0.25	1	252.94	40.75	37.58
10	0.25	2	444.99	89.17	75.51
10	0.25	3	593.11	136.39	108.82
10	0.3	1	270.74	46.73	37.82
10	0.3	2	473.19	102.24	77.81
10	0.3	3	656.17	154.98	112.81
10	0.35	1	294.40	55.38	38.87
10	0.35	2	538.22	118.87	80.72
10	0.35	3	722.68	180.90	120.48
20	0.1	1	364.62	63.35	68.39
20	0.1	2	582.23	125.43	110.09
20	0.1	3	748.25	178.88	139.57
20	0.15	1	382.75	69.22	69.89
20	0.15	2	610.79	137.53	115.29
20	0.15	3	793.68	195.37	147.65
20	0.2	1	411.03	75.65	70.45
20	0.2	2	664.91	152.72	122.06
20	0.2	3	855.65	217.24	158.25
20	0.25	1	439.35	84.38	71.76
20	0.25	2	718.96	171.48	129.61
20	0.25	3	935.39	242.42	168.38
20	0.3	1	471.71	96.94	74.45
20	0.3	2	783.38	195.02	136.84
20	0.3	3	1016.17	280.49	184.99
20	0.35	1	521.37	113.23	77.14
20	0.35	2	876.22	228.53	149.65
20	0.35	3	1156.55	322.84	200.37
30	0.1	1	474.78	94.93	92.02
30	0.1	2	744.96	176.49	138.81
30	0.1	3	970.83	253.03	180.64
30	0.15	1	500.77	103.66	95.25
30	0.15	2	800.66	192.21	146.45
30	0.15	3	1027.30	278.04	192.38

E	ν	Penetration (mm)	Plunger stress (kPa)	Average Bulk stress(kPa)	Octahedral shear stress(kPa)
30	0.2	1	534.34	114.10	98.39
30	0.2	2	852.26	212.36	155.25
30	0.2	3	1125.41	302.99	206.39
30	0.25	1	575.33	127.67	102.43
30	0.25	2	924.17	238.95	166.74
30	0.25	3	1208.84	338.74	220.61
30	0.3	1	629.72	145.10	107.03
30	0.3	2	1026.46	272.10	180.65
30	0.3	3	1338.38	386.23	242.60
30	0.35	1	698.95	168.97	113.21
30	0.35	2	1149.92	318.55	199.17
30	0.35	3	1506.16	446.21	266.65
40	0.1	1	576.70	121.51	108.19
40	0.1	2	897.39	224.06	164.86
40	0.1	3	1170.84	318.52	214.81
40	0.15	1	606.21	133.50	113.85
40	0.15	2	947.06	246.11	175.85
40	0.15	3	1258.09	345.05	228.80
40	0.2	1	647.30	147.28	125.28
40	0.2	2	1019.45	270.35	201.58
40	0.2	3	1332.45	382.57	264.62
40	0.25	1	697.25	164.85	125.28
40	0.25	2	1106.77	302.18	201.58
40	0.25	3	1457.53	422.86	264.62
40	0.3	1	767.11	187.89	133.73
40	0.3	2	1233.42	343.34	219.45
40	0.3	3	1616.13	482.16	292.70
40	0.35	1	851.94	219.70	144.72
40	0.35	2	1372.34	398.92	241.79
40	0.35	3	1836.77	548.85	320.96
50	0.1	1	656.80	147.56	123.27
50	0.1	2	1039.39	268.67	188.45
50	0.1	3	1343.24	379.97	246.06
50	0.15	1	701.80	161.31	130.29
50	0.15	2	1095.37	295.66	202.08
50	0.15	3	1446.58	412.20	263.34
50	0.2	1	749.45	177.94	137.43
50	0.2	2	1192.41	324.34	215.91
50	0.2	3	1568.15	452.35	283.68
50	0.25	1	810.09	199.36	145.99
50	0.25	2	1289.37	362.15	233.58
50	0.25	3	1716.61	504.44	310.60
50	0.3	1	883.99	227.92	157.05
50	0.3	2	1433.83	409.47	254.41
50	0.3	3	1857.33	567.39	337.83
50	0.35	1	990.53	265.92	171.58

E	ν	Penetration (mm)	Plunger stress (kPa)	Average Bulk stress(kPa)	Octahedral shear stress(kPa)
50	0.35	2	1607.17	477.09	283.41
50	0.35	3	2107.70	642.90	368.69
60	0.1	1	738.61	171.86	137.35
60	0.1	2	1149.10	313.46	211.28
60	0.1	3	1518.55	436.55	276.30
60	0.15	1	784.32	187.90	144.92
60	0.15	2	1225.67	341.57	225.58
60	0.15	3	1791.96	0.00	296.17
60	0.2	1	842.98	206.51	153.39
60	0.2	2	1326.89	375.80	243.10
60	0.2	3	1763.12	523.34	320.47
60	0.25	1	909.62	231.40	163.83
60	0.25	2	1463.09	416.95	263.39
60	0.25	3	1910.31	577.74	349.00
60	0.3	1	997.70	264.26	177.17
60	0.3	2	1617.03	472.82	288.30
60	0.3	3	2106.85	644.14	378.60
60	0.35	1	1120.27	308.96	195.07
60	0.35	2	1800.39	545.64	319.61
60	0.35	3	2070.89	641.77	369.24
70	0.10	1	813.44	194.37	149.41
70	0.10	2	1273.55	356.21	233.48
70	0.10	3	1682.56	490.98	304.64
70	0.15	1	869.38	212.36	158.47
70	0.15	2	1357.96	385.65	248.17
70	0.15	3	1819.45	534.85	327.70
70	0.20	1	925.89	233.39	168.06
70	0.20	2	1473.01	424.64	268.70
70	0.20	3	1977.12	581.28	352.42
70	0.25	1	1009.19	261.51	180.21
70	0.25	2	1609.15	470.46	291.10
70	0.25	3	2097.02	639.10	380.19
70	0.30	1	1108.07	298.87	196.02
70	0.30	2	1790.76	533.12	320.64
70	0.30	3	2165.39	654.21	382.17
70	0.35	1	1250.26	347.71	215.61
70	0.35	2	1981.57	605.60	351.09
70	0.35	3	2040.64	631.28	363.92
80	0.10	1	881.33	216.78	161.17
80	0.10	2	1403.68	391.18	253.41
80	0.10	3	1824.23	543.30	329.64
80	0.15	1	936.74	237.73	171.78
80	0.15	2	1497.18	429.39	272.19
80	0.15	3	1978.78	586.19	354.43
80	0.20	1	1005.28	261.52	183.13
80	0.20	2	1606.27	467.68	291.20

E	ν	Penetration (mm)	Plunger stress (kPa)	Average Bulk stress(kPa)	Octahedral shear stress(kPa)
80	0.20	3	2098.12	632.75	376.40
80	0.25	1	1106.85	292.32	197.61
80	0.25	2	1758.86	523.08	319.15
80	0.25	3	2117.93	645.30	382.03
80	0.30	1	1220.02	332.19	214.03
80	0.30	2	1969.46	583.97	348.87
80	0.30	3	2158.31	641.24	378.44
80	0.35	1	1363.91	385.51	235.86
80	0.35	2	2099.85	647.42	373.82
80	0.35	3	2084.82	638.35	368.55
90	0.10	1	957.90	240.32	174.25
90	0.10	2	1507.94	428.85	270.91
90	0.10	3	1992.18	588.16	355.83
90	0.15	1	1011.38	261.85	184.49
90	0.15	2	1605.06	467.13	291.33
90	0.15	3	2122.87	634.20	380.10
90	0.20	1	1091.42	286.04	196.36
90	0.20	2	1730.60	512.26	314.46
90	0.20	3	2214.84	657.90	391.09
90	0.25	1	1183.01	323.55	205.21
90	0.25	2	1889.81	568.97	395.21
90	0.25	3	2098.50	635.39	362.10
90	0.30	1	1319.85	365.56	231.93
90	0.30	2	2080.72	637.74	374.52
90	0.30	3	2088.48	633.49	371.09
90	0.35	1	1470.04	422.81	255.85
90	0.35	2	2086.91	634.28	367.39
90	0.35	3	2128.32	645.96	372.85
100	0.10	1	1017.71	260.05	221.58
100	0.10	2	1617.37	467.24	325.12
100	0.10	3	2111.09	635.58	375.25
100	0.15	1	1092.94	284.94	197.16
100	0.15	2	1709.91	504.52	310.16
100	0.15	3	2112.67	642.41	379.14
100	0.20	1	1162.90	314.41	211.13
100	0.20	2	1892.81	553.51	338.06
100	0.20	3	2081.69	633.14	371.87
100	0.25	1	1269.55	350.68	228.43
100	0.25	2	2017.90	610.41	365.57
100	0.25	3	2104.91	639.04	378.04
100	0.3	1	1411.51	370.51	232.41
100	0.3	2	2134.63	621.52	372.51
100	0.3	3	2110.82	651.21	381.67